Marco Polo

Near-Earth asteroid sample return mission

Assessment Study Report

European Space Agency
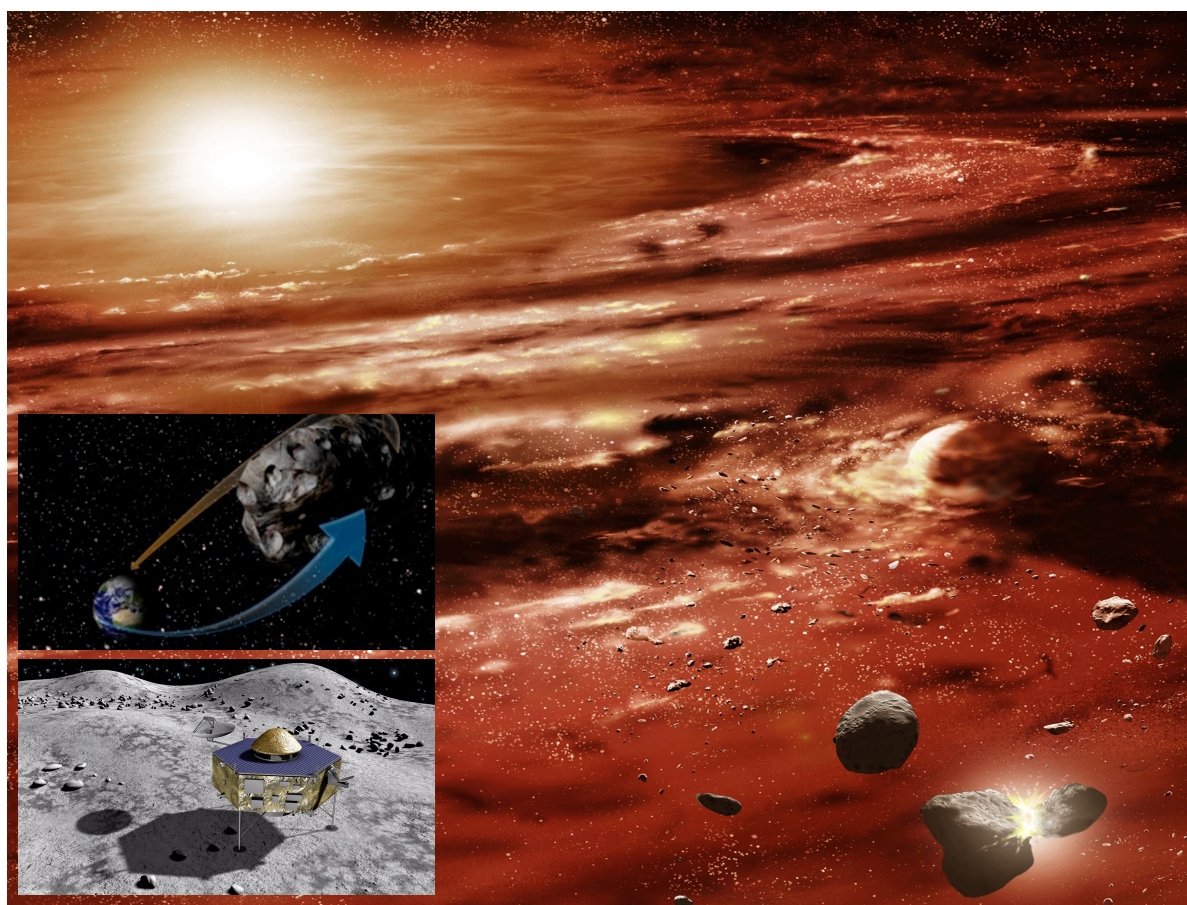
The front page shows an artist's impression of the solar-system formation in the background. The inserts show an asteroid sample return mission based on a European design.

Marco Polo Assessment Study – Mission Summary (ESA-defined scenario)[1]	
Key scientific goals	**Marco Polo will return a sample from a near-Earth asteroid (NEA).** *Marco Polo aims at answering the following key questions:* 1) What were the processes occurring in the early solar system and accompanying planet formation? 2) What are the physical properties and evolution of the building blocks of terrestrial planets? 3) Do NEAs of primitive classes contain pre-solar material yet unknown in meteoritic samples? 4) What are the nature and the origin of the organics in primitive asteroids and how can they shed light on the origin of molecules necessary for life?
Reference core payload	Narrow and Wide Angle Cameras, Close-Up Camera, radio science experiment, visible/near-infrared and mid-infrared spectrometers, laser altimeter, neutral particle analyzer, all benefiting from strong heritage from previous space missions.
Overall mission profile	• Launch into direct escape by Soyuz-Fregat 2-1B (Kourou), Nov./Dec. 2018, to the near-Earth asteroid 1999 JU3 (backup launch one year later), main spacecraft + re-entry capsule composite • Two outbound Earth swing-bys (one for the backup transfer) - Rendezvous with asteroid in Feb. 2022 - 18 months of asteroid proximity operations (global/local characterisation at km to 200 m altitude, 7-8 months, selection of sampling site, sampling operations) - Return to Earth in Dec. 2024: 6 year mission duration (5 years for backup), parachute-based re-entry • Total mission Δv: 1394 m·s⁻¹ (excl. proximity operations and navigation) • Sample curation in receiving facility and investigating analytical laboratories – curation for 50 years, initial analytical programme 4 years.

Spacecraft modules	**Main spacecraft**	**Earth re-entry capsule**
Stabilization	3-axis	Spin
Specific capabilities. Two sampling strategies presented, second one in parentheses	• Descent strategy: precision vision-based navigation aided by altimetry measurement • Sampling strategy: short-term landing, rotating corer transferred to Earth re-entry capsule (ERC) via robotic arm (touch and go, fast pusher transferred to ERC via landing legs and elevator system)	• Direct re-entry from hyperbolic trajectory • Descent under parachute • Ground landing
Sizing-case power (peak)	555 - 910 W (global characterisation phase at maximum solar distance)	< 10 W
Telemetry band	X-band	UHF beacons for recovery
Total downlink capacity	400 – 600 Gbit	--
Payload mass	~30 kg (science instruments)	1.3 - 4.6 kg (sample container)
Dry mass (incl. all margins)	710 - 745 kg (excl. ERC)	25 - 69 kg
	Main spacecraft + ERC: 745 - 810 kg	
Total launch mass	**1450 – 1560 kg**	
Key capabilities	• Autonomous precision GNC for proximity operations • Landing/touchdown - legs for low-gravity environment • Sample collection, transfer and containment system • High heat flux ablative material • Re-entry capsule parachute	

Astrium
OHB
TAS

---

[1] *3 options were astudied; the range between minimum and maximum numerical values is given. Other scenarios have been investigated for collaborations both with JAXA and NASA. The mission is modular and cooperation efforts can easily be envisaged and adapted to the available resources.*

Foreword
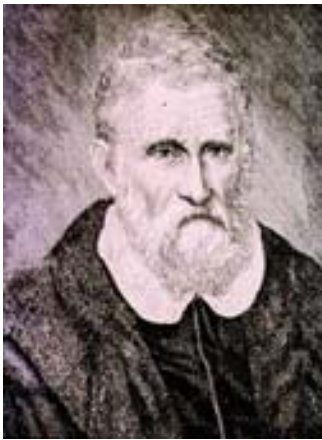
Figure 1: Marco Polo, traveller and author of the book "The travels of Marco Polo", describing Asian provinces in the 15th century.

Marco Polo is a mission to return a sample from an asteroid. It was proposed as a contribution to a JAXA mission to ESA's Cosmic Vision programme as a response to a call for mission proposals by ESA in 2007. The proposal was produced under the leadership of Antonella Barucci from Paris Observatory, with about 450 scientists supporting the proposal. The mission will contribute to our understanding of the solar system and involves many different research areas: the formation of the solar system; synthesis of the elements; planet formation; and the origin of life.

The first ideas for the mission came up in 2004 and resulted in a number of meetings of people interested in the mission. A European group formed which started to write a proposal, in close collaboration with colleagues from Japan and the USA. The name 'Marco Polo' reflects this collaboration: Marco Polo (see Figure 1) was the first European who after his travels brought back to Europe the news of the existence of Japan. This Yellow Book presents an ESA mission and identifies possible collaboration scenarios.

This Assessment Study Report, the so-called Yellow Book of Marco Polo, was written by the Marco Polo Science Study Team and compiled on their behalf by the Study Scientist. It was made possible because of the dedication of a number of scientists and engineers both in Europe and in Japan who, just like Marco Polo, want to explore new worlds and return samples from them. In this case the new world would be a near-Earth asteroid. Thanks to all of those who were involved in preparing this work.

Detlef Koschny, Marco Polo Study Scientist

Bookkeeper of this document

Authorship, acknowledgements

This report has been prepared by the Marco Polo Science Team listed below.

The Marco Polo Science Team

ESA Science Study Team (SST)		
Maria Antonietta Barucci (lead proposer)	LESIA-Paris Observatory	Paris, France
Hermann Böhnhardt	MPS	Katlenburg-Lindau, Germany
John R. Brucato	INAF – Obs. of Arcetri	Florence, Italy
Elisabetta Dotto	INAF – Obs. of Roma	Roma, Italy
Ian Franchi	Open Univ.	Milton Keynes, UK
Simon F. Green	Open Univ.	Milton Keynes, UK
Jean-Luc Josset	Space Exploration Institute	Neuchatel, Switzerland
Patrick Michel (co-lead proposer)	Univ. Nice, CNRS, Cote d'Azur Obs.	Nice, France
Karri Muinonen	Univ. Helsinki and FGI	Helsinki and Masala, Finland
Jürgen Oberst	DLR Berlin and TU Berlin	Berlin, Germany
ESA study team		
David Agnolon (Study Manager)	ESA	Noordwjik, The Netherlands
Detlef Koschny (Study Scientist)	ESA	Noordwjik, The Netherlands
Jens Romstedt (Payload Manager)	ESA	Noordwjik, The Netherlands
NASA representative		
Richard P. Binzel	MIT	Massachusetts, USA
JAXA representatives		
Jun-Ichi Kawaguchi	JSPEC, JAXA	Japan
Makoto Yoshikawa (co-lead proposer)	JSPEC, JAXA	Japan
Hajime Yano	JSPEC, JAXA	Japan

Table of contents

1 Executive summary

Marco Polo is a sample return mission to a near-Earth asteroid (NEA), see Figure 2. This mission will rendezvous with a primitive NEA, scientifically characterise it at multiple scales, and return a sample to Earth unaltered by the atmospheric entry process or terrestrial weathering and most likely unlike any known meteorite. This will be the first sample ever returned from a primitive asteroid. Marco Polo thereby contributes to our better understanding of the origin and evolution of the solar system, the Earth, and life itself. Moreover, Marco Polo provides important information on the volatile-rich (*e.g.* water) nature of primitive NEAs, which may be particularly important for future space resource utilization.

Small bodies, as primitive leftover building blocks of the solar-system formation process, offer clues to the chemical mixture from which the planets formed some 4.6 billion years ago. Current exobiological scenarios for the origin of life invoke an exogenous delivery of organic matter to the early Earth: It has been proposed that primitive bodies could have brought these complex organic molecules capable of triggering the pre-biotic synthesis of biochemical compounds on the early Earth. Moreover, collisions of NEAs with the Earth pose a finite hazard to life. For all these reasons, the exploration of such objects is particularly interesting and urgent.
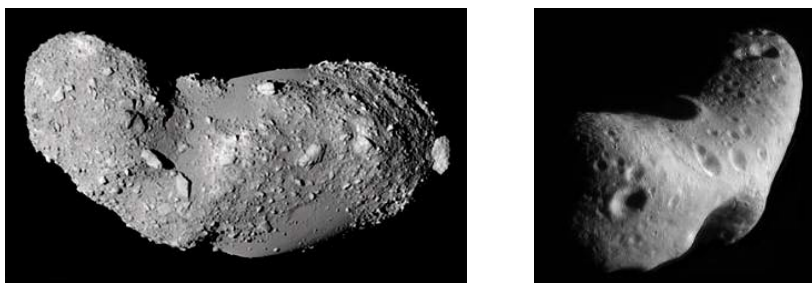
Figure 2: (433) Eros (right) and (25143) Itokawa (left), the two only asteroids which have ever been orbited by spacecraft. Both of them are compositionally evolved (images: NASA/JAXA).

The main goal of the Marco Polo mission is to return unaltered NEA material to allow it to be studied with ground-based laboratories. The limited sampling provided by meteorites does not offer the most primitive material available in near-Earth space. More friable material, and likely even more primitive material with less parent body processing, would not have survived atmospheric entry in any discernible amount.

Marco Polo will allow us to study the most primitive materials available to investigate early solar-system formation processes. Moreover, Marco Polo provides a sample from a known target and known geological context. Direct investigation of both the regolith and fresh interior fragments is also impossible by any means other than sample return.

Marco Polo will provide fundamental elements to answer the following key questions:

1) What were the processes occurring in the early solar system and accompanying planet formation?

2) What are the physical properties and evolution of the building blocks of terrestrial planets?

3) Do NEAs of primitive classes contain pre-solar material yet unknown in meteoritic samples?

4) What are the nature and the origin of the organics in primitive asteroids and how can they shed light on the origin of molecules necessary for life?

Answers to these fundamental questions can be provided only by the analysis of the returned sample in terrestrial laboratories (with exceptionally high precision and sensitivity), thereby obtaining measurements that cannot be performed from a robotic spacecraft. The most demanding measurements are those required to date the major events in the history of a sample, plus measurements to determine organic components. Laboratory techniques can determine the time interval between the end of nucleosynthesis and agglomeration, the duration of agglomeration, time of accumulation, crystallization age, the age of major heating and degassing events, the time of metamorphism, the time of aqueous alteration, and the duration of exposure to cosmic radiation.

The *scientific objectives* of the mission are:

A. Characterise the chemical and physical environment in the early solar nebula
B. Define the processes affecting the gas and the dust in the solar nebula
C. Determine the timescales of solar nebula processes

D. Determine the global physical properties of an NEA
E. Determine the physical processes, and their chronology, that shaped the surface structure of the NEA
F. Characterise the chemical processes that shaped the NEA composition (*e.g.* volatiles, water)
G. Link the detailed orbital and laboratory characterisation to meteorites and interplanetary dust particles (IDPs) and provide ground truth for the astronomical database

H. Determine the interstellar grain inventory
I. Determine the stellar environment in which the grains formed
J. Define the interstellar processes that have affected the grains

K. Determine the diversity and complexity of organic species in a primitive asteroid
L. Understand the origin of organic species
M. Provide insight into the role of organics in life formation

NEAs are among the most accessible bodies of the solar system. For several tens of NEAs, the Δv involved to transfer and insert a spacecraft in orbit around them is lower than required for the Moon. Many of them have flexible launch windows and short mission durations (*e.g.* less than 5-6 years for a sample return). A number of possible primitive targets of high scientific interest have been selected covering a wide range of possible launch windows in the time span 2017-2019, *e.g.* 1999 JU3, 1989 UQ, 2001 SG286 and 2001 SK162. A very operationally and technically efficient mission has been found for 1999 JU3 which was selected as the baseline target for the mission profile described in this document. In order to assess the feasibility of such a mission, ESA financed three different industrial studies. The baseline mission scenario, common to all three studies, is as follows:

A single primary spacecraft, carrying the Earth re-entry capsule (ERC), will be launched by a Soyuz-Fregat 2-1b rocket from Kourou on a direct escape trajectory to 1999 JU3. The launch will be in November/December 2018 with a backup in November/December 2019. From this moment on, both baseline and backup missions are identical, with an arrival at the NEA in February 2022. All manoeuvres are carried out via a chemical propulsion system. The outbound and inbound transfer Δv-budget is lower than 1500 m s^{-1} (incl. margins, dispersions, navigation). The Δv for the asteroid proximity operations is lower than 100 m s^{-1} (incl. margins). This leads to a spacecraft total mass at launch between 1450 and 1557 kg depending on the proposed industry design. The first ~ 6-7 months are dedicated to instrument calibration, far and close orbital science global observations, gravity field determination and hazard mapping above 2 km altitude. A number of potential sampling sites (up to 5) are then characterised at high resolution at a 200 m safe altitude. After a number of sampling rehearsals, the spacecraft, designed to cope with hazards up to 50 cm scale, attempts to sample surface material on the most suitable site (*i.e.* yielding the best compromise between science return and risk-mitigation). Three landing legs enable a safe touchdown. For this particular operation, two solutions are proposed: a landing of a few minutes using hold-down thrust to keep the spacecraft on the surface, or a touch and go of less than 3 seconds using elastic energy in the landing feet to re-ascend.

The sampling tool is based on a rotating corer in the first case which is transferred to the ERC via a separate extended arm. In the second option the sampler, accommodated on the landing feet, is pushed into the soil and transferred via folding of the landing legs. After confirmation that a sample has been collected, it is transferred to the re-entry capsule and sealed. The spacecraft could continue performing orbital science, or wait for departure in a safe position. If the sample collection is not confirmed, the spacecraft could undertake up to two additional sampling attempts. The total stay duration of the spacecraft is in the order of 18 months. The spacecraft departs from the asteroid in July 2023 and returns to Earth in December 2024, both in the baseline and backup scenario. The re-entry capsule is then released and undertakes a high-speed Earth re-entry at v_{entry} ~ 11.9 km s^{-1}. The capsule will be retrieved on the ground in the Woomera Test Range (Australia), a non-habited military area, which is already equipped to receive the Hayabusa capsule in 2010, potentially containing a sample of a non-primitive stony asteroid, and transported safely to the curation facility.

The curation facility must guarantee the preservation of the sample in their pristine condition, avoiding any kind of chemical and physical alteration of materials by the Earth environment. The levels of contamination that the sample is exposed to must be controlled with appropriate tools. A preliminary characterisation of all the principle components will be performed within the facility to provide sufficient information to understand the variation of material types present and to allocate appropriate sub-samples to the scientific community (*e.g.* organic rich material may be prioritised for organic studies, low aqueous alteration for interstellar grain and early solar-system studies, *etc.*). Aliquots of the returned sample or specific fragments will be available world-wide (subject to peer review) for detailed analyses. Initial studies will be divided according to scientific information that can be gained: bulk properties, mineral properties, isotopic composition, age dating, and chemical composition. Modern instruments and analytical tools will be used to study the sample with the highest accuracy attainable so far. However, a fraction (1/3) of the returned sample will be stored in the facility for future generations of scientists and advances in analytical instrumentations.

In order to achieve the scientific goals of the mission a multi-scale approach is proposed with different resolution requirements for global and local characterization as well as context measurements. The scientific payload includes: a high resolution imaging system (Narrow Angle Camera, Wide Angle Camera, Close-Up Camera), spectrometers covering visible, near-infrared and mid-infrared wavelengths, laser altimeter, neutral-particle analyzer and a radio science experiment. Some optional instruments can be added if resources are available. All the proposed instruments are based on already existing technologies or technologies under development.

The Marco Polo mission is modular such that cooperation efforts can be easily envisaged and adapted to the available resources. Various scenarios can be considered, including the Marco Polo mission as a 'mission of opportunity' for ESA and are presented in the appendix. In this Yellow Book, the ESA baseline scenario is presented. Other space agencies are interested in NEA sample return missions, namely JAXA and NASA.

JAXA is in the selection process to define the next space mission programme that includes small body sample return missions. Strong links already exist between European science team members and JSPEC/JAXA colleagues which would facilitate implementing a collaboration.

NASA is in the process of selecting the next New Frontier mission (announcement early 2010). Two NEA sample return mission proposals are under consideration and there is a wide interest both at NASA Headquarters and on the level of scientific teams to consider a possible merge with Marco Polo after NEA sample return mission selection by each agency.

Moreover, discussions with other National Space Agencies (DLR and CNES) are ongoing to investigate the possibility to include a small lander on board.

In addition to addressing the exciting science goals, the Marco Polo mission also involves technologies for which maturation programmes are well underway. It is the ideal platform to:

a. Demonstrate innovative capabilities such as: high-speed Earth re-entry capsule, sample collection, transfer and containment techniques, accurate planetary navigation and landing, as well as sample return operational chain;
b. Prepare the next generation of curation and laboratory facilities for extraterrestrial sample storage and analysis;
c. Pave the way as a pathfinder mission for future sample returns from bodies with high surface gravity.

The public outreach possibilities of Marco Polo are considerable because of the enormous fascination of the general public for asteroids in general and challenges such as landing a spacecraft on a planetary body, taking close-up pictures as well as bringing a sample back from this alien world. Moreover, on the strategic and political front there is considerable interest in prediction and mitigation of an NEA impact.

2   Scientific objectives

2.1   Scientific overview

Small bodies of the solar system are believed to be the remnants - either fragments or "survivors"- of the swarm of planetesimals from which the planets were formed. In contrast to the planets, which have experienced major alteration during their history, most asteroids and (dormant) comets, due to their small sizes, are believed to have retained a record of the original composition of our solar system's proto-planetary disk. Abundant within the inner solar system, small bodies may have been the principal contributors of the water and organic material essential to create life on Earth (Figure 3). Thus, small bodies can be considered to be equivalent to DNA for unravelling our solar system's history, offering us a unique window to investigate both the formation of planets and the origin of life. Moreover, in the current epoch, these small bodies also represent both a potentially rich resource for future space exploration and a threat to the very existence of humankind on Earth.

Near-Earth asteroids (NEAs) are a continuously replenished population of small bodies with orbits that come close to the Earth's orbit. Their median lifetime is 10 Myr (Gladman et al. 2000). Most of them end up in a Sun-grazing state, or are ejected from the solar system, while about 10-15 % collide with a terrestrial planet, in particular the Earth or Venus. Objects in near-Earth space are a precious source of information as they represent a mixture of the different populations of small bodies, *i.e.* main-belt asteroids and cometary nuclei, and a link with meteorites (Morbidelli et al. 2002, Binzel et al. 2004, DeMeo and Binzel 2008). They have the orbital advantage of being much more accessible for scientific research and space missions than small bodies in other more distant populations (comets and main-belt asteroids). Moreover, an NEA offers the particular advantage of being directly related to a specifically known birth region, which from dynamical studies, places most between Mars and Jupiter (Bottke et al. 2002).
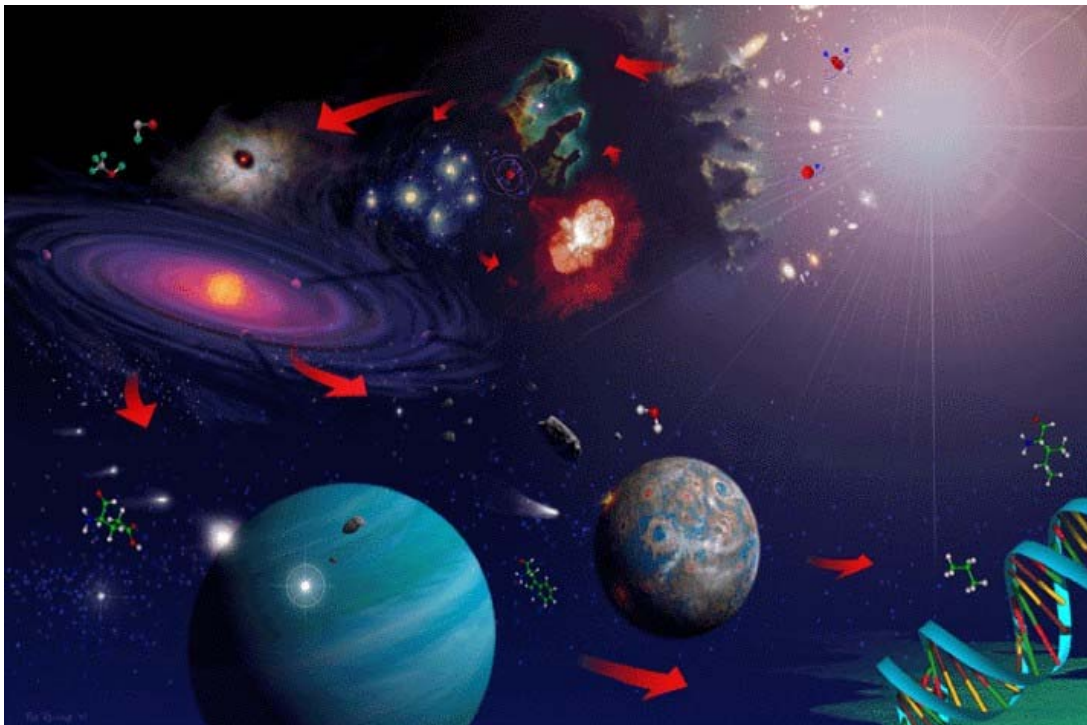
Figure 3: The 15-billion-year-long chain of events from the birth of the universe at the Big Bang, through the formation of chemical elements, galaxies, stars, planets, asteroids and comets, through the mixing of chemicals and energy that cradles life on Earth, to the earliest self-replicating organisms — and the profusion of life (courtesy NASA/JPL-Caltech).

A space mission to an NEA thus provides major opportunities for advancement in our understanding of some of the fundamental issues on the origin and early evolution of the solar system. NEA missions enable an entirely new approach for investigating the primordial cosmochemistry of the solar protoplanetary disk and the formation and properties of the building blocks of terrestrial planets. Moreover, considering the threat represented by those NEAs classified as potentially hazardous objects, knowledge of the physical properties of NEAs (composition and internal structure) is the first essential step towards developing efficient methods to deflect an object whose trajectory leads to a possible collision with the Earth.

The NEA population presents a high degree of diversity as revealed by ground-based observations. More than 10 major spectral classes have been identified (Barucci et al. 1987, Bus and Binzel 2002a, b). These classes group objects with similar spectral properties, suggesting similar surface composition, and probably similar evolution. The most intriguing objects, which represent the highest priority for NEA missions, are those having the most primitive compositions with the most direct link to the chemistry and conditions of the early solar system. Typically, such compositions are found among NEAs having low albedos in the "C" and "D" asteroid classes which are widely believed to have preserved materials that witnessed the condensation of the early phases of the formation of the solar system. These may also contain pre-solar grains[2] that retain information on the interstellar medium (ISM) and even their genesis in evolved stars.

Therefore, a mission to a primitive NEA (dark C, D, and similar spectral classes) will provide crucial elements to answer the following fundamental questions, later called *science goals* (see also Figure 9):

   1) What were the processes occurring in the early solar system and accompanying planet formation?

   2) What are the physical properties and evolution of the building blocks of terrestrial planets?

   3) Do NEAs of primitive classes contain pre-solar material yet unknown in meteoritic samples?

   4) What are the nature and the origin of the organics in primitive asteroids and how can they shed light on the origin of molecules necessary for life?

Answers to these fundamental questions can only be derived by use of laboratory instrumentation, and therefore Marco Polo will return a sample from a low-albedo, primitive NEA. Only one low-albedo asteroid, namely (243) Mathilde, has been observed by spacecraft to date (Yeomans et al. 1997) and only during a brief fly-by and with limited instrumentation. Marco Polo will thus return fundamental and exciting science, within a mission that will excite the public during all phases, in particular during the in-situ observations and laboratory-based investigation of the returned material. Orbital observations will provide a characterization of the target necessary for sample selection and for relating laboratory samples to the asteroid population as a whole. Marco Polo will return a sample providing new information on organic-rich solar-system materials and the formation of habitable planets. It will also improve our knowledge of a potentially threatening object, which is a necessary step to future hazard mitigation.
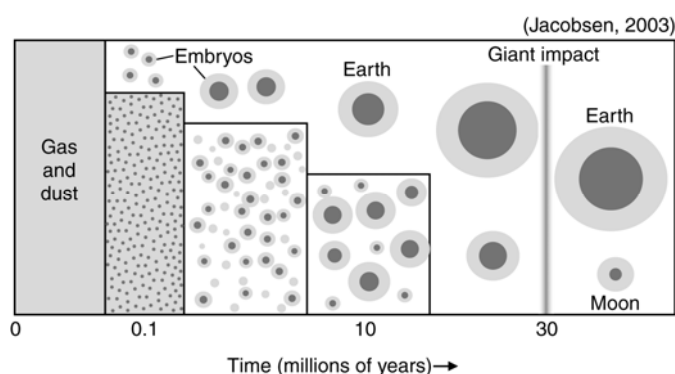
Figure 4: In the primordial solar nebula dust and ices condensed to form planetary embryos that accumulated to larger protoplanets eventually forming bodies of the sizes of the terrestrial planets (after Jacobsen, 2003).

---

[2] A 'grain' contains one single mineral crystal, c.f. a 'particle' is composed of several or many grains.

2.1.1   Fundamental science goals of Marco Polo

What were the processes occurring in the early solar system and accompanying planet formation?

The solar system formed from a disk of gas and dust orbiting around the Sun. These dust grains then collided with each other, growing into larger objects named "planetesimals", which eventually reached a size of tens to a thousand kilometres, although some key aspects of this process are not fully understood. Details of the formation of the principal components formed in the solar protoplanetary disk, and the timing of these events relative to the formation of different asteroidal bodies, is beginning to emerge (Figure 4).

From meteoritic studies it would appear that the formation of the solar system, from collapsing nebula to planetary embryos, was a rapid process, lasting just a few million years. The chronology of these events is still poorly understood. Subsequently, once the first planetesimals were formed, a *runaway growth* occurred, in which the largest planetesimals started to accrete mass from the smaller objects, growing bigger and increasing the relative mass difference with the remaining objects. Thus, the planetesimals represent the building blocks of the planets, and in this respect their analysis is expected to bring us crucial information on the nature of the protoplanetary disk.
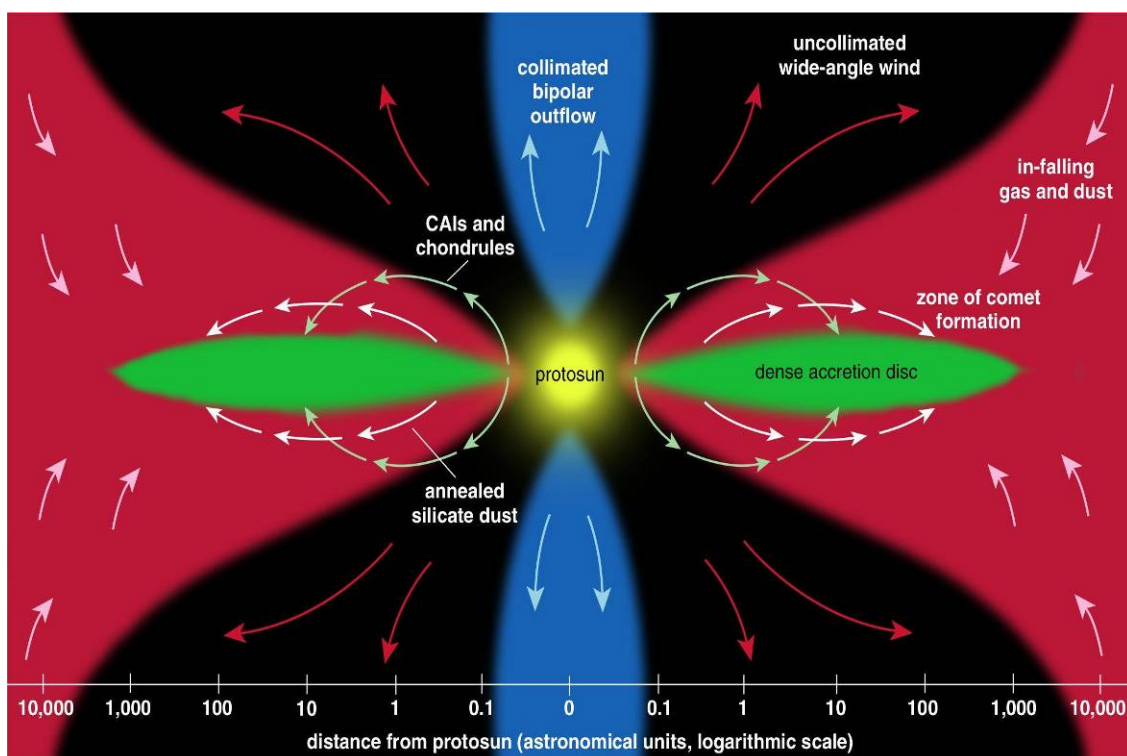
Figure 5: A schematic diagram of the solar nebula as it was still accreting dust. Planets have not yet formed. Materials heated near the Sun circulate to the outer solar system (from Nuth 2001).

Primitive objects include material made and/or modified by stellar outflows, the ISM, and the solar protoplanetary disk (Figure 5), as well as by parent-body processing. Because large-scale mixing was a major phenomenon in the early solar system, they include materials formed in different regions of the solar nebula and at different times under very different physico-chemical conditions. The isotopic composition of various elements, the nature of the organics and the mineralogy of the rocky elements in early solar system bodies are requisite data to obtain information on the great variety of processes that took place during solar-system history. Marco Polo, by returning primitive material from a small body and knowing the geological context it was residing in, offers the possibility of distinguishing between effects of solar-nebula processing and effects of alteration from asteroidal parent-body processing.

Primitive material also permits determination of the abundance of a number of short-lived radionuclides present at the time of formation of a variety of early solar-nebula components – essentially free from the concerns of partial re-setting or secondary process effects – offering a clear insight into the timing of the formation of these components and determining whether they have a local (*e.g.* irradiation and ejection by X-

wind[3]) or remote (*e.g.* stellar nucleosynthesis) origin. The abundance of the various short-lived nuclides provides an important constraint on possible triggering mechanisms for the collapse of the proto-solar molecular cloud.

What are the physical properties and evolution of the building blocks of terrestrial planets?

The current physical and chemical properties of an asteroid have been shaped by its evolution since the condensation and agglomeration that formed its parent planetesimal in the asteroid belt. This evolution includes some or all of: thermal metamorphism, aqueous alteration, collisional disruption, re-accumulation, regolith processing and space weathering. For primitive asteroids, the effects of these processes are expected to be minor, or even minimal, and will not obliterate the record of early nebular conditions at formation. The sample of mixed NEA regolith returned by Marco Polo will likely contain components displaying varying degrees of asteroidal processing that must be accounted for to permit study of the earliest stages of solar-system formation, but will also allow detailed investigation of the evolution of the solar system from its formation to the present day.

The evolution of asteroids can be divided into two stages. The first state is characterised by high impact rates within the first ~100 Myr, heating by short-lived radionuclides, and dynamical evolution of the main belt. Two detailed scenarios are currently discussed. The first one sees a peak in the impact rate about 3.9 Gy after the formation of the solar system, called the Late Heavy Bombardment coinciding with planetary migration and the formation of lunar basins (Gomes et al. 2005). Alternatively, the initial heavy bombardment decayed continuously (Hartmann et al. 2007). In the second stage, after 3.9 Gy, evolution has been less extreme with a lower frequency of collisions (Bottke et al. 2005).

Thermal heating of asteroids, as documented in meteorite analyses, reveals extended periods of heating resulting in considerable modification and even obliteration of the accreted primitive material. Temperatures to >800 ˚C in the ordinary chondrites (see Figure 6), or even higher temperatures in the achondrites result in the re-crystallisation or melting of minerals, loss of volatiles, including water and organics. While potentially of interest in terms of heat sources and planetesimal differentiation these effects are incompatible with the principle objectives of Marco Polo. However, these changes result in a residue with higher albedo and different spectral features and therefore we can be confident that the low-albedo target asteroid of Marco Polo will not have suffered such processes.

Aqueous alteration is a low-temperature chemical alteration of compounds by liquid water which acts as a solvent and produces secondary minerals such as phyllosilicates, sulphates, oxides, carbonates, and hydroxides and plays a major role in the modification and synthesis of organics. Several transfer transitions are only possible in the presence of liquid water on the surface of the object. Related spectral features, found for several meteorites and low-albedo main-belt and outer-belt asteroids, indicate that liquid water was present on their surface during some previous epoch.

About 60 % of the C-class asteroids, at heliocentric distances between 2.5 and 3.5 AU, are thought to have undergone some kind of aqueous alteration process (Barucci et al. 1998). While D-class bodies have no clear relation with any kind of meteorites (with the tentative exception of Tagish Lake), C-classes appear to be related to carbonaceous chondrite meteorites, which are the best preserved witnesses of the early phases of the solar-system formation on the Earth. The sample of mixed regolith returned from an NEA by Marco Polo will likely contain a number of components sampling regions of the parent asteroid with different geological histories. It will thus offer a unique opportunity to follow the effects of progressive aqueous alteration on the mineralogy and organic inventory of a suite of rocks, where we can be confident that the starting materials had homogeneous properties.

It remains unclear from where the water for the Earth's oceans came. Models of the early solar system indicate that accretion at 1 AU and the energy released during this process would have led to a body poor in water. Comets are a major available source of water in the solar system, but the D/H ratio of water measured in a number of comets is much higher (by a factor of 2-3) than that of the Earth's oceans (Dauphas et al. 2000 and Robert 2006; new results for 8P/Tuttle by Villanueva et al. 2009).

---

[3] The X-wind is a fast stream of material ejected from the inner regions of the proto-solar nebula.
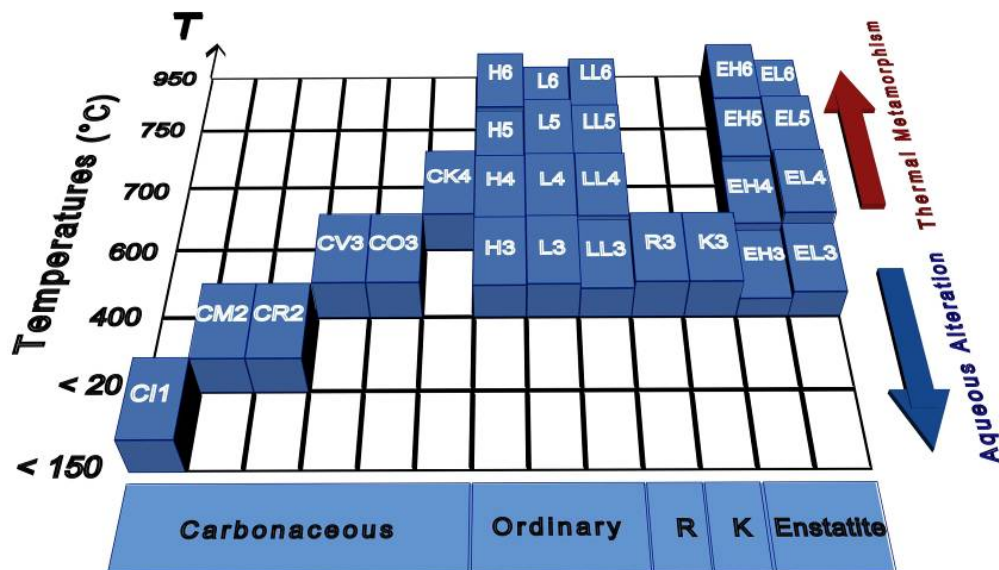
Figure 6: The chondrite classification as a function of the estimated temperature required for producing the petrographic types. Arrows on the right indicate the degree of aqueous alteration or thermal metamorphism. This highlights the fact that most meteorites have experienced extensive aqueous alteration or significant levels of thermal metamorphism (Dotto et al. 2005).

The D/H ratio of carbonaceous chondrites appears to be much closer to that of the oceans – and therefore primitive asteroids originally from the main belt may be considered as the potential delivery mechanism for the abundance of water now present on the Earth that is so essential for all life. A sample of a primitive NEA will provide further insight to the abundance and isotopic signatures of water originally accreted at 3-5 AU.

All but the largest asteroids (diameter > ~100 km) are part of a collisionally evolved population (see Figure 7). The bulk density (porosity), shape (*e.g.* ellipsoidal to highly elongated), rotation rate and morphology (grooves, crater shapes and abundance, crater chains, slope variation) provide clues about the internal structure. This could range from monolithic objects (mostly sizes ~ tens of m), through fractured or shattered objects or contact binaries, to true "rubble piles" of re-accumulated fragments with porosities up to 40 % (Richardson et al. 2002).

Space weathering, the physical and chemical alteration of materials exposed to the space environment, starts to affect the surface layers of NEAs as soon as they are exposed by collisional disruption or subsequent surface movements. The effects are most apparent on the extreme surfaces of grains (solar radiation and particle flux) but can significantly affect the light-scattering properties. Dating of disruption or resurfacing events is possible via sample analysis (exposure ages from more deeply penetrating cosmic rays) or asteroid imaging (cratering rates).

The returned sample from the asteroid which has undergone negligible thermal alteration will allow us to study the chemical evolution of material from the formation of planetesimals (the building blocks of the terrestrial planets) to their current state in NEAs. In-situ observations of the known source object will provide the large-scale properties as well as surface and regolith features and their variation across the whole body that define the physical evolution of the NEA and place the collected sample in context.

Do NEAs of primitive classes contain pre-solar material yet unknown in meteoritic samples?

Primitive material is expected to contain abundant pre-solar grains, in particular silicates, and offers the best opportunities for obtaining pristine grains.

One of the major achievements in meteoritics over the past 20 years has been in the isolation and detailed analyses of a wide range of different pre-solar grains found in primitive meteorites. They have offered insight which was previously undreamed of into specific nucleosynthetic processes and the thermo-physical conditions of the accompanying circumstellar shells associated with a wide variety of nucleosynthetic processes. The latest and potentially the most important group of grains identified in meteoritic material is the one composed of interstellar silicates. Within meteorites these silicate grains are only found in specific areas of matrix composed of very fine-grained anhydrous phases. To date very few have been found where

aqueous alteration has been prevalent. This highlights the susceptibility of these grains to processes occurring on the parent asteroids – particularly the effects of water. Similarly, the abundance of other, rarer pre-solar grains such as nanodiamonds, SiC and graphite all show marked decreases in abundance with increasing metamorphism and/or aqueous alteration (Huss *et al.* 2003). Marco Polo will offer the opportunity to investigate the abundance of such grains accreted to the parent body and to search for new, less robust grains which have not survived the meteorite formation processes.
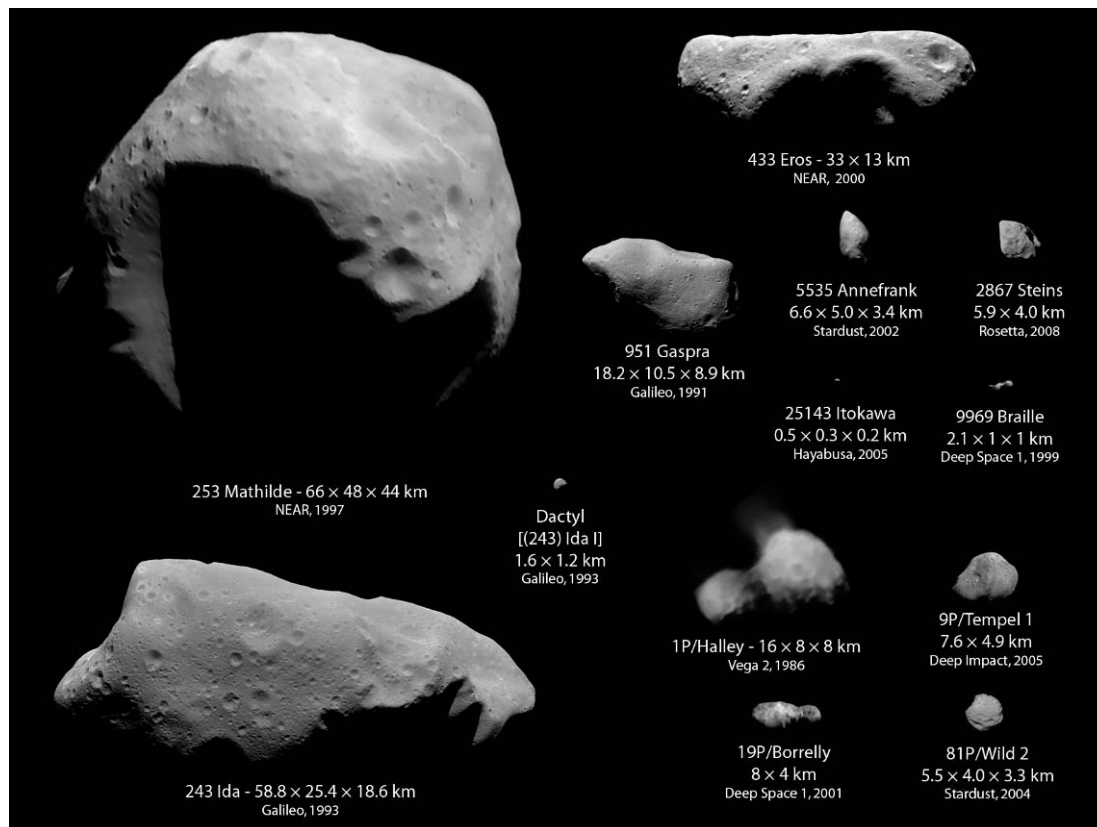
Figure 7: Images of all small bodies (asteroids and comets) visited so far by a space mission at relative scales, showing the great diversity in size, shape and surface characteristics.

An area of meteorite interstellar grain research that is starting to open up with a range of analytical tools capable of generating samples and performing complex measurements on much less than micron-scale features is the study of mantles and reaction rims around the grains (*e.g.* Bernatowicz et al. 2003, Lyon et al. 2007). Such features should record a wealth of information about the environments and processes the grains experienced since their formation – offering insight into the ISM and early nebula. However, by their very nature these rims or mantles are likely to be particularly susceptible to modification or destruction during meteorite formation on the parent body. Once again, primitive material collected from the surface of an NEA offers the best opportunities for obtaining pristine grains.

What are the nature and the origin of organics in primitive NEAs and how can asteroids shed light on the origin of molecules necessary for life?

Current exobiological scenarios for the origin of life invoke an exogenous delivery of organic matter to the early Earth. It has been proposed that carbonaceous chondrite matter (in the form of planetesimals down to cosmic dust) could have imported vast amounts of complex organic molecules capable of triggering the prebiotic synthesis of biochemical compounds (*e.g.* Maurette 2005 and references therein). For example, amino acids are abundant in meteorites and have recently been discovered in returned Stardust samples (Elsila et al. 2009).

The organic compounds found in meteorites display great structural diversity. Figure 8 shows the large number of different aliphatic and aromatic hydrocarbons that can be extracted from one meteorite. Comparable diversity exists for other types of compounds – *e.g.* heterocyclics, polar compounds such as amino acids, carboxylic acids, *etc*. The origin of the organics present in meteorites, particularly for the

dominant form – an insoluble macromolecule – is still debated (*e.g.* Remusat et al. 2006), but clearly involves a complex series of reaction pathways occurring in the ISM, solar nebula and during aqueous alteration on the parent asteroids.
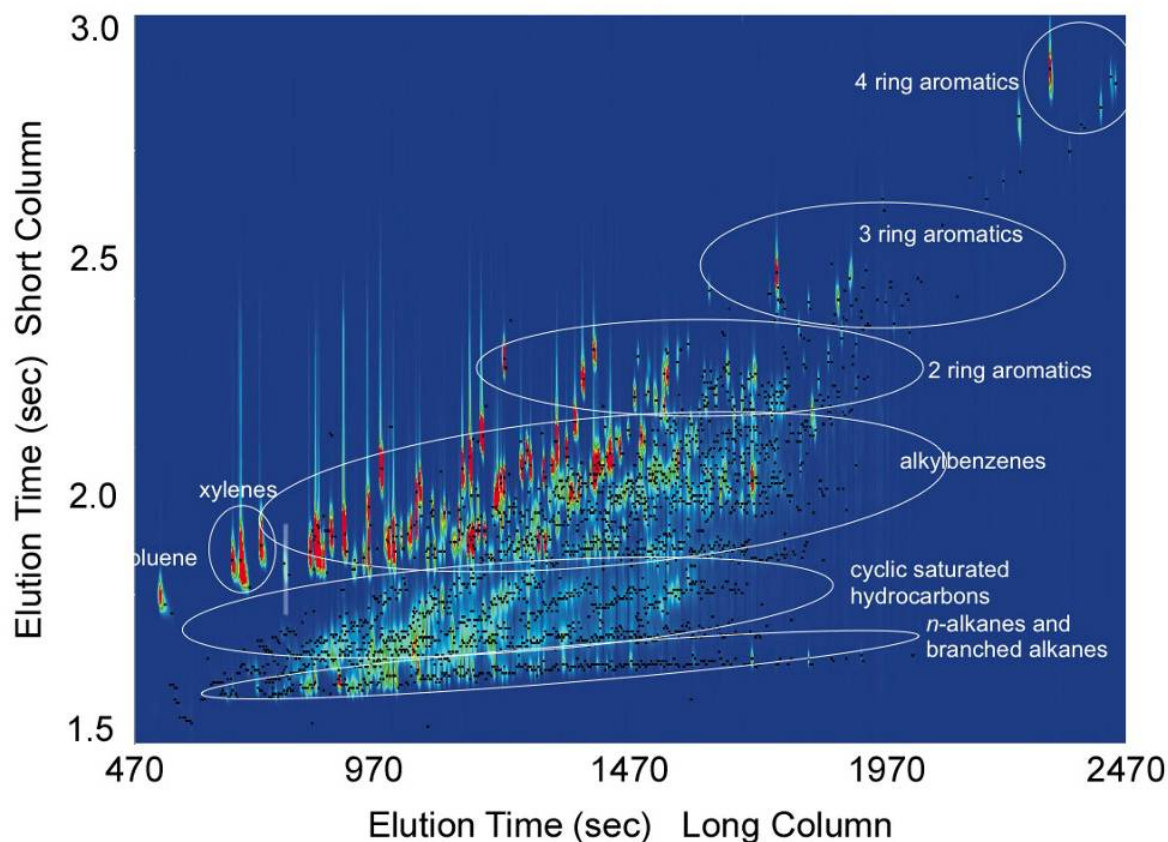
Figure 8: 4D GC-MS chromatogram (elution time from two columns in series along x-axis (long column) and y-axis (short column) of the volatile compounds extracted from the Orgueil meteorite using hydro-pyrolysis. Combining dual-chromatography (GC) and time-of-flight mass spectrometry (MS) permits the different types of compounds identified and more than 1000 individual compounds (individual black dots) to be readily resolved within this complex mixture.

Current investigations of the most primitive organic materials available from samples such as the Stardust cometary samples, interplanetary dust particles (IDPs) and micrometeorites are limited to a few techniques – *i.e.* those offering exceptional spatial resolution or sensitivity, but due to the very small sample size, lacking detailed abundance and isotopic information available from the meteorite samples.

One of the most important observations to date has been the identification of chiral excesses in the soluble fraction of meteoritic organic matter (*e.g.* Pizzarello and Cronin 2000). It was demonstrated that some of the most abundant amino acids display an excess of the left-handed version (L-enantiomer) over the right-handed version (D-enantiomer) of up to 15%, called enantiomeric excess. It has been suggested that the observed preference for left-handedness may be related to the left-handedness of biological molecules in life on Earth, strengthening the possibility that the meteoritic organics played a role in the origin of life on Earth.

Understanding the origin of the amino acids and their distribution in the early solar system will contribute to assessing the likelihood of this scenario, and indeed its applicability to planets or other bodies around other stars. Processes currently considered for the origin of the enantiomeric variations observed include enantio-selective photo-dissociation in the ISM (Bonner 1991) and various synthesis reactions on the parent bodies, including those requiring asymmetric catalysts and precursors (*e.g.* Peltzer and Bada, 1978; Pizzarello et al. 2006; Arteaga et al. 2009).

An even greater analytical challenge is determining the presence and origin of nucleobases in primitive materials. Like amino acids, the nucleobases are fundamental building blocks of life, being integral parts of DNA and RNA. There is evidence that such compounds are present in meteorites (*e.g.* Martins et al. 2008), but their detection and study are hindered by their ubiquitous presence in life on Earth and low abundances in meteorites. Contamination is a major problem, particularly as all nucleobases are involved in terrestrial

life processes. The delivery of rocks, loaded with amino acids, nucleobases, sugar-related compounds, carboxylic acids and other organic materials (*e.g.* carbonaceous chondrites, (CCs)) could have had a major influence in the initial stages of the development of life on Earth. Measurements of such pre-biotic compounds in samples from other worlds will trigger a tremendous discussion on the origin of life and its ubiquity in the universe.

A sample of mixed regolith from a primitive NEA containing a number of components with varying degrees of aqueous alteration (where we can be confident that the starting materials had homogeneous properties) would give definitive answers on the formation processes of carbonaceous matter in interplanetary material. It would help to determine the origin of compounds such as the amino acids – by monitoring how the abundance of the amino acids, and their possible precursor, evolves with the degree of aqueous alteration (as determined by mineralogy). By returning a sample free from terrestrial contamination, any ambiguity created by life on the Earth is eliminated.

In the following, we describe the rationale for a sample return mission to a primitive object.
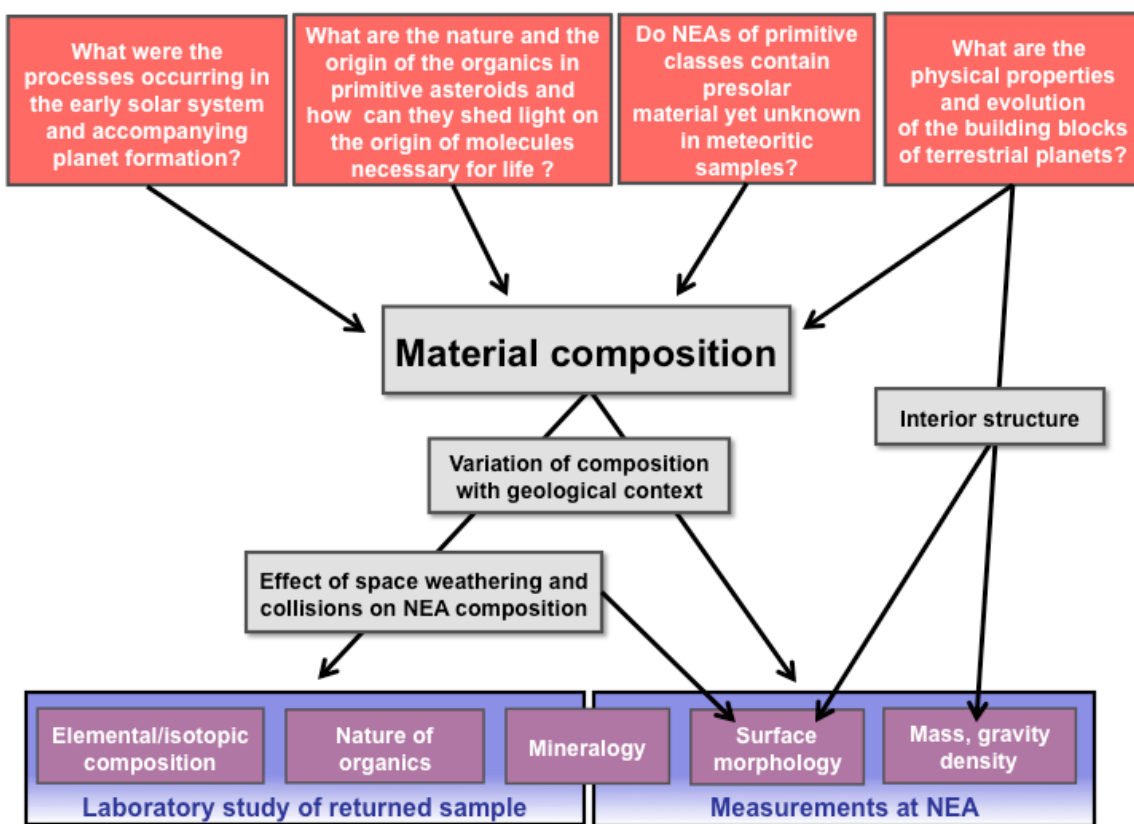
Figure 9: Science goals and objectives of Marco Polo.

2.1.2 Why a sample return?

Many of the science questions we are attempting to resolve stem from detailed knowledge obtained from high-precision and high-sensitivity measurements of meteorites. The anticipated scientific advances, with the new sample from a primitive asteroid, will only be achievable with the level of analytical capability provided by laboratory instruments. The ability of in-situ or remote-sensing instruments to emulate lab-based instruments in providing high-sensitivity, high-precision or high spatial resolution measurements is compromised by constraints due to limitations of size, mass, power, data rate, and reliability imposed by the practical aspects of space missions.

The NASA Stardust mission to comet 81P/Wild 2, a periodic comet captured from the outer solar system on its current orbit only recently, is the first space mission to return solid extraterrestrial samples other than those from the Moon. Several thousand micron-sized dust particles from the coma were trapped during the

fly-by on 2 January 2004, in a collector made of silica aerogel, and returned in a capsule to Earth on 15 January 2006 by direct re-entry. Their analysis highlights the wealth of information that can be achieved from sample return (Brownlee et al. 2006). For instance, the presence of high-temperature minerals (forsterite and calcium aluminium-rich inclusions or CAIs), that formed in the hottest regions of the solar nebula, provided dramatic evidence for extensive radial mixing at early stages of the solar nebula (Brownlee et al. 2006, Zolensky et al. 2006). The organics present in the cometary samples display considerable variability and complexity, even at a very fine scale, indicating multiple formation processes (see Figure 10; *e.g.* Cody et al. 2008, Rotundi et al. 2008).
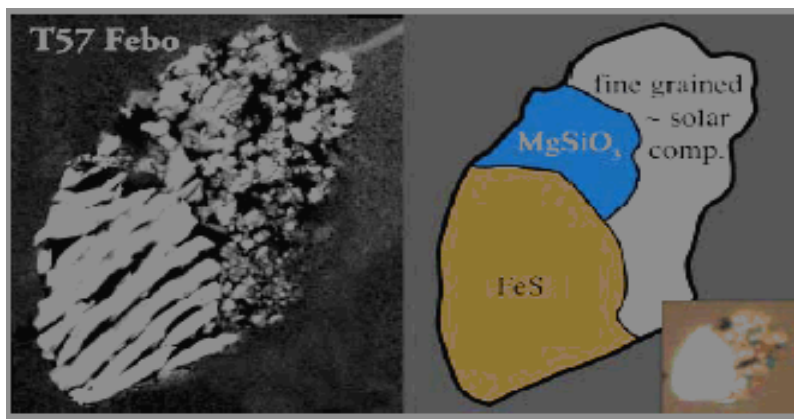
Figure 10: Stardust 8-μm particle from comet 81P/Wild 2. Laboratory analyses show the presence of three major components: sulphide pyrrhotite, enstatite grain and fine-grained porous aggregate material with chondritic composition (Brownlee et al. *2006). Thus, in a single grain, materials which formed in different regions in a protoplanetary disk can co-exist, which was not expected.*

Nevertheless, the samples collected by Stardust are far from ideal when attempting to understand the incredibly complex materials and organic compounds found in primitive materials. Moreover, it is difficult to draw extensive conclusions about many of the contrasts between comet 81P/Wild 2 samples and other primitive bodies because the capture process of the grains has obliterated or greatly modified the more fragile or volatile components of the coma dust. This is particularly important for the organic material (*e.g.* Cody et al. 2008). Very limited evidence exists for volatile-rich silicates (*e.g.* phyllosilicates) which would have a low survival rate during the capture process.

The science questions which Marco Polo addresses require many different types of analyses, providing a framework of understanding about the history of the sample, the parent asteroid, the solar nebula and beyond. Examples of the types of analyses include:

Detection of elemental abundances at the ppm-level or even ppb-level, with a precision of a few percent, of components within the sample are required to provide context between components and with known meteorite groups. Laboratory-based techniques such as mass spectrometry and neutron activation are routinely employed for such measurements. In-situ analyses of the elemental composition from the spacecraft could be performed by APXS – however, typical detection capability limits analyses to elements present at the 0.1 to 1 wt% level (*i.e.* only a handful of elements, and excludes some key element groups such as rare-earth and platinum-group elements). Even more challenging is the need to understand diffusion/exchange processes (*e.g.* gas dust in nebula, aqueous alteration on parent asteroid, *etc.*) operating over <<mm scales which requires analyses to be performed of the order of microns or even less – again readily achieved by techniques in the laboratory such as LA-ICPMS, SIMS, XAFS, EMPA, but generally not possible by in-situ techniques with the required sensitivity or precision.

Isotopic measurements are a key tool in understanding the processes in the solar nebula and parent asteroid. Light-element isotopic measurements (*e.g.* H, C, N, O, S) of primitive materials can be achieved with relatively modest instruments in the laboratory, readily providing the required precision (≈0.1 ‰) and sensitivity (analysis of <mg amounts of sample) to understand the processes under consideration. Space flight instrumentation has been developed to perform similar analyses, but to date the, as yet un-tested, analytical precision has been limited to 10 ‰ (Ptolomy on Rosetta) and 1 ‰ (Gas Analysis Package on Beagle 2) for $^{13}C/^{12}C$ measurements. The $^{17}O/^{16}O$ ratio is much smaller, and is a much more challenging measurement that cannot be performed with any meaningful precision (in the context of solar-system

variations) by space flight instruments. Measurements of other isotopic ratios, such as Mg or Fe, are even more difficult, with extra challenges due to problems of ionisation, even greater precision requirements and high mass resolution to resolve isobaric interferences. Such analyses have only been achieved by large magnetic sector instruments and therefore cannot be considered for spaceflight (lower mass quadrupole or TOF-MS provide insufficient mass resolution or sensitivity, respectively).

One of the major goals of Marco Polo is to provide a detailed understanding of the chronology of early solar-system events, which we know to span only a few million years from the analysis of meteorites. Using mass spectrometry, these are perhaps the most challenging measurements – requiring precise isotopic ratio measurements of trace elements (*e.g.* Pb) of well characterised specific components. These challenges are such that useful geo-chronology measurements have never been attempted by spaceflight instruments (although Beagle2 was to make some ^{40}Ar measurements in conjunction with K measurements by APXS in an attempt to perform K/Ar dating on Mars, albeit with an expected uncertainty of the order of 10^9 years. But the requirements for Marco Polo are approximately 10^3 times greater, *i.e.* $<10^6$ years).

Organic analyses require a wide array of techniques – based on the use of liquid solvents to extract key life-implicated compounds such as amino acids and nucleobases. Detection of such compounds, and those from thermal decompositions could be performed using space flight instruments. Precise isotopic measurements are far more demanding (see above). Investigation of the insoluble macromolecule would require use of NMR (with large super-conducting magnets) and synchrotron radiation, neither of which could ever be envisaged for space flight.

Notwithstanding the technical requirements of individual measurements and the high levels of stability (thermal, vibration, power, *etc.*) that the instruments demand, multiple analyses of the same sub-sample employing a range of techniques are usually necessary in order to unravel the history of each component and to understand the earliest process involved in their formation. In order to achieve high quality measurements, careful sample selection is required along with complex sample preparation – *e.g.* production of very flat, polished surfaces for precise spot elemental and isotopic measurements, irradiation with high neutron fluxes for Ar-Ar and I-Xe dating of asteroidal and early solar-system processes, demineralisation by harsh acids for NMR investigation of macromolecules and concentration of interstellar grains.

It will thus be important to compare the sample returned by Marco Polo from a primitive asteroid, with its geologic context, to the dust sample from comet Wild 2 returned by Stardust, as well as the collections of meteorites, micrometeorites and IDPs, across the full range of compositional and physical properties.

Marco Polo will collect at least 4 orders of magnitude more material than Stardust, permitting more sample-specific selection from the expected complex mixture of asteroid regolith. Most importantly, Marco Polo will be able to collect the sample such that its physical content is not modified during its collection. There will also be a strong control on any possible contamination, particularly by and for the organics.

The study of the Marco Polo sample within the larger context of extraterrestrial primitive materials will greatly advance the understanding of the nature and origins of primitive materials in the solar system.

It is clear that in order to answer the science questions that Marco Polo seeks to address, laboratory analysis of a sample of a primitive asteroid is required. The great added benefit of sample return is that the analyses can be refined to account for unexpected features of the sample, and that material is available to address new scientific questions which may arise or for new techniques that are developed during the long lead times of such a mission.

Why can meteorites in our collections not answer these key science questions?

Approximately 40000 meteorites now exist in collections across the world (including large collections from Antarctica and the hot deserts), although the number of individual falls is much less – reflecting the presence of unidentified shower falls and mechanical break up of single bodies into numerous fragments. However, even after correcting for such effects, we have strong scientific indications that our terrestrial record is biased. Various clues point to an abundance of material that does not survive atmospheric entry. The C-class asteroids account for ≈ 75 % of all main belt asteroids (MBA) – and while largely located in the mid/outer asteroid belt, their nearest meteoritic equivalents, the somewhat friable carbonaceous chondrites (CCs), are present in our meteorite collections at the level of less than 5 %. Although carbonaceous meteorites

belonging to the so-called CM class constitute by far (~35 %) the majority of carbonaceous chondrites, it is possible that they come from one asteroid only (Morbidelli et al. 2006).

Since only the strongest material reaches the Earth, it is not known whether this material is representative of the dominant material in space. For instance, the measured compressive strength of the Murchison meteorite is 50 MPa (Tsuchiyama et al. 2008), which is an order of magnitude higher than the compressive strength of porous materials on the Earth. This could explain the apparent overrepresentation of "ordinary chondrites" in the meteorite collections compared to dominant interplanetary matter as inferred from populations of asteroid classes.

The strength of meteorites is the result of metamorphism and/or aqueous alteration on the parent asteroids – with effects that extend well beyond the mechanical properties of the meteorites as they mobilise elements and isotopic ratios within and between minerals, re-set radio-isotope chronometers, destroy and modify primitive materials, and synthesise and mobilise organic compounds. IDPs display mineralogical, chemical and isotopic signatures, not found in meteorites. This strongly indicates formation and/or residence in the ISM or solar accretion disk. Such primitive material must have been stored somewhere for the past 4.5 x 10^9 years. On a more macroscopic scale, the Tagish Lake meteorite is perhaps the most friable carbonaceous chondrite recovered to date. Recovery of useful amounts of material was only possible as the fall was witnessed and happened over a frozen lake. In some respects it appears to be a particularly primitive meteorite, with high carbon content and unusual organic inventory, It has been linked with the very primitive D-class asteroids (*e.g.* Hiroi et al. 2001), but the high levels of aqueous alteration affecting this meteorite are not consistent with the fact that water features in D-class spectra are rarely observed (*e.g.* Kanno et al. 2003). Moreover, the recent experience of the Sudan meteorite 2008 TC3 emphasises the uncertainty and incompleteness of our understanding. This fall is the first instance where an object was observed astronomically as an asteroid and then was recovered as a meteorite. It was identified as an F-class object, similar to C-class (bluer in the visible), but the meteorite is unexpectedly a ureilite (Jenniskens et al. 2009), a carbon-rich achondrite with a fragile matrix. These rare and unique samples demonstrate that mechanically weak material does exist in significant quantities within the inner solar system and that the existing meteorite collection is significantly biased towards heavily processed material. Nonetheless, we still miss primitive materials that are probably even weaker and would not survive atmospheric entry.

The spectacular falls mentioned above highlight two crucial lessons, in addition to the obvious one that our knowledge from the current meteorite collection is incomplete. First, carbonaceous chondrites preserve material and information from the solar nebula as well as from the pre-solar environment. However, carbonaceous chondrites also underwent thermal and aqueous processing on their parent body. Carbonaceous chondrites, alone among the chondrites, display evidence of little asteroidal processing, but we will never understand such processing of primitive materials unless we return a sample from a primitive asteroid. Clearly, we do not have access to all the information recorded in primitive materials too fragile to be recovered on the Earth.

Unless we return a sample from a primitive asteroid, which is the primary goal of Marco Polo, we will never know what a primitive material is.

2.1.3   Why an NEA?

NEAs are the most accessible targets containing primitive materials for scientific research and space missions. They offer two main advantages: (i) most of them come from the asteroid belt, which makes them representative of the whole asteroid population, and (ii) contrary to more distant MBAs, they are highly accessible targets for spacecraft missions. Starting from the classical definition of "accessibility" of a celestial body in terms of the velocity change (Δv) needed for a rendezvous mission (*e.g.* orbiting around an object), it is possible to show that some NEAs are even easier to get to than the Moon (Perozzi et al. 2001). Although the list of accessible NEAs for space missions already contains many objects, their number is likely to grow dramatically in the near future thanks to current and up-coming observational programmes, such as Pan-STARRs (Jedicke 2008). Moreover, the Warm Spitzer programme has awarded 500 h of the warm Spitzer time to derive albedos and diameters for some 700 NEOs. Amongst them, already 35 NEOs with Dv< 6 km/s and 165 with Dv < 7 km/s have been identified for which albedo and size determination will be derived from Spitzer observations. It is likely that some of these bodies will have a low albedo, making them additional potential targets. The ESA space mission Gaia will enormously improve the accuracy of the characterization for hundreds of thousands of asteroids (Mignard et al. 2007, Dell'Oro and

Cellino 2008). Follow-up observations will identify and characterise the NEAs that constitute the list of the scientifically interesting targets for space missions.

Several thousand objects in near-Earth space are currently known. According to model estimations, the whole near-Earth population contains somewhat more than 1000 objects with diameter larger than 1 km and hundreds of thousands greater than 100 m (Morbidelli et al. 2002, Stuart and Binzel 2004).

2.1.3.1 *Link to the main asteroid population*

The near-Earth population includes both asteroids and comet nuclei in orbits with perihelion distances $q < 1.3$ AU. Thus, they periodically approach or intersect the Earth's orbit. The median lifetime of the population is about 10 Myr (Gladman et al. 2000) although the number of objects is believed to be constant on average. Indeed, the chronology of craters on the Moon up to 3.8 Gyr, which has been calibrated by crater counting and dating the surface samples brought back by the Apollo missions, indicates that the flux of impactors was approximately constant during the last 3.8 Gyr, with some fluctuations due to stochastic events. Therefore, the near-Earth population must be continuously replenished from small body reservoirs. Numerical studies have determined that most of these reservoirs are located in the inner solar system (Mars crossing zone and main belt; Michel et al. 2000, Bottke et al. 2002) with a small component coming from the Jupiter Family Comets. The near-Earth population is therefore representative of asteroids and comets, both considered as the remnants of the primitive leftover building blocks (planetesimals) of solar-system formation processes.

Numerical analysis of the orbital histories of thousands of particles from each reservoir has allowed, as a by-product, the estimation of the most likely reservoir of a real object before its transport to its current orbital position. Thus, it is possible to estimate the relative probability that a body with known semimajor axis, eccentricity and inclination of its orbit in near-Earth space comes from a particular reservoir. For instance, Michel and Yoshikawa (2006) have shown that the asteroid Itokawa, the target of the Hayabusa mission, most likely comes from the inner part of the main belt. Thus, this tool provides a powerful means to relate the target from which a sample will be taken to its most likely source region in the solar system.

Our knowledge of the structure and composition of the near-Earth population is still rather poor, since only a few percent of the known near-Earth objects have diagnostic spectral or photometric observations. The most striking characteristic is the high degree of diversity in terms of physical properties. The population's diversity is also emphasised by the fact that all the taxonomic classes known from MBAs are present.

2.1.3.2 *Impact Hazard*

The study of the physical nature of NEAs is relevant to the assessment of the potential hazard imposed by NEA impacts on our planet. NEAs are responsible for most meteorite falls and for the occasional occurrence of major catastrophic impact events. Figure 11 shows the position of all known minor bodies in the inner solar system with respect to the planet orbits on 09 Nov 2009, demonstrating their nearness to Earth. Whatever the scenario, it is clear that the technology needed to set up a realistic mitigation strategy depends upon knowledge of the physical properties of the impacting body. For example, deflecting a body using a kinetic impactor depends on the response of the body to the impact, which in turn depends on the body's physical properties. Using the concept of a gravitational tractor (Lu and Love 2005) for mitigation against an NEA impact also requires precise determination of the mass, shape and rotation state of the object.

The return of a surface sample from an NEA by the Marco Polo mission and its subsequent laboratory analysis will not only help to answer questions related to planetary formation, but will also provide for the first time a good knowledge of the material properties of a potential impactor. Up to now, because of the lack of constraining measurements, numerical codes applied for simulating asteroid impacts and deflections as a mitigation strategy have used properties of terrestrial materials to model an asteroid, and they would greatly benefit from the measurements of some properties of a real asteroid sample taken in-situ. Better knowledge of the physical properties of a whole object and its material properties would then allow a better optimization of mitigation strategies, and Marco Polo can provide a significant contribution to this objective.
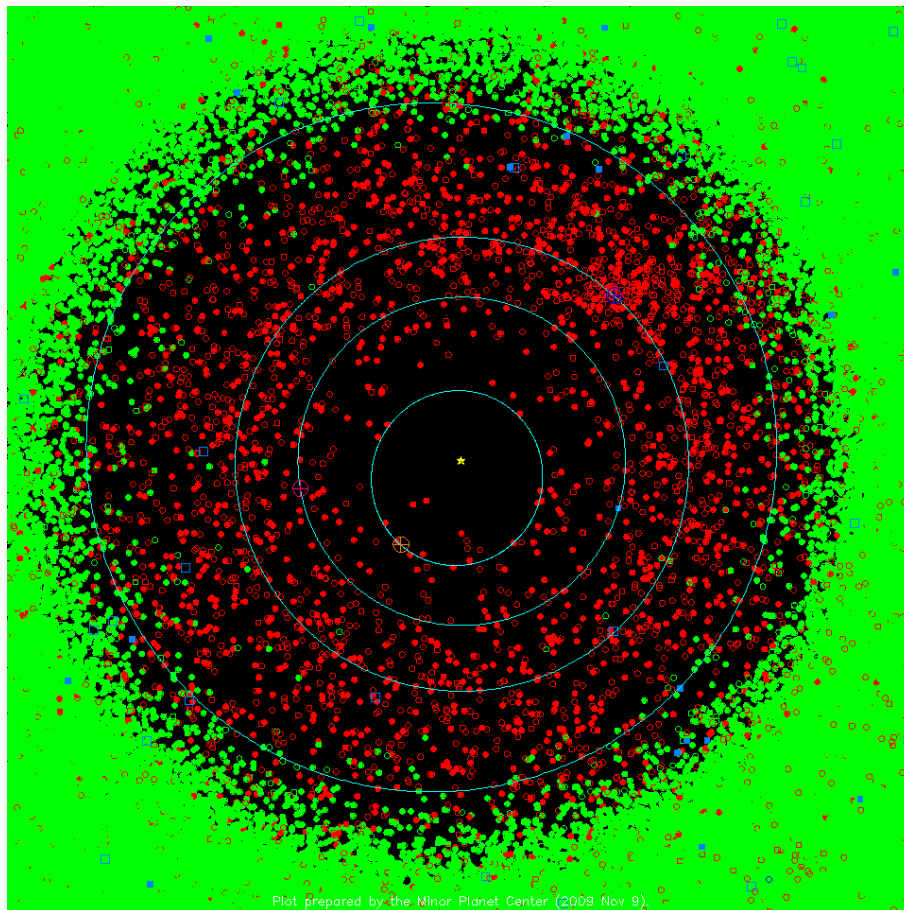
Figure 11: A plot of the inner solar system as of 09 Nov 2009. The orbits of the inner planets Mercury, Venus, Earth, and Mars are shown as circles. The dots indicate the current location of the minor planets. Objects with perihelia within 1.3 AU (NEAs) are shown by red dots (http://www.cfa.harvard.edu/iau/lists/InnerPlot.html).

2.1.4   The missing links

Considerable effort has been made linking reflectance spectra obtained from asteroids with those of meteorites. Good matches have been achieved for highly evolved (melted) bodies (*e.g.* 4 Vesta and the basaltic achondrites), but become increasingly more tenuous with decreasing albedo (increasing organic content) and other characteristics of more primitive mineralogy. For instance, spectra of the E-class asteroid (2867) Steins obtained by the ESA space probe Rosetta do not match any existing reflectance spectra of meteorites (Keller et al. 2009). However, from spectral observations of asteroid 2008 TC3 and the analysis of fragments recovered on Earth, we now have evidence that there is a discrepancy between the expected composition of a small body based solely on its spectral properties and the actual one from recovered fragments (Jenniskens et al. 2009).

Because of their spectral similarity in the visible and near-infrared regions, C-class asteroids have always been associated with CI and CM meteorites especially due to their matching weak absorption features in the shortest wavelength regions. However, the interpretation of the continuum of reflectance or thermal emissivity of an asteroid surface is difficult and not unique, since asteroid surfaces are composed of mixtures of minerals whose spectral properties are non-linearly combined.

A significant complication comes from space weathering (from solar wind irradiation and impact processing) which can alter the surface properties of airless bodies. The effects of space weathering are very difficult to simulate in the laboratory, but have been studied in great detail using returned lunar samples. However, the the space environment at the lunar surface is quite different from that of asteroids.

Interpretation of all remote observation data will be greatly enhanced by "ground truth" analysis. Laboratory reflectance spectra of individual components from a returned sample of a primitive NEA can be compared with telescope spectra. The level of space weathering each component has experienced can also be determined mineralogically and geochemically (*e.g.* noble gas studies), by comparison with the mineralogy

and chemistry of known meteorite types. Only on the basis of Marco Polo sample analysis will it be possible to apply the knowledge obtained from meteorites to the vast amount of information available from asteroid observations.

2.2   Scientific objectives and related measurements

From the top level *scientific goals* as given in the previous Section the following more detailed *scientific objectives* were derived:

> A. Characterise the chemical and physical environment in the early solar nebula
> B. Define the processes affecting the gas and the dust in the solar nebula
> C. Determine the timescales of solar nebula processes
>
> D. Determine the global physical properties of an NEA
> E. Determine the physical processes, and their chronology, that shaped the surface structure of the NEA
> F. Characterise the chemical processes that shaped the NEA composition (*e.g.* volatiles, water)
> G. Link the detailed orbital and laboratory characterisation to meteorites and interplanetary dust particles (IDPs) and provide ground truth for the astronomical database
>
> H. Determine the interstellar grain inventory
> I. Determine the stellar environment in which the grains formed
> J. Define the interstellar processes that have affected the grains
>
> K. Determine the diversity and complexity of organic species in a primitive asteroid
> L. Understand the origin of organic species
> M. Provide insight into the role of organics in life formation

In the following, we outline the sample analysis that will be performed in the laboratory and the measurements that will be performed at the NEA in order to address these objectives. The global characterization of the NEA is crucial to understand the geological and global context of the sample.

2.2.1   Sample analysis in the laboratory

Marco Polo will allow us to analyze the sample of a primitive NEA in terrestrial laboratories, thereby obtaining measurements that cannot yet be performed from a robotic spacecraft (*e.g.* dating the major events in the history of a sample: laboratory techniques can determine the time interval between the end of nucleosynthesis and agglomeration, the duration of agglomeration, time of accumulation, crystallization age, the age of major heating and degassing events, the time of metamorphism, the time of aqueous alteration, and the duration of exposure to cosmic radiation).

The key scientific questions to be addressed by this mission, primarily through the sample analysis programme on the returned sample are given at the beginning of this section. Breaking The relation of these aspects to the science goals as outlined in the previous section and the required measurements are listed in Table 1.

There is a vast array of analytical tools for the characterization of returned materials encompassing many techniques spanning the principal approaches of microscopy and spectroscopy/spectrometry. These are shown in Table 2, together with an estimate of the required mass for a given measurement. For each science area, the range for the minimum amounts of consumed material is shown in column 'single analysis mass'. However, the actual amount of material required for each analysis is much greater, as given in the column 'required mass'. In many cases, this is because very specific phases are required, from specific components with known histories or relationships to other components (*e.g.* chronology measurements) and multiple analyses of different components are required to develop an understanding of a process, *e.g.* thermal history or space weathering. Such phases may be present at very low abundances (as low as ppm levels). Some of the instruments demand very precise sample preparation – usually very flat surfaces (*e.g.* SIMS and EMPA) and this usually necessitates the preparation of mounts or slices, with the added benefit of providing contextual information for any given grain.

Table 1: Science goals, objectives and related measurements; and the method to perform the measurement.

Science Goals	Science Objectives	Measurements	Method
1. What were the processes occurring in the early solar system and accompanying planet formation?	A. Characterise the chemical and physical environment in the early solar nebula B. Define the processes affecting the gas and the dust in the solar nebula C. Determine the timescales of solar nebula processes	Bulk chemistry Mineralogy, petrology Isotopic chemistry in inclusions (*e.g.*, chondrules or CAIs), matrix; pre-solar grains and volatiles, water	Sample analysis
2. What are the physical properties and evolution of the building blocks of terrestrial planets?	D. Determine the global physical properties of an NEA E. Determine the physical processes, and their chronology, that shaped the surface structure of the NEA F. Characterise the chemical processes that shaped the NEA composition (*e.g.* volatiles, water) G. Link the detailed orbital and laboratory characterisation to meteorites and interplanetary dust particles (IDPs) and provide ground truth for the astronomical database	Volume, shape, mass Surface morphology and geology Mineralogy, petrology Isotope geochemistry & chronology Weathering effects Thermal properties	Imaging and laser altimetry Visible and Near-IR Imaging-spectrometry Sample analysis Neutral particle analysis Mid-IR spectrometry
3. Do NEAs of primitive classes contain pre-solar material yet unknown in meteoritic samples?	H. Determine the interstellar grain inventory I. Determine the stellar environment in which the grains formed J. Define the interstellar processes that have affected the grains	Bulk chemistry Grain mineralogy and composition Isotope chemistry of grains	Sample analysis
4. What are the nature and origin of organics in primitive asteroids and how can they shed light on the origin of molecules necessary for life?	K. Determine the diversity and complexity of organic species in a primitive asteroid L. Understand the origin of organic species M. Provide insight into the role of organics in life formation	Abundances and distribution of insoluble organic species Soluble organics Global surface distribution and identification of organics	Sample analysis Visible and Near-IR Imaging-spectrometry

Other sample preparation techniques (particularly for organics) require extracting specific components from a large sample, in either a relatively non-destructive manner (e.g. solvent extraction for CS-GS-MS analyses) or in a highly destructive manner (*e.g.* demineralisation for NMR analyses). Finally, considerable variability in the abundance of specific components, phases or elements is expect in a mixed regolith sample and therefore the requirements from fragment to fragment could readily change by one to two orders of magnitude for some analyses.

The requested mass has been derived in such a way as to guarantee the scientific success of the mission. Different aspects have been taken into account to evaluate the returned mass, specifically: the probability that an amount of each sample component sufficient for analysis was estimated; a statistical analysis of the returned sample has to be done in the laboratory (*e.g.* at least three different measurements in three different

Table 2: Scientific information obtained analysing various types of materials expected in the returned sample and sample requirements to achieve the scientific results.

Component	Scientific aspects			Measurement requirements			
	Goal	Objective	Theme	Measurement type	Techniques	Required mass	Single analysis mass
Chondrules, refractory inclusions, matrix	1	C	Age	Isotopic abundances	SIMS, LA-ICPMS, MC-ICPMS, TIMS	Gram	10s pg (SIMS) to 10s mgs (TIMS) per analyses
	1	B	Disk dynamics	Mineralogy & mineral chemistry	EMPA, SEM, TEM, XRS, FTIR, Raman, SIMS, LA-ICPMS	Gram	ng (EMPA) to µgs (LA-ICPMS) per analysis
	1	A	Volatility fractionation	Elemental and isotopic abundances	SIMS, LA-ICPMS, GS-MS, NG-MS	100s mgs	10s pg (SIMS) to 100s µgs (NG-MS) per analyses
	1	B	Processing	Elemental and isotopic abundances	SIMS, LA-ICPMS, MC-ICPMS, GS-MS, NG-MS	Gram	10s pg (SIMS) to 10s mgs (MC-ICPMS) per analyses
	1	B, C	Thermal history	Mineralogy and mineral chemistry	EMPA, SEM, TEM, XRS, FTIR, Raman, SIMS, LA-ICPMS	Gram	ng (EMPA) to µgs (LA-ICPMS) per analysis
	1	A, B, C	Accretion dynamics	Mineral chemistry	EMPA, SEM, TEM, XRS, FTIR, Raman, LA-ICPMS, SIMS	Gram	ng (EMPA) to µgs (LA-ICPMS) per analysis
	2	L	Interstellar processes	Elemental and isotopic abundances	SIMS, CS-GS-MS, NMR, GC-MS, XANES, STXM, µL^{2}MS	10 grams	10s ag (GC-MS) to gram (NMR) per analyses
Organics	1	A, B	Early solar-system processes	Chemical analyses, elemental and isotopic abundances	SIMS, GS-MS, NMR, Raman, XANES,	Several grams	10s ag (GC-MS) to gram (NMR) per analyses
	3	K, L	Asteroidal processes	Chemical analyses	NMR, Raman, XANES, HPLC, GCMS, µL^{2}MS	100s mgs	10s ag (GC-MS) to gram (NMR) per analyses
	3	K, L, M	Origin of life	Chemical analyses	Laser GSMS, NMR, Raman, XANES, HPLC, GCMS, µL^{2}MS	Several grams	10s ag (GC-MS) to gram (NMR) per analyses
	3, 4	D, L	Collisional history	Mineral composition	EMPA, SEM, TEM, XRS, FTIR, Raman	100s mgs	10s pg (Raman) to ngs (EMPA) per analyses
Lithologies & breccias	4	F	Aqueous alteration	Mineralogy	EMPA, SEM, TEM, XRS, FTIR, Raman, GS-MS, SIMS	Several grams	10s ag (GC-MS) to 100s µgs (GS-MS) per analyses
	4	D	Shock processes	Mineralogy	EMPA, SEM, TEM, XRS, FTIR, Raman	Several grams	10s pg (Raman) to ngs (EMPA) per analyses
	4	F, L	Thermal alteration	Mineralogy	EMPA, SEM, TEM, XRS, FTIR, Raman, SIMS, GS-MS	Several grams	10s ag (GC-MS) to 100s µgs (GS-MS) per analyses
	4	F, G, L	Space weathering	Mineralogy	EMPA, SEM, TEM, XRS, FTIR, Raman, Opt. spectro., ESR, NG-MS, SIMS, GS-MS, susceptometer	Gram	10s pg (SIMS) to mgs (susceptometer) per analyses
	4	D	Physical properties	Strength, porosity, thermal diffusivity	Helium pycnometer, differential scanning calorimeter.	Gram	mgs (differential scanning calorimeter) to 100s mgs (Helium pycnometer)
	4	D, L	Age	Mineralogy & isotopes	EMPA, SEM, TEM, XRS, FTIR, Raman, SIMS, NG-MS, ICPMS	Gram	10s pg (SIMS) to 10s mgs (ICPMS) per analyses
Pre-solar grains	2	H, I	Nucleosynthesis	Elemental and isotopic composition	SIMS, NG-MS, TEM, SEM	Several grams	10s pg (SIMS) to 100s µgs (NG-MS) per analyses
	1, 2	B, H, I	Circumstellar processes	Mineralogy and mineral chemistry	SEM, TEM, Raman, SIMS, Auger spectr.	Gram	10s pg (SIMS) to 100s µgs (NG-MS) per analyses
	2	H, J	Interstellar processes	Isotopes and mineralogy	SEM, TEM, Raman, SIMS, Auger spectr.	Gram	ags (Auger) to 10s pgs (SIMS)
	1, 2	C, I, J	Age	Isotopes	SIMS, NG-MS	Several grams	10s pg (SIMS) to µgs (NG-MS) per analyses

laboratories have to reproduce the same results); and finally 1/3 of the returned mass has to be stored for an indefinite time in the curation facility for future analysis.

In the last few decades, revolutionary changes in instrumentation have increased the use of highly sophisticated instruments for obtaining analytical information on the composition, chemistry, surface, and internal structures of solids at the micrometre and nanometre scales. These techniques are based on various underlying principles and cannot be put under one umbrella. Therefore, it is important to define the scope of techniques that can be used to provide answers to the scientific objectives of the Marco Polo mission.

In almost all cases no single measurement, or type of measurement, will provide the complete answer to any of the questions. Instead, our understanding will be derived from the results of many analyses of different components of the returned sample, and by a plethora of techniques. A sample returned from the surface of a primitive asteroid is expected to be a mixed regolith, containing components from different parts of the body, each having experienced a unique geological history on the asteroid.

For instance, it is only through careful characterisation of each component that the most primitive components can be identified, necessary for investigating solar-system formation and pre-solar processes. Such a characterisation is also necessary for a thorough assessment of the geological variability of the asteroid that can help us understand the structure, history and formation of the asteroid.

The sample of primitive material from an NEA returned by Marco Polo will be heterogeneous at different scales, from centimetres to nanometres and, even at the molecular scale. Each component will be a remnant directly connected to specific astrophysical environments and processes, such that the chemical, isotopic, mineralogical and molecular information records the place where it formed, the processes experienced, the timescales elapsed, and the environments crossed in space. Thus, any reliable laboratory analysis must be able to resolve these discrete components within the sample.

The analytical approach is now described as component-oriented, with each section highlighting the materials expected within the returned sample, the principal techniques that will be employed for the analyses, the data generated and the sample requirements.

2.2.1.1 Early stages of solar-system formation

Details of the birth of the solar system remain unclear. What caused the pre-solar cloud of gas and dust to collapse, triggering the formation of the solar system? What were the conditions within the proto-stellar disk? What phases were formed, destroyed and reacting, and what were the conditions prevailing at each stage? How did a mass of predominantly gas condense, agglomerate and accrete to form the planetesimals that ultimately went on to form the planets? What were the timescales for the various steps and environments?

The analytical campaign can be considered as tackling scientific challenges on a number of scales from the whole-rock properties through the different types of materials present to the individual grain or molecule.

Studies of meteorites have revealed that the oldest known components available for study formed in the solar nebula are the CAIs. These sub-millimetre- to centimetre-sized clasts, found in chondritic meteorites have a mineralogy setting them apart from other chondrite components. They record some of the earliest stages of solar-system formation. Chondrules, generally slightly smaller spherical particles of silicate with less refractory compositions, appear to have formed 2 to 3 million years after CAIs. One of the debates centres on the difficulty of making CAIs in the vicinity of where their current parent bodies formed - the asteroid belt in the case of chondrites or indeed much further out following evidence of fragments of CAI in the comet 81P/Wild2 samples returned by the Stardust mission. The conditions and processes of condensation are retained within these fragments of early solar-system formation, but much of the detail has been fogged or obliterated by processes occurring on the meteorite parent bodies. The sample of an NEA returned by Marco Polo is expected to contain components that have experienced little or no processing on the parent asteroid – providing a unique opportunity to have a clear sight of processes occurring in the early solar nebula. There are many aspects to the study of the early solar nebula that will be significantly advanced by the Marco Polo sample – the following are examples of some of the more important areas:

Condensation and gas-dust reactions - After the formation of the refractory inclusions and chondrules, there is evidence from meteorites that these components continued to exchange material, possibly during re-cycling of the material through chondrule/CAI formation mechanisms, with a gas phase that was not in

equilibrium with the solid material. Such processes are recorded in the element diffusion profiles and isotopic heterogeneity imparted into these early solar-system components. Unfortunately, redistribution of the same elements and isotopes are also a consequence of later events on the parental asteroids of the meteorites. Major and trace element distributions in CAIs and chondrules derived using techniques such as EMPA, LA-ICPMS and SIMS offer the possibility of determining the composition of the gaseous reservoir, the temperature and even pressure of the environments where these processes occurred (*e.g.* Galy et al., 2000; Alexander et al. 2008).

The oxygen isotopic heterogeneity in the early solar nebula was clearly considerable – with CAIs and chondrules displaying variations of almost 10 % (*e.g.* Franchi 2008). The origin of this heterogeneity remains a contested issue, although the results from the Genesis mission do point towards the possibility of mass-independent fractionation of an oxygen reservoir by some form of self-shielding of CO gas as the principle mechanism (McKeegan et al. 2009). However, details of this process, and where it may have occurred remain to be established. The exact signatures of the mass-independent fractionation, the end member compositions and slope of the mixing line, are obscured by the effects of asteroidal aqueous alteration. Low temperature alteration results in large mass fractionation effects, and therefore even very mild alteration can have significant effects. High-precision GS-MS and SIMS analyses of well characterised components free of asteroidal processing will provide clear measures of the primordial signatures in the solar nebula.

Timescales - Recent advances in the dating of ancient materials found in meteorites indicate that the formation of CAIs and chondrules through to planetesimals took only a few to ten million years (Russell et al 2006). Absolute ages via the Pb-Pb dating technique (from the decay of ^{235}U to ^{207}Pb and ^{238}U to ^{206}Pb) offer the possibility of determining crystallisation ages for individual components such as CAIs and chondrules with a temporal resolution of 1 Myrs or better. However, Pb is a very mobile element under a range of geological conditions and therefore great care in selection of meteoritic samples is required in order to minimise the effects of any post-crystallisation re-setting that may have occurred. Primitive materials from an NEA offer the possibility to date components free of re-setting and therefore to obtain a clear understanding of the formation ages of the earliest-formed solar nebula components.

Absolute dating with Pb-Pb chronometers (Figure 12) requires very specific components with high initial U/Pb ratios as well as undisturbed histories. Further insight into the age of different components present in the early solar nebula can be obtained through the now extinct, short-lived radionuclides known to be present at the birth of the solar nebula. While only providing relative ages, isotope measurements assessing the initial abundance of radioisotopes including ^{41}Ca (half life ≈ 0.1 Myr), ^{36}Cl (≈ 0.3 Myr), ^{26}Al (≈ 0.74 Myr), ^{10}Be (1.5 Myr), ^{60}Fe (1.5 Myr), ^{53}Mn (3.7 Myr) offer a range of chronometers that can be analysed using SIMS, ICPMS and TIMS techniques to provide dates spanning a range of ages relevant to the formation of the solar system. Cross calibrating the relative and absolute chronometers with common samples provides the opportunity, with primitive NEA material, to provide a rigorous understanding of the timescales of early solar-system formation.

Irradiation history - Powerful X-ray flares observed in many pre-main sequence solar-like stars are likely accompanied with intense fluxes of accelerated particles (Feigelson and Montmerle 1999), yet our understanding of the irradiation history of early solar-system components remains poor. Such processes may play an important role in the production of short-lived radionuclides (such as ^{26}Al), the most likely heat source that powered the alteration and differentiation of the planetesimals. There is evidence for spallogenic production of isotopes such as ^{10}Be and ^{6}Li in CAIs (*e.g.* McKeegan et al. 2000) and some evidence for the presence of ^{7}Be in some CAIs (*e.g.* Chaussidon and Gounelle 2006). With a half life of only ≈ 53 days, the presence of ^{7}Be argues for production at the same epoch as the formation of CAIs. This possibly happened close to the proto-Sun with subsequent ejection out towards the asteroid belt (or beyond) by strong X-winds (*e.g.* Shu et al. 1994). Such an environment may also be expected to generate significant amounts of other short-lived radionuclides such as ^{26}Al, ^{41}Ca and ^{53}Mn (*e.g.* Chaussidon and Gounelle 2006). Production of short-lived radionuclides by this mechanism is likely to lead to a significant heterogeneity of short-lived radionuclides in the early solar nebula – rendering the chronometers based on these nuclides invalid.

(Courtesy of A. Krot, University of Hawaii.)
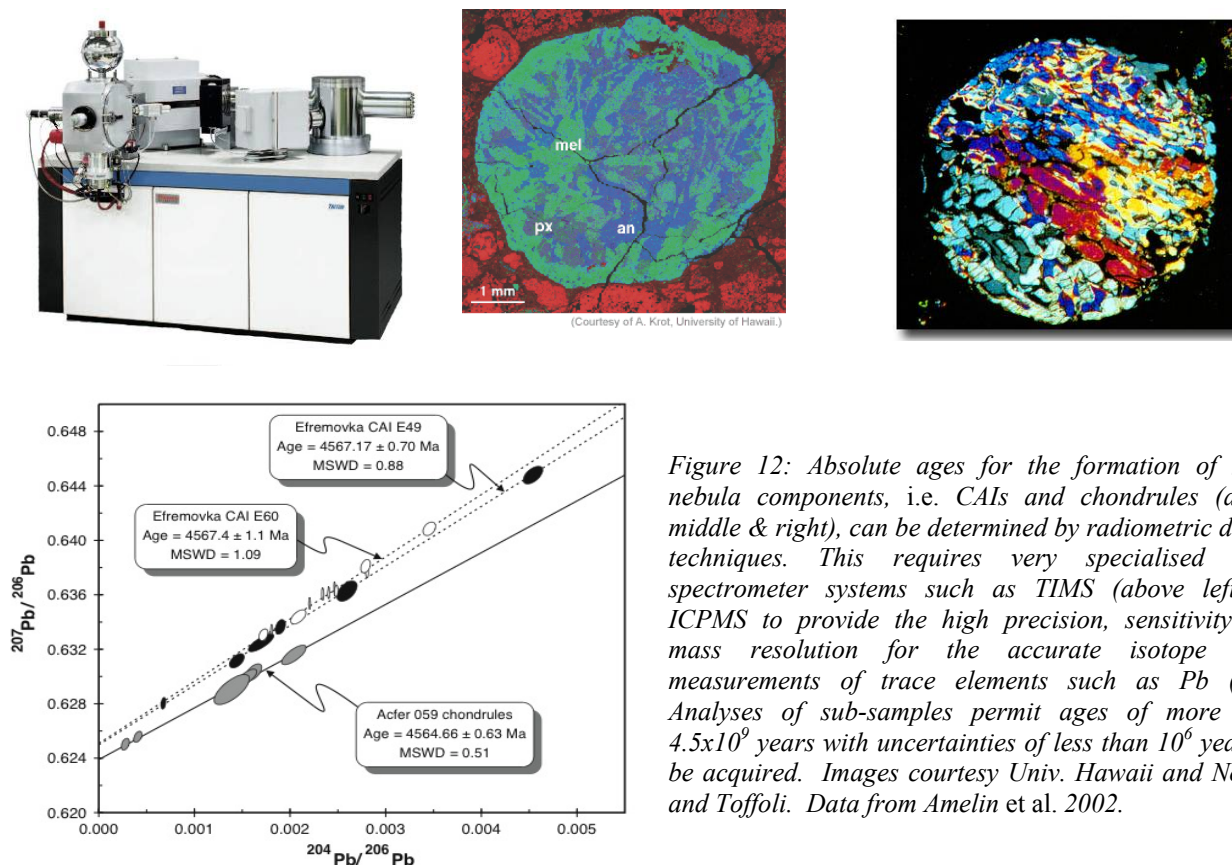
Figure 12: Absolute ages for the formation of solar nebula components, i.e. CAIs and chondrules (above middle & right), can be determined by radiometric dating techniques. This requires very specialised mass spectrometer systems such as TIMS (above left) or ICPMS to provide the high precision, sensitivity and mass resolution for the accurate isotope ratio measurements of trace elements such as Pb (left). Analyses of sub-samples permit ages of more than 4.5×10^9 years with uncertainties of less than 10^6 years to be acquired. Images courtesy Univ. Hawaii and Norton and Toffoli. Data from Amelin et al. *2002.*

However, the X-wind type models cannot produce all the observed short-lived radionuclide abundances – and therefore one of the major challenges ahead is to understand the role irradiation played in the early solar nebula and the origin and distribution of short-lived radionuclides. Some of the elements of interest, such as Li, are particularly mobile and therefore materials from an NEA with little asteroidal processing offer the best opportunity to unravel this pressing problem. As the various short-lived radio-nuclides known to be present are generally considered to have been synthesised in only a small number of different nucleosynthetic sites, their relative abundances provide important constraints on solar-system formation initiation such as the supernova trigger.

The combined output from such studies of the solar nebula components will also contribute to further understanding of many aspects of the formation and evolution of the solar nebula and the first steps towards the accretion of the planetesimals.

2.2.1.2 Pre-solar components

Pre-Solar grain inventory: While meteorites display a variety of interstellar grains, these are generally the most chemically and mechanically robust materials – such as diamond, carbide and even the rare nitride, as well as some less robust materials such as silicates and graphite (*e.g.* Meyer and Zinner 2006). It is clear that geological process on the asteroidal parent bodies has a detrimental effect on the abundance of all types of interstellar grains (*e.g.* Huss et al. 2003), and that the pre-solar silicates that have been found in meteorites have almost exclusively been found in meteorites that have experienced the least effects of aqueous alteration. Therefore, portions of the sample returned by Marco Polo identified during the initial characterisation as having experienced the least asteroidal processing will be those expected to contain the highest abundances of pre-solar grains. This material will offer the best opportunity to assess the abundance of pre-solar grains that survived their passage through the solar nebula to be accreted into the planetesimals at 3-5 AU. Isotope ratio imaging using ion microscopes such as the IMS 1280 or ion probes such as the NanoSIMS for a range of different elements and isotopes on polished slices of whole rock and pre-solar grain concentrated acid residues will provide an assessment of the pre-solar grain inventory in the sample, seeking to establish the abundance of grains most susceptible to destructive asteroidal processes (Figure 13). We will search for pre-solar grains hitherto unknown in the meteorites – providing new insights into nucleosynthetic processes.
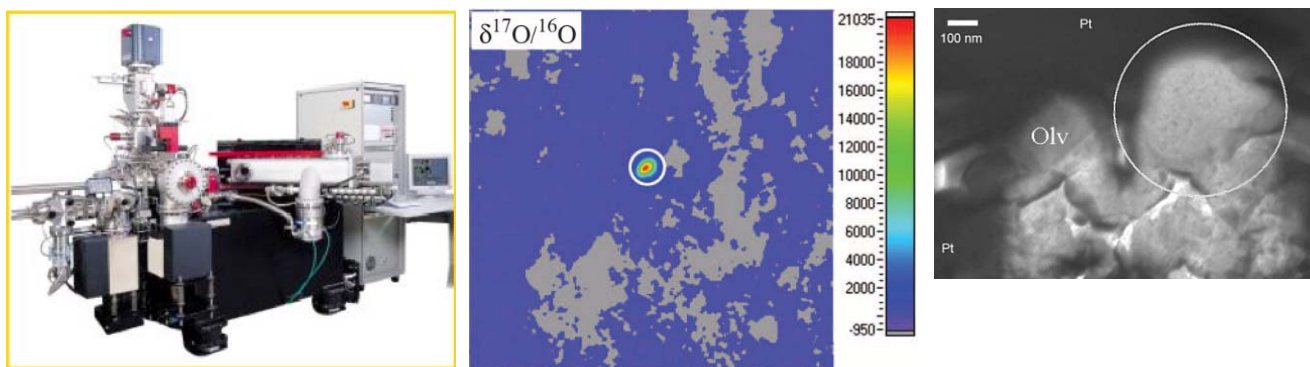
Figure 13: Pre-solar grains can be identified by isotopic compositions far from typical solar-system values. Ion microprobes such as NanoSIMS (top) provide detailed isotope ratio maps (middle - showing very ^{17}O enriched silicate grain approximately 400 nm in diameter, in fine silicate meteorite matrix). Isotopic ratios provide information on nucleosynthetic processes. Characterisation of the mineralogy and elemental composition of the grains using TEM (bottom – pre-solar silicate circled), Auger spectroscopy, etc. provides insight into condensation environment and subsequent history in ISM and solar nebula. Data images from Nguyen et al. *(2007).*

A major challenge in the coming years is understanding the residence times in the ISM for the interstellar grains. Recent analyses of rare, large, (50 micron) grains show residence times up to 10^9 years in the ISM (Heck et al. 2009). The challenge now is to extend this to more representative grains (micron sized) and with different chronometers (*e.g.* heavy r-process elements). Primitive material from an NEA offers the best opportunity to accurately determine these unknown ages.

Nucleosynthetic processes: The study of pre-solar grains permits information to be obtained about individual stars, albeit unidentified ones, complementing astronomical observations of elemental and isotopic abundances in stars, by extending measurements to elements that cannot be measured astronomically, or with precision and/or sensitivity beyond that achievable with telescopes. By extending the known range of interstellar grains the Marco Polo sample may provide fresh insight into nucleosynthetic processes. Knowledge of the nucleosynthetic processes combined with constraints of the mineralogy, controlled by the composition of the gas from which the grains condense, offers unparalleled insight into stellar processes. For example, a small fraction of the pre-solar silicon carbide grains carry isotopic signatures clearly indicating that they formed during type II supernovae. However, the composition of these grains demands mixing from several non-adjacent zones within the precursor star, with the challenge of doing so without significant incorporation of intervening oxygen-rich zones in order to preserve C>O ratios suitable for condensation of phases such as silicon carbide and graphite (Meyer and Zinner, 2006). The detailed mineralogy of grains can be further investigated by sectioning with FIB-SEM for TEM analyses – revealing seed grains, internal structures, *etc.* which provide detailed understanding of the condensation sequences, formation intervals, pressures and temperatures in the circumstellar shells (Bernatowicz et al 2006). The study of new grain types will provide new insight into stellar environments.

Interstellar processes: The identification of interstellar grains in-situ, or concentrated via gentle separation techniques such as freeze/thaw disaggregation combined with density and settling techniques permits study of the mantles and reaction rims found on some grains using techniques such as NanoSIMS, TEM, XANES. These mantles offer a unique insight into the post-formation history of these grains which will include processes in the ISM and solar nebula. Such mantles are readily destroyed in acid treatment concentration methods and are probably significantly modified during the extensive asteroidal processing that is required to generate meteorites. Therefore, the more primitive material returned from an NEA will offer an unprecedented opportunity to investigate the history of these grains in the ISM and the processes occurring there.

2.2.1.3   Organic components

A detailed assessment of the major classes of organic compounds present in the different fractions (Table 3) is required to assess the nature of the processes which contributed to the organic inventory on the asteroid. Very little is known about the conditions and processes that could have altered, destroyed or formed organic compounds during the proto-solar nebula collapse, solar-system formation and evolution. Evidence from meteorites indicates that processes occurring in the ISM, the solar nebula and the asteroids all contributed to

the organics found in meteorites. Primitive material from an NEA returned by Marco Polo will contain lithologies largely unaffected by evolutional processing, in which case there will be a clear window to ISM and nebula processes, or there will be a range of lithologies with varying degrees of alteration from a common source which will permit a detailed understanding of the history of these processes. The study of biologically important molecules in meteorites has been hampered by the problem of terrestrial contamination as even with isotopic characterisation it is impossible to unequivocally resolve molecular abundances indigenous to the meteorites. Many of the astrobiologically important molecules in meteorites are present in the soluble organics fraction. The collection of a pristine sample by Marco Polo, un-processed by an atmosphere re-entry and the subsequent handling with strict control on the introduction of terrestrial contamination, provides the opportunity for an un-compromised investigation of the origin of these compounds. It will allow accurate characterisation of the organics present including important measurements such as the extent and magnitude of the enantiomeric excesses present in some compounds such as the amino acids and some of the carboxylic acids, *etc.* Understanding the sources and nature of organic molecules and the chemical processes that led to their formation is the primary goal.

The carbon content of the returned sample can be considered as consisting of two distinct, but potentially intimately related fractions: a soluble and an insoluble component which may be heterogeneously dispersed in the bulk material. The carbon content of the more primitive carbonaceous chondrites suggests that we should expect approximately 2 to 8 weight percent of the total returned mass as organic carbon, although some so-called carbonaceous chondrites can contain less carbon by up to a factor of 30. While there may be abundant organic matter within the sample, it is present as a vast number of different types of molecules. Table 3 shows the possible range of abundances giving two examples, the Tagish Lake meteorite and the Murchison meteorite.

The soluble fraction can be extracted from the sample with a series of solvents of different polarity, which leads to complex mixtures of compounds in the individual extracts. This total soluble fraction is typically 5-10 % of the total organic carbon in the most primitive, carbon-rich meteorites. Thus, the insoluble fraction is the majority of the total carbon content (>80 %).

Investigation of the organic matter in the sample, and its distribution within the principal lithologies requires a wide array of analytical techniques, tackling different, but related aspects of the organic inventory, its composition, structure, its distribution within the sample and how it is related to the silicate mineralogy. In order to provide quantitative measurement of these compounds it is usually necessary for them to be separated out via various fractionation and chromatographic techniques to facilitate analysis. This requires destructive analyses, and in some cases considerable (gram) amounts of rock sample because many of the astrobiologically important individual molecules are present at ppm or less level.

Soluble fraction: The study of soluble organic molecules needs an extraction process first (*i.e.* isolated from the silicate and macromolecule matrix). A number of approaches are typically employed – such as ultra-sonication in a range of different solvents or super-critical fluid extraction. For example, non-polar solvents (*e.g.* toluene) can be used to primarily extract aliphatic and aromatic compounds while more polar solvents (*e.g.* formic acid or water) can extract far more polar molecules – *e.g.* nucleobases and amino acids. Each extract will contain a large number of different compounds (Table 3) which need to be separated out prior to detection/analysis. There are mainly two important chromatographic methods in use for the analysis of organics: Gas (GC) and Liquid Chromatography (LC) equipped with a number of different detector types according to the nature of compound to be detected.

Combining the different extraction, chromatography and detection methods will provide a complete analysis of the identification and abundance of the different molecules present. The types of structures present and their relative abundances provide important insight into possible formation mechanisms (*e.g.* surface catalysed synthesis and gas phase addition reactions have very different outcomes in the generation of branched variants within some types of compounds).

The stable isotopic composition of H, C, N, O, and S of individual compounds can provide important information on the origin of the organics. This important technique is a major driver on sample requirement, as less sensitive instruments (for higher precision) are being employed to detect less abundant (minor isotope abundance) species, such that sample requirement can be increased by several orders of magnitude.

Table 3: Soluble organic compounds in the Tagish lake and Murchison meteorites (from Pizzarello et al. *2006).*

Class	Tagish Lake		Murchison	
	Concentration (ppm)	Compounds Identified	Concentration (ppm)	Compounds Identified
Aliphatic hydrocarbons	5	12	>35	140
Aromatic hydrocarbons	>1	13	15-28	87
Polar hydrocarbons	n.d.	2	<120	10
Carboxylic acids	40	7	>300	48
Amino acids	<0.1	4	60	74
Hydroxyl acids	n.d.	0	15	7
Dicarboxylic acids	17.5	18	>30	17
Dicarboximides	5.5	9	>50	2
Pyridine carboxylic acids	7.5	7	>7	7
Sulfonic acids	>20	1	67	4
Phosphonic acids	n.d.	n.d.	2	4
N-heterocycles	n.d.	n.d.	7	31
Amines	<0.1	3	13	20
Amides	<0.1	1	n.d.	27
Polyols	n.d.	n.d.	30	19
Imino acids	n.d.	n.d.	n.d.	10

Isotopic measurements of individual compounds across the compound classes will provide confirmation of extra-terrestrial origin of the compounds, source region information (*e.g.* high D/H ratios indicative of ISM origin) as well as the formation processes. Isotopic measurements are the only means to provide direct evidence of commonality between different types of compounds, *i.e.* do left- and right-handed enantiomers have the same isotopic signatures (*i.e.* sources), and are there similarities between different compound types? They can also be used to determine the relationships with the non-organic components within the sample (*e.g.* oxygen isotope can be tracked across to silicates, D/H with the aqueous alteration components (*i.e.* role of fluids), carbon can be compared to carbonate signatures, *etc.*).

As all nucleobases are involved in biological systems, the Marco Polo sample, collected under strict contamination control and handled appropriately subsequently, offers a unique opportunity to assess the indigenous levels in the asteroidal material of this group of compounds very much at the heart of life on Earth. Other groups of compounds important to life can be analysed similarly to the amino acids or nucleobases, usually from the same extraction (focussing on different elutions from the initial separation) or the non-polar extracts.

Insoluble fraction: More than 70 % of the organic matter in carbon-rich carbonaceous chondrites is a complex macromolecular form of carbon that remains in the rock even after repeated solvent extractions. The insoluble organic fraction consists of molecules that cannot be readily separated and analysed individually, and therefore a range of techniques distinct from those applied to the soluble fraction are usually employed in the study of the macromolecule.

Solid state ^{1}H and ^{13}C NMR spectroscopy constitutes one of the most powerful spectroscopic approaches to the study of the organic macromolecule – establishing the types and distribution of the different functional groups in the amorphous macromolecular material. This can be used to provide a quantitative, albeit averaged, determination of the structural picture of the macromolecule and its elemental composition. A number of NMR methods applicable to small amounts (a few tens of mg) of a powdered sample at natural abundance have been used – although first the sample must be demineralised to remove the paramagnetic nuclei present in the silicate matrix, as they have a major impact on the quality of the NMR spectra in terms of both signal strength and sensitivity – and therefore gram amounts of whole-rock sample must be processed.

A variety of pyrolysis-GC-MS techniques (flash heating, hydrous and hydro-pyrolysis) provide a complementary approach to the NMR studies, offering detailed characterisation of the molecular species or components within the macromolecule. Such techniques convert a portion of the macromolecule to free compounds, providing a means to compare the nature of the soluble and insoluble fractions. Primitive material from an NEA returned by Marco Polo will allow investigation of the nature of the organics accreted to the asteroidal parent and the role of asteroidal processes in the formation of the macromolecular material.

While the molecular abundance patterns obtained for the macromolecule pyrolysis experiments and that obtained from the soluble organic fraction can offer some hints at relationships, this can most readily be determined by performing isotopic measurements on the pyrolysis products in the same way as described for the soluble fraction, *i.e.* with GC-isotope-ratio-MS attached to the pyrolysis sample introduction system. Such analyses are therefore key to developing an overall understanding of the nature and origin of the organic material present in the sample.

In terms of understanding the relationship between the silicate matrix and the organics - parameters of interest would include determining correlations with aqueous alteration and the distribution of pre-solar grains - all the conventional microscopy techniques (SEM and TEM) and the SIMS techniques for elemental and isotopic techniques provide complementary information to the organic distributions.

A number of further techniques (*e.g.* Figure 14) provide detailed structural or molecular information on the distribution of organic compounds with high spatial resolution (*e.g.* μL^2MS, XANES, Raman and Infrared micro spectroscopy, *etc*.). Most of these techniques require small samples, little or no sample preparation (microtome sections are needed for XANES), offer very high sensitivity (down to the level of attograms) and are non- or partially-destructive.
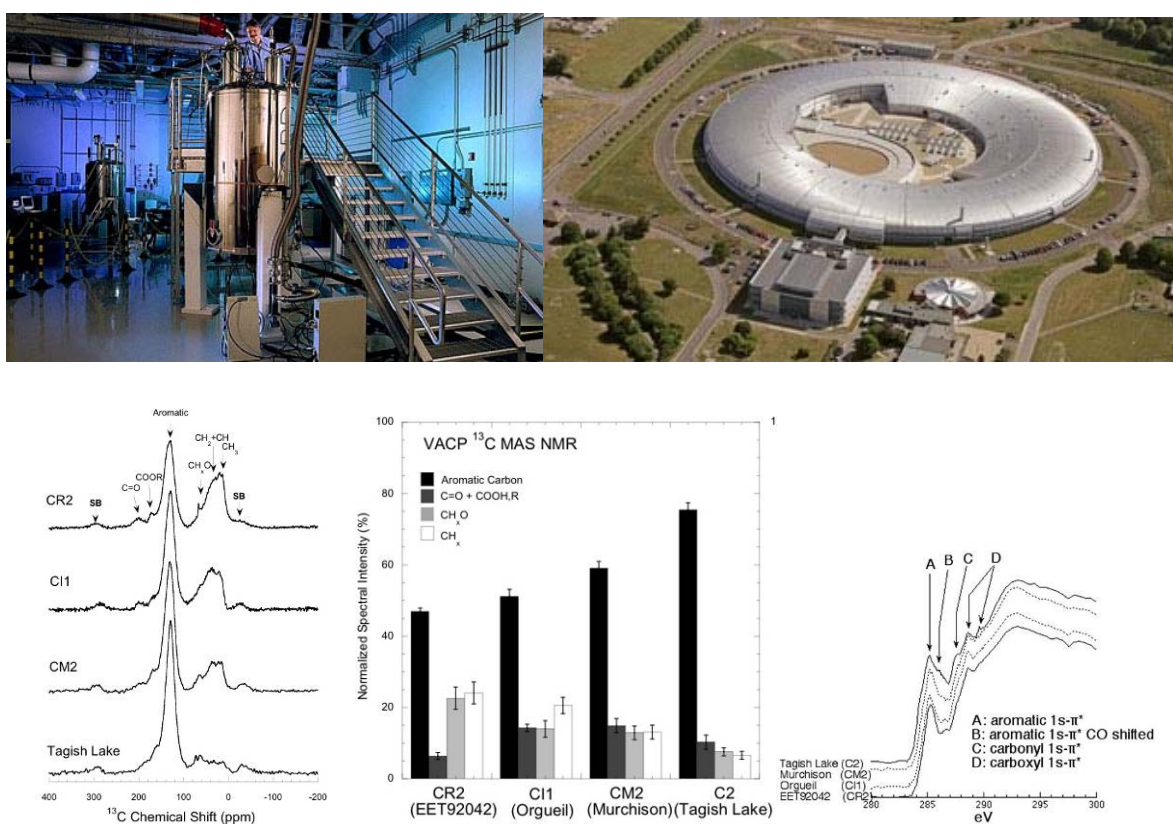
Figure 14: Probing the complex structure of the organic macromolecules requires sophisticated instrumentation such as ^1H and ^{13}C NMR (top left) spectroscopy (of demineralised samples to remove matrix interferences) to establish the types and distribution of functional groups (bottom left), providing information on formation and evolution processes. The spatial distribution of the organics structures can be determined through spot analyses techniques such as synchrotron (top right), XANES measurements allowing distribution of specific bonds (bottom right) to be mapped on the scale of microns. The results can be correlated with mineralogical, isotopic and elemental variations in the rock to provide a detailed understanding of the formation history of the organics (bottom middle & right). NMR data from Cody and Alexander (2005), XANES data courtesy Cody (Image from: http://people.gl.ciw.edu/cody/meteorite.html).

2.2.1.4   Asteroidal components

Asteroid evolution: It is anticipated that the surface of the NEA will be a mixed regolith, and therefore it is expected that there will be many different lithologies present in the returned sample. Evidence from the only small NEA visited to date, Itokawa (Fujiwara et al. 2006), indicates that the particle size may typically be in the range of mm to cm, and therefore there will be significant quantities of many of the lithologies present in the returned sample.

A range of petrographic techniques are needed to determine the exact phases present, their form and their inter-mineral relationships. Techniques, spanning a range of scales from the mm to nm will include optical microscopes, SEM and TEM, with a wide range of mineral characterisation techniques including X-ray diffraction and spectrometry (electron and synchrotron sources), electron diffraction, EELS, cathode luminescence, FTIR and Raman spectroscopy, XANES, a variety of SIMS techniques, LA-ICPMS.

This information is required to understand the variability in the materials present on the surface of the asteroid and the causes of this variation. Specifically, and in part drawing upon knowledge gained from meteorites, it will permit identification of those components which are of nebula origin, and the extent to which each lithology has suffered from asteroidal processing: impact events, thermal and aqueous metamorphism, space weathering.

The basic mineralogy and textural relationships will provide some of the detailed information on the nature of the asteroidal processes that the sub-samples have experienced. For instance, the nature of any aqueous alteration that has affected the various lithologies: The degree of alteration by relative proportions of secondary and primary (nebula) minerals, the types of secondary minerals, and their chemical compositions, including oxygen isotopic measurements, reflecting the fluids and conditions of alteration. Similarly, for thermal events the mineral chemistry and rock textures provide well-established measures of the thermal history a rock has experienced. Shock history can also be determined from mineral structure and defects.

The oxygen and hydrogen isotopic composition of hydrated phases of the different components in the sample of regolith determined by SIMS and GS-MS will provide an understanding of the aqueous alteration history of the parent asteroid. This will determine the isotopic signature and abundance of water that could be delivered by such bodies to the early Earth. Combined with measurement of other volatiles, particularly noble gases by NG-MS, this will provide a test of the viability of primitive asteroids from the main belt as a source of the Earth's oceans.

The chronology of the different asteroidal processes identified in the sample can be measured through high-precision radio-isotope measurements. Carbonate minerals are a common product of aqueous activity, and information on the timescales of formation can be gathered from a number of approaches such as Rb-Sr or Pb-Pb dating for younger ages (*e.g.* Borg et al. 1999) and Mn-Cr (from short-lived ^{53}Mn) for older ages (*e.g.* de Leuw et al. 2009). Shock age information can be readily gathered from Ar-Ar ages. Sample requirements are small – a few mg or even less if in-situ SIMS techniques can be employed. However such analyses can only be performed on suitable mineral grains of the right composition formed at the same time (*e.g.* Mn-Cr dating will require a number of grains with a range of Mn contents, including some high Mn content).

Understanding of the different geological events experienced by the different lithologies (*e.g.* Figure 15), coupled with spectral characterisation of these components can then be combined with the spacecraft observations at different scales to develop a detailed knowledge about the formation and history of the asteroid. Bulk density, grain density and porosity of the sample can be determined with a pycnometer and CT scans, providing further constraints for models of the bulk physical properties determined from spacecraft observations.

Asteroidal surface components: Space weathering is the physical and chemical alteration of surfaces of airless bodies exposed to the space environment (Hapke 2001) such as the bombardment by ions from the solar wind, magnetosphere ions, energetic electrons, cosmic rays, ultraviolet photons, and fast interplanetary dust (micrometeorites), with the relative flux of each of those projectiles depending on the location of the surface in the solar system.

The NEA region is irradiated by solar wind particles dominated by ion population. Solar wind ions have an energy of about 1 keV/amu with flux in the range of 10^8 (protons) to 10^2 (Ar ions) cm^{-2} sec^{-1} at 1 AU and decreasing as the square of the distance from the Sun. The 1 keV protons, although by far the most abundant, penetrate only the very thin skin of the asteroid and their effects are to sputter the surface material and to re-deposit it on a rough surface (Hapke 2001). This process alters the structure and composition of the surface material in such a way that it affects the optical properties in the UV–visible spectral region (Strazzulla et al. 2005, Loeffler et al. 2009). This process is so far more efficient than the effect due to micrometeoritic impacts (Yamada et al.,1999; Sasaki et al. 2001). A timescale for the weathering of NEA surfaces is on the order of 10^4–10^6 yr.

Effects of space weathering on the mineralogy can be identified by conventional electron microscopy (SEM/TEM). Development of nanophase iron, an important effect on the lunar surface, can be determined by techniques such as Mössbauer spectroscopy, Electron Spin Resonance (ESR) and magnetic susceptibility. The timescales of the gardening rate of the asteroidal regolith can be determined through measurement of short lived radionuclides – both by decay counting shortly after return and by accelerator mass spectrometry in order to establish cosmic ray exposure (CRE) histories (saturation, multiple episodes, *etc.*). Noble gas and other light elements implanted into grain surfaces will provide a measure of the solar wind composition independent of the Genesis collectors and the Apollo samples (offering additional temporal variation). As the Earth's upper atmosphere may be a further source of ions contributing to the solar wind impacting the lunar surface (excesses of ^{40}Ar and N, as well as highly variable oxygen and nitrogen isotopic signatures in the implanted component are well documented), there may be distinct differences between the implanted components in NEA and lunar regoliths. Analyses by noble gas mass spectroscopy (NG-MS), gas source mass spectroscopy (GS-MS) and SIMS will provide precise determination of the composition of the solar wind component implanted into the surface material. A sample returned from the surface of a primitive asteroid will also offer the opportunity to provide some "ground truth" for remote observations (spacecraft and telescope) for the vast amount of information gathered on asteroids. Visible to near-IR and mid-IR spectroscopy of specific components within the sample, with well determined mineralogy, physical properties and known exposure history will provide unique information that will be invaluable for a better interpretation of the spectra that currently exist for minor bodies in the solar system.
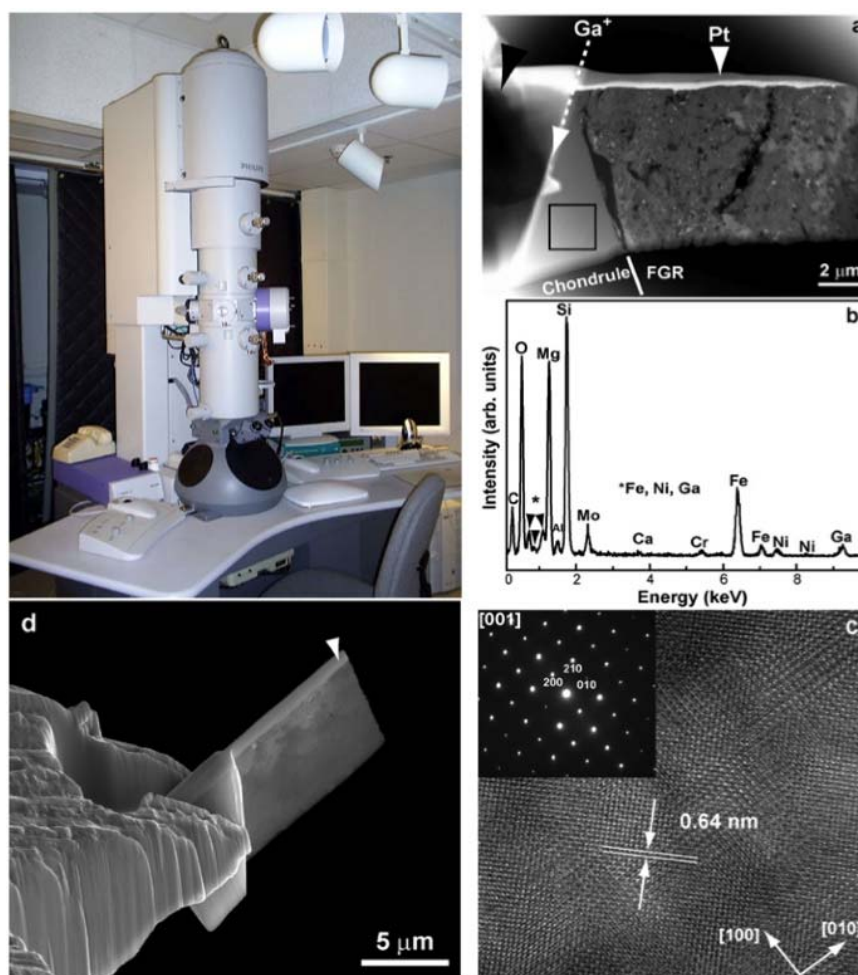
Figure 15: Asteroidal alteration processes result in modification of existing mineralogy. Tracking the effects of such processes, operating over very small scales (<μm), requires the use of scanning (SEM) and transmission (TEM – top left) electron microscopes. Preparation and manipulation of electron transparent sections (bottom left) from areas of specific interest for TEM can be achieved with combined electron microscope-focussed ion beam instruments. Analyses of the prepared sections allow detailed investigation of the mineral relationships (e.g. top right shows interface between chondrule and fine grained material), full characterisation of the chemical composition (EDX spectra – middle right) and structure (electron diffraction – bottom right) of specific components at the nm scale. Further analyses on the same

*area such as isotopic (*e.g. *NanoSIMS) or chemical (*e.g. *XANES),* etc. *provide a complete picture of the processes and environments experienced by these components. Images and data from Zega* et al. *(2007).*

2.2.2   Remote sensing analysis

The scientific goals of the remote sensing analysis are the global exploration and characterization of the asteroid, the search and identification of surface sampling sites, and the local characterization of the sampling sites. The global characterization of the body is required to obtain a picture as complete as possible of the physical nature of the NEA in order to relate the properties of the sample to those of the parent body.

2.2.2.1   Sampling site selection

For the overall success of the mission, the global characterization will allow the selection of a number of surface areas as potential locations for the intended surface sampling.

Geometrically correct shape models and maps must be produced for correct pointing of the remote sensing instruments and to safely manoeuvre the spacecraft towards its intended sampling sites. The characterization of the selected areas by close and in-depth investigations will then be performed. Imaging, spectroscopy and in-situ analysis have to join forces for the accomplishment of this goal. The in-depth characterization requires local exploration of the selected sites from closer range. The task of the imaging is the provision of the three-dimensional topography of the landing sites at the best possible resolution. The spectroscopic and in-situ tools contribute the compositional profile of the surface areas. All investigations have to consider the context of the selected landing sites, *i.e.* it must be possible to put the local characterization, obtained for the sampling region, into the larger context of the surrounding surface region, even at a global scale.

The search for potentially interesting areas is performed using comprehensive maps of the NEA surface produced by the various instruments during dedicated mapping campaigns.

Temperature maps can distinguish areas with high and low thermal inertia. For instance lower thermal inertias are characteristic of a high regolith fraction. Therefore such maps can help in the choice of the sampling site as they correspond to different surface conditions.

Marco Polo must be able to land on a surface with unexpected conditions and extract a sample. For instance, the asteroid Eros has abundant fine particulate regolith, whereas Itokawa has much higher areal densities of large blocks (Fujiwara et al. 2006). About 1/3 of Itokawa's surface area is covered by blocks larger than 1 m, and the regolith (particle sizes << 1 m) is globally segregated and ponded in gravitational lows to create smooth areas (see Figure 16). On Itokawa, 20 % of the total surface area is rather smooth. Obviously, Marco Polo will look for the most appropriate areas for sampling.

The remote sensing analyses described in the following sections, are essential to select the best sampling site.

2.2.2.2   Size, shape, and rotation

Size, shape, and rotation are basic physical parameters for any planetary body which, in the case of Marco Polo, will be obtained from combinations of imaging and laser ranging data. The determination of these parameters is also crucial for sampling site selection and safe navigation at close proximity. Even simple shape models will reveal general characteristics of the asteroid, *i.e.*, if the asteroid is a single monolithic rock, a contact binary, or a rubble pile. The existence of major impact craters on the asteroid surface can be interpreted on the background of evolutionary processes and impact events over the past 4.6 billion years (see *e.g.* Michel et al. 2009).

From shape models, the YORP effect (see Section 2.2.2.9) that may modify the rate and direction of the body rotation (Rubincam 2000) and associated redistribution of surface material can be modelled. For instance, the YORP effect has been predicted for Itokawa using its detailed shape model, rotation pole, mass estimate, and optical properties derived from the Hayabusa mission.
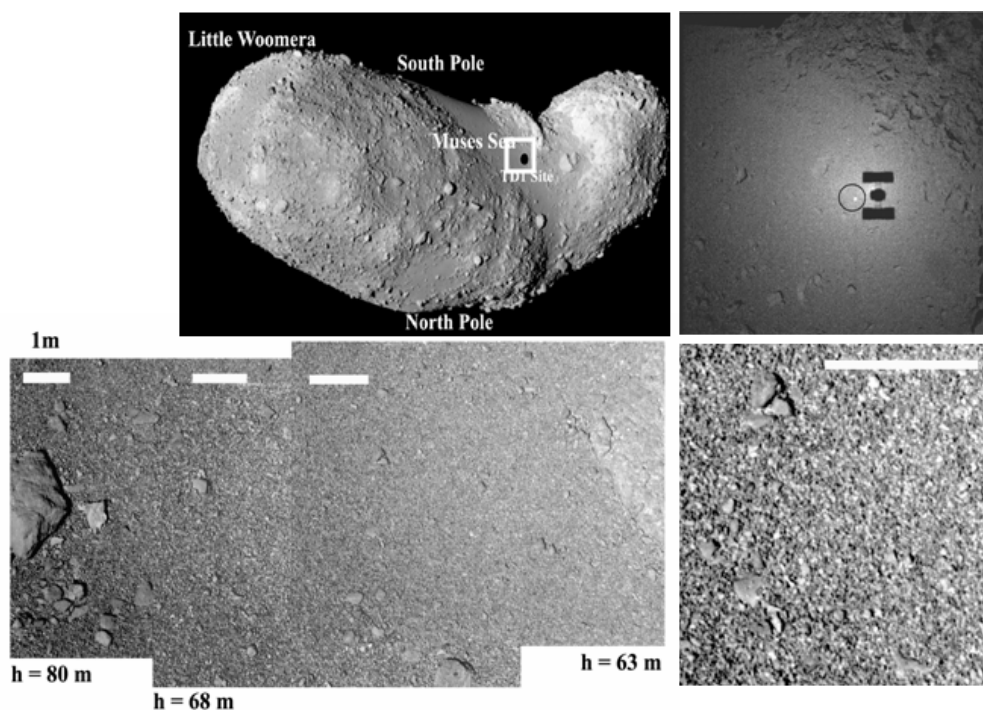
Figure 16: The best spatial resolution images of Hayabusa's landing site on the asteroid Itokawa. The bottom right image is a very close-up image of the Muses Sea gravel field taken by Hayabusa: its resolution is <1 cm (Yano et al. 2006).

Based on these shape predictions, the modelled deceleration rate for Itokawa was suggested to halve its rotation rate in only 50–90 thousand years (Scheeres et al. 2007). The diamond-shape morphology of asteroid Steins (Figure 17) as seen during the Rosetta fly-by in 2009 (Keller et al. 2009) is also believed to be caused by redistribution of material towards the equator owing to increased rotation rate and centrifugal forces (Walsh et al. 2008).

The combination of imaging and ranging data will allow us to determine parameters of the body rotation model with great accuracy. Precise identification of excitation modes of the body rotation would indicate the action of external torques, for instance due to a very recent impact event (perhaps still evident in the image data), tidal interaction during recent planet encounters, or the long-term action of the YORP effect. Other rotation states (*e.g.* tumbling) would then provide indications on the internal energy dissipation within the body and on the precise way YORP modifies the spin rates of small bodies (Vokrouhlicky et al. 2007).
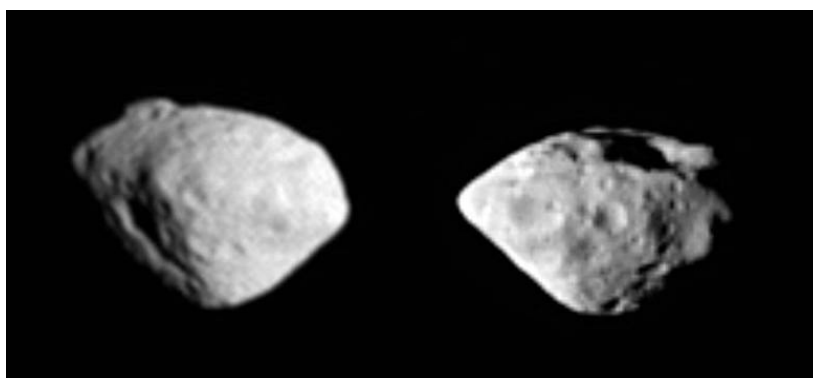
Figure 17: The best Rosetta camera images taken around close approach at a phase angle of 57° show the surface of (2687) Steins with a scale of 80 m/px to 100 m/px. The viewing directions between both images are 87° apart providing information on the side of the asteroid body not seen during close approach. The large crater lies near the south pole.

The rotational axis orientation can be compared with the shape model for implications on the asteroid's interior, which is of fundamental importance. This allows us to relate the potential macroporosity of the whole asteroid to the microporosity of the returned sample. While structural information cannot be inferred directly, moment of inertia tensors of the asteroid can be determined to identify offsets between centre of

mass and centre of figure, i.e., imbalances in the internal mass distribution of the body. This can help us determine whether the body is monolithic or an aggregate, which has great implications on its past history and for mitigation studies. For instance, the non-detection of YORP for Itokawa as of 2008, despite predictions that YORP should have been evident by now, shed light on the density distribution within that body. The theory supports a shift of the asteroid centre of mass towards Itokawa's neck region, where there is an accumulation of finer gravels, or towards the asteroid's "Head" region (Scheeres and Gaskell 2008).

Shape models in combination with rotation determine local gravity that affects local crater morphologies and regolith escape. Surface slopes will reveal the magnitude and orientation of local gravity vectors to study redistribution of surface masses, such as regolith and boulders ("mass wasting"). Slopes are also of utmost importance for determination of precise surface illumination angles, which in turn are needed for studies of surface photometry and surface physical properties, such as roughness, porosity, and particle size. Shape models also pose the framework for thermal models and internal heat transport.

2.2.2.3   Mass, density, and gravity field

From spacecraft tracking, mass estimates of the asteroid will become available. Using volume information in combination with mass, the bulk density and the porosity index of the body, by comparison with meteorite analogues can be determined, which are indicators for the internal body structure and associated formation scenarios. Low density and high porosity are expected for primitive, widely unaltered asteroids, such as C-class objects (Britt and Consolmagno 2000), that have not been affected by internal condensation processes during their evolution. Thanks to the analysis of the returned sample and mass/volume determination of the asteroid, we will be able for the first time to determine the true porosity of an asteroid by direct comparison of its bulk density with that of a sample coming from its surface.

If gravity models of higher order become available, a combination of shape and gravity model will provide hints on the mass distribution in the interior of the body, and may allow us to model mass concentrations or layering, which cannot be done on the sole basis of a bulk density estimate. Determining whether the mass is distributed more or less homogeneously can also tell us whether the porosity inferred from both the bulk density and that of the sample is dominated by the presence of large voids or due to microporosity inherent to the material itself.

This exercise has been done for the two asteroids that have been visited by a space probe so far. The NASA NEAR-Shoemaker probe used its Radio Science Experiment (RSE) to determine the mass and the gravity field of Eros (Yeomans et al. 2000) up to degree and order 10. The differences between the measured gravity field and one determined from a constant density shape model were detected relative to their uncertainty only to degree and order 6 (Miller et al. 2002). The offset between the centre of figure and the centre of mass is only about 30 m, indicating that Eros has a very uniform density (1% variation) on a large scale (35 km), although it is heavily fractured (Buczkowski et al. 2008). Variations to degree and order 6 (about 6 km) may be partly explained by the existence of a 100-m deep regolith or by small internal density variations.

Owing to its small (500 m) size and weak gravitational field, the total mass of asteroid Itokawa was measured with an uncertainty of 5 % by the Hayabusa spacecraft (Abe et al. 2006). The analysis suggests for Itokawa a mean density of 1.9 ± 0.15 g/cm^3 and a bulk porosity of 40% (assuming chondritic meteorite composition). A model representing Itokawa as a contact binary has also been proposed (Scheeres 2007).

This information is important for defining scenarios of the body's history. Indeed, the collisional lifetime and history of a small body depends on its response to impacts which in turn depends on the kind and degree of porosity that constitutes its interior. Marco Polo will thus allow us to estimate the potential history and lifetime of a body from which a sample will be analysed in the laboratory, which will certainly be an asset for interpreting some of the measurements performed during sample analysis.

2.2.2.4   Morphology and geology

Imaging maps of the whole body from a closer distance (order of a few hundred metres to two kilometres) provide the database for the detailed and synoptic geological analysis and interpretation of the NEA surface. Such information is important in order to place the returned sample into a geological environment and to relate it to the surface history. The crater statistics (cumulative number vs. size) provide the 'age' of the

surface which at most goes back to the creation of the NEA itself either as a planetesimal during its formation or as a product of a major impact on the parent body (see *e.g.* Michel et al. 2009). The crater statistics may also reveal global or local resurfacing events covering or completely erasing earlier stratigraphic layers. It is noteworthy that crater chains as imaged at the surface of asteroid Steins (Figure 17), could indicate (former) voids underneath the surface – of yet unknown origin – that have been partially filled by surface regolith. Other geological surface features like flat and hilly terrains, reefs, edges, or scarfs, *etc.* (Figure 18) are to be interpreted in the framework of restructuring processes in the body's interior (for instance, rearrangement of 'rubble in the pile') or during creation of the body.

Terrain models are also crucial tools for a variety of geological applications and for sample site selection. For instance, the analysis of the small-scale topography of Itokawa by the Hayabusa mission greatly helped to characterise the surface properties of the asteroid and gain some inferences on its internal structure (Barnouin-Jah et al. 2008).
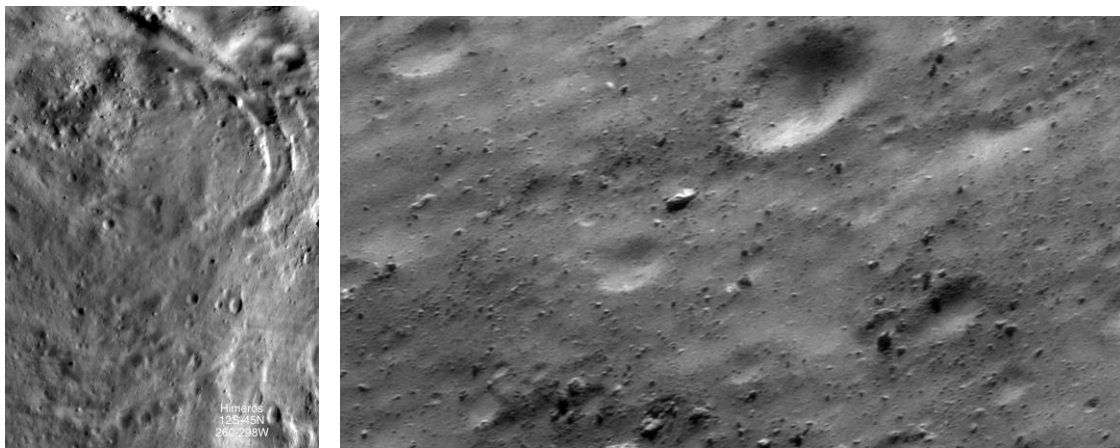
Figure 18: Left*: 7-km wide mosaic of Eros' largest depression (10 km-wide). The curving trough at the top and upper right, as well as more subtle curving depressions near the bottom of the mosaic, reflect fracturing of Eros. The bright and dark banding near the top results from material accumulating at the base of the nearly vertical scarp that forms one wall of the curving trough. More subtle dark lineations near the lower right result from thin layers of loose material moving down an approximately 20-degree slope. Many impact craters dotting the area are somewhat eroded and infilled.* Right*: Most of this 350-m wide image is covered in rocks of all sizes and shapes, but the floors of some craters are smooth, suggesting accumulation of fine regolith. For scale, the large boulder near the centre of the picture is about 15 m across. The smallest visible rocks are about 1.4 m across. (NEAR/JHUAPL).*

Colour maps of the surface allow us to study the regional distribution of the surface material, through continuum bands and/or specific absorption dips. Although these maps are less indicative of the possible wide variety of surface composition than those provided by spectroscopic imaging, they demonstrate impressively – thanks to their higher spatial resolution – the extent of geological units and correlations of colour data with surface morphology. For instance the global analysis of Eros colour units acquired by high-resolution imaging with the NEAR spacecraft illustrates complex regolith processes and grain sorting that may hold clues to understanding space weathering processes and the link between asteroids and meteorites (Riner et al. 2008).

2.2.2.5   Regolith

Regolith on an asteroidal surface can be envisaged as being a porous random medium of particles, with rough interfaces towards free space to the exterior and solid rock towards the interior. Particles can range from fine sub-micron and micrometre grains to particles of centimetre, decimetre and even metre sizes. Regolith is present, at least to a varying extent, on all asteroids, natural satellites, and terrestrial planets. The key physical parameters describing the regolith relate to the porosity and surface roughness of the medium, and size, shape, and orientation distributions of the particles. Whereas it is clear at the outset that the last three quantities are distributions, it is also probable that the porosity and surface roughness vary substantially across the surface of an object. Regolith particles are subject to various physical processes that change size and constitution, such as impact comminution, impact melting, formation of agglutinates, solar-wind sputtering, impact vaporization, impact vapour condensation, and shock and thermal welding of particles.

However, each regolith is unique and contains information about the origin of the body itself and its geological evolution.

For most NEAs, regolith supposedly constitutes a large portion of the surface. However, little is known of the detailed physical conditions of the surface material of NEAs and in particular of the vertical extent of the regolith. he two asteroids that have been visited so far by spacecraft have the same taxonomic class (S), but totally different regolith properties reflecting different collisional histories. However their surface geologies are similar in there is a lack of small craters that may be due to seismic shaking. Knowledge of the surfaces of C-class asteroids is even poorer and a wide range of possible regolith characteristics have been postulated. For example, will the compositional difference be associated with different surface geology, like compression cratering (Housen et al. 1999)?

The depth and extent of regolith layers can be studied on the basis of regolith mobility on steep surface slopes (Michikami et al. 2007), for which information on terrain topography and gravity are required. The prevalence of regolith has been studied extensively for the Martian satellite Phobos (Thomas et al. 2000), which possibly represents a captured asteroid. Also, both Eros and Itokawa show the presence of a mobile regolith (Cheng 2002, Saito et al. 2006). Millimetre resolution imaging of the surface of Itokawa has revealed it to be covered with unconsolidated millimetre-sized and larger gravels (Miyamoto et al. 2007). Locations and morphologic characteristics of this gravel indicate that Itokawa has experienced considerable vibrations, which have triggered global-scale granular processes like granular convection, landslide-like granular migrations, and particle sorting, resulting in the segregation of the fine gravels into areas of potential lows. It is believed that granular processes become major resurfacing processes for small size regolith-bearing bodies.

Surface imaging at high (mm) resolution contributes to the determination of the particle size distribution and can even resolve the geometric shape of the larger particles. Extending the size and shape analysis into the sub-millimetre range, for instance by surface imaging from very close distance while sampling on the surface of the NEA, is beneficial for understanding of the regolith processing either during its formation or while embedded in the body. Light-scattering parameters such as single-scattering albedo, scattering phase function, surface roughness, and porosity are further important physical parameters for the characterization of the regolith ensemble on the surface, also partially constraining the composition of the regolith material. The regolith structure and layering as well as the related different thermal conductivity also affect the thermal behaviour of the surface, *e.g.* the surface temperature and its changes with time and across the surface. Marco Polo will thus provide information that will greatly contribute to a better understanding of granular material behaviour in a low gravity environment.

2.2.2.6   *Compositional characterization and mineralogy*

Global compositional characterization of the entire target by Marco Polo is important primarily for the sample selection but also for scientific study of the nature of the object. In particular, it is crucial to determine the degree of homogeneity of the surface composition. Discovery of any inhomogeneities leads to the follow-up questions: *What is the cause of these surface differences? What are the implications of these differences with respect to the primitive nature of the asteroid surface?* Only by a complete and thorough characterization can these questions be addressed so that the optimal site for sample collection can be determined.

Spectral characterization in the visible and near-IR (400 nm – 3300 nm) will allow us:

- to explore the presence of the primary silicates such as olivine and pyroxene and their chemistry (abundance of Fe in olivine and of Ca in pyroxene);
- to understand the relation between clinopyroxene (high Ca) and orthopyroxene (low Ca);
- to identify the presence of undissociated water in minerals and OH groups like hydroxyls;
- to analyse the mineralogy of clays and other phyllosilicates, which can imply aqueous alteration processes;
- to identify the presence of carbonates, which are important to recognise because of their known presence in interstellar dust and their primordial signatures as unaltered material condensing directly from the solar nebula.

Primitive asteroids (tentatively associated with carbonaceous chondrites) can show on their surface the presence of hydrated silicates and are expected to include organic materials as indicated in Table 4. Marco Polo will allow us to verify this.

Knowledge of the hydrated mineral inventory of asteroids is important for deducing the origin of Earth's water, interpreting the meteorite record, and unravelling the processes occurring during the earliest times in solar-system history. The presence of the 3000 nm absorption feature detected on many primitive asteroids tells us that hydrated minerals can persist on the surfaces of airless bodies, presumably since early in the solar system's history. The band may constrain the maximum heating a body has experienced in the past. Water abundances as low as fractions of weight percent are observable around 3 microns (Salisbury et al. 1991).

Table 4: Possible signatures of organics in NEA near-infrared spectra (absorption regions for some important groups and vibrations).

Group	Type of Vibration (stretching, bending)	Wavelength in nm
Free OH	3ν (2nd overtone)	960-980
Bound OH	3ν (2nd overtone)	1000-1130
C-H (CH$_3$, CH$_2$)	3ν (2nd overtone) and combination	1150-1220 1360-1390
Free OH	2ν (1st overtone)	1400-1420
C-H (CH$_3$, CH$_2$)	Combination	1410-1450
Free NH	2ν (1st overtone)	1490-1540
Hydrogen bonded NH	2ν (1st overtone)	1510-1600
S-H	2ν (1st overtone)	1730-1750
CH$_3$ and CH$_2$	2ν (1st overtone)	1660-1800
C=O	3ν (2nd overtone)	1910-1950
Free OH	Combination	1920-1980
C-H and C=C	Combination	2150-2170
C-H (CH$_3$, CH$_2$)	Combination	2250-2380
CH	Aromatic CH stretch	3270-3290
CH	Aliphatic stretch	3370-3500

Spectral observations of the whole surface of the NEA will allow the identification of organics and their distribution on the surface.

Many of the major rock-forming elements and their complexes have fundamental vibration frequencies corresponding to mid-IR wavelengths, 5000–50000 nm. Thus, spectral measurements in the mid-IR will allow determination of the presence of silicates, carbonates, sulfates, phosphates, oxides, and hydroxides which show spectral signatures in these wavelengths (*e.g.* Lyon 1962, Hunt and Salisbury 1974, 1975). Phosphates and sulfates also have diagnostic absorption bands associated with their anion complexes (PO 3–4 and SO 4–4), as do oxides, nitrites, and nitrates. Sulfides and halogenide salts are also readily distinguished (Hunt and Salisbury 1975).

Emission spectra in the thermal infrared are well suited to addressing silicate mineralogies. This spectral region contains the Si-O stretch and bend fundamental molecular vibration bands (typically in the ranges 9000-12000 and 14000-25000 nm, respectively). Interplay between surface and volume scattering around these bands creates complex patterns of emissivity highs and lows which are very sensitive to, and therefore diagnostic of, mineralogy as well as grain size and texture. The three main types of feature observed (Figure 19) in mid-IR spectra are:

- Christiansen feature, which is directly related to the mineralogy and the grain size.
- Reststrahlen features which are due to the vibrational modes of molecular complexes. They are strongly dependent on grain sizes; for smaller grain sizes, the main reststrahlen features decrease their spectral contrast.
- Transparency features. In the spectral region where the absorption coefficient decreases, grains become more transparent. If the grain size is small, volume scattering occurs and transparency features are observable due to a loss of photons crossing many grains.

Asteroid spectra are affected not only by the chemical composition of the surfaces, but also by several physical parameters, such as particle size, porosity, packing, and thermal gradients. Mid-infrared spectroscopic analysis will give stronger constraints on this subject.
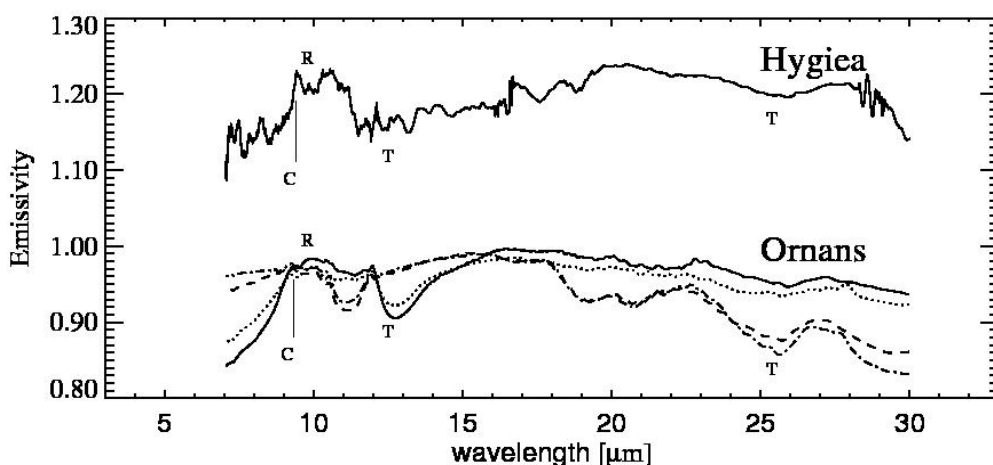
Figure 19: The emissivity of the main-belt asteroid 10 Hygiea, based on ISO data, compared with the laboratory emissivities of four samples of the carbonaceous chondrite meteorite Ornans (from Barucci et al. *2002) at grain dimensions smaller than 20 micron (continuous line), between 20-50 micron (dotted line), between 50-100 micron (dashed line), and larger than 100 micron (dashed-dotted line). Christiansen, Reststrahlen and Transparency features are noted as C, R, and T, respectively. The spectrum of Hygiea is vertically offset for clarity.*

2.2.2.7 Space Weathering

The effects of space weathering are different according to the heliocentric distances of the bodies and their surface composition. In particular, it is important to study the effects of space weathering on an NEA because it can give hints on how surface spectral properties are altered in the space environment, to provide ground truth for astronomical observations of reflectance and thermal emission. The visits to S-class asteroids by the missions NEAR and Hayabusa showed evidence of alteration of spectral properties by space weathering, which creates redder slopes and weaker mafic absorption bands. Results from the Sloan Digital Sky Survey suggest the opposite colour trends for C-class asteroids than for S-class asteroids (Nesvorny et al. 2005), although this is contradicted by other studies (Lazzarin et al. 2006). These results are very intriguing and generate many questions that can only be answered by returning a sample. We may also find evidence for surface movements on the asteroid through spatial variations of spectral features.

Marco Polo will measure any gas species expanding from the asteroid surface, which is crucial for the identification and localization of the physical processes acting on its surface as well as estimation of their efficiency. Identifying the rate of surface aging and space weathering, due to all types of release processes, is of particular importance for the airless NEAs. However, different release processes produce particles within different energy ranges (Wurz and Lammer 2003) and of different kinds of material.

The surface release processes relevant at NEA distances from the Sun are ion sputtering, photon stimulated desorption, thermal desorption and micrometeoroid impact vaporization (Plainaki et al. 2009). The ion sputtering process, active in many planetary environments in the solar system (*e.g.* Mercury, Moon, Europa), is defined as the removal of a part of atoms or molecules from a solid surface, due to the interaction of a projectile ion with target electrons and nuclei, as well as secondary cascades of collisions between target

atoms (Sigmund 1981). It is one of the most important processes, the products of which depend on the composition and the chemical structure of the surface. Photon stimulated desorption refers to the desorption of neutrals or ions as a result of direct excitation of surface atoms by photons (Hurych et al. 1988), whereas the thermal desorption exists when the thermal energy of an atom exceeds the surface binding energy. The micrometeoroid impact vaporization refers to the impact vaporization caused by micrometeoroids hitting the surface of an asteroid. Since the other surface release processes are mainly active on the dayside, micrometeoroid impact vaporization is likely to be the most important process for the night side of airless bodies (Killen and Ip 1999).

In particular, the analysis of released material from the surface of an NEA as measured by an orbital particle analyser will allow us to investigate:

- the composition of the escaping material and consequently the composition of the NEA surface;
- the processes happening on the surface of the NEA as a result of exposure to the space environment and collisions;
- the efficiency of each process as a function of environment conditions;
- the efficiency of particle release processes in the NEA's surface;
- the role of the surface release processes in the body's evolution.

Investigation of active release processes, as a function of external conditions and NEA surface properties, is crucial for obtaining a clear view of the body's present loss rate as well as for getting clues on its evolution, which depends significantly on space weathering. This investigation can be done by comparing the released particle observations with the solar wind data available from other near-Earth spacecraft and with surface remote sensing observation performed by other experiments onboard the Marco Polo orbiter. Discrimination between the contributions of different release processes will reveal the most important erosion mechanisms under different environmental conditions. Consequently, surface release processes and, in particular, solar wind sputtering investigation provide important clues on the evolution of a planetary body.

2.2.2.8   *Thermal properties*

The thermophysical properties of an NEA's surface are of fundamental importance in determining the surface temperature distribution, its diurnal and seasonal cycles and variation with depth. Mid-infrared spectroscopy provides the tool from which the temperature and thermal properties are derived or constrained using thermal models. Earth-based mid-IR observations are used for determination of asteroid diameters and albedos using the radiometric method. In the absence of detailed knowledge of shapes and rotation properties, simple equilibrium thermal models (*e.g.* Lebofsky and Spencer 1989, Harris 1998) are adopted and yield diameters to a precision of ~10 % and albedos to ~20 %, but do not provide great insight into the nature of the asteroids' surfaces. Thus, while this is a powerful tool, the disk-integrated data require models with a number of assumed or poorly constrained parameters and derivation of thermal properties is difficult. In-situ, spatially resolved measurements, in conjunction with shape, rotation and topography from imaging, will allow the investigation of heterogeneity in the thermophysical properties, the variation of emissivity with direction, possible improved regolith particle size determination for landing site selection, and validation of the radiometric method. In addition, the wavelength-dependence of emissivity will provide further constraints on surface composition and the improved thermal models can be used to determine the magnitude of the Yarkovsky and YORP effects (see the following section), of fundamental importance for the orbital and spin history of asteroids.

Thermal inertia is the key parameter affecting the diurnal variation of temperature (Figure 20). It represents the ability of the subsurface to store and conduct heat energy from the surface to the interior during the day and to return that heat energy to the surface through the night. Deriving and understanding the thermal inertia of a surface can help to identify the small-scale characteristics of that surface. Fine-grained and loosely packed material typically exhibits a low value of thermal inertia (Γ ~50 J m^{-2} K^{-1} s$^{-1/2}$ for large main-belt asteroids and for the Moon, Müller and Lagerros, 1998), while higher values (Γ ~2000) are common for rocks and exposed bedrocks. NEAs show a trend of higher globally averaged values (Γ = 100 – 1000; *e.g.* Delbo et al. 2007, Campins et al. 2009) with decreasing size, indicative of increasing dominant particle size in the regolith. Spatially resolved thermal IR data can be used to constrain the regolith particle size distribution in different regions (local gravity slopes, craters, correlations with morphological features or different surface mineralogies) to provide greater insight into surface evolution and particle mobility.

The surface and subsurface temperatures of a surface element of an NEA can be calculated using a thermophysical model. The average NEA surface inertia appears to be considerably greater than that of (large) MBAs. These data have been obtained from disk integrated models observed at one or more solar phase angles, and are therefore an average of the overall surface visible at that time. Spatially resolved data obtained at a range of rotational phases and local phase angles will allow study of the influence of local topography (shadowing and beaming) and regolith properties (composition, size distribution), providing more powerful constraints on the surface conditions.

The thermal history of an NEA is determined by its dynamical history and physical properties and is important for assessing the degree of thermal processing that any regolith sample may have undergone. This is of particular interest for the potential thermal processing of organics. Thermal models which are used to fit the observed IR emission continuum implicitly produce temperature profiles as a function of depth.

Although, in the absence of knowledge of subsurface properties, there is an *a priori* assumption that the thermal inertia is constant with depth (at least up to a few thermal skin depths – cm scales for particulate surfaces), models with depth-dependent properties are possible.

Thermal infrared data are of additional value for operations. The data may also provide sufficient constraints on the regolith particle size distribution to influence selection of a landing (touch-and-go) site suitable for the chosen sampling techniques.
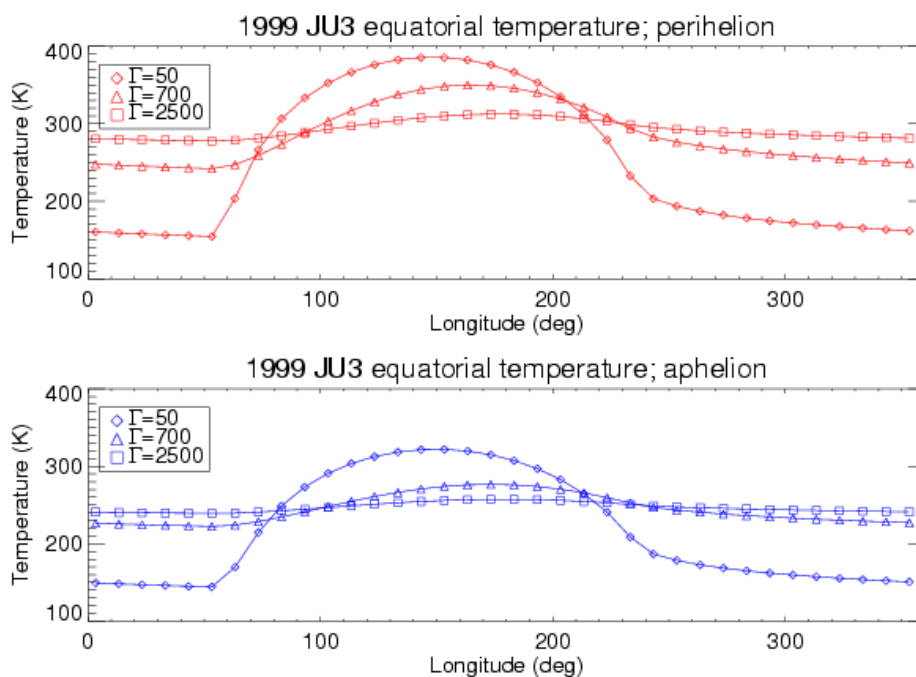
Figure 20: Diurnal temperature profiles (surface temperature as a function of the longitude) at the equator of asteroid 1999 JU3, the baseline target of Marco Polo, assuming sub-solar latitude equal to zero for different values of the thermal inertia (Γ). A bolometric Bond albedo of 0.03, an infrared emissivity of 0.9, a smooth surface and a rotation period of 7.7 hours are assumed. Upper panel: temperatures at perihelion; lower panel: temperatures at aphelion.

The spatial and rotational phase resolutions of in-situ mid-IR data, and the further constraints on surface properties from other instruments will allow major advances in quantifying thermophysical properties of NEAs and interpretation of surface evolutionary processes.

2.2.2.9   *Yarkovsky and YORP effects*

Knowledge of the thermal inertia (combined with a detailed shape model, spin properties, and mass) is essential to characterise thermal effects on the motion of an asteroid. Because of thermal inertia, which produces asymmetries in thermal radiation, radiation reaction can yield both a net force (Yarkovsky force) and a net torque (Yarkovsky-O'Keefe-Radziewski-Paddack (YORP) effect). Yarkovsky, a size-dependent effect which slowly moves asteroid orbits (by changing semimajor axes) is believed to be the dominant

mechanism for injecting small asteroids into gravitational resonances which causes their escape from the main belt and replenishes the NEA population. Although suggested theoretically in the late 90s (see *e.g.* Farinella and Vokrouhlicky 1999), the critical role of the Yarkovsky effect was only fully recognised, when a non-gravitational acceleration consistent with this effect was first detected in 2004 from the small NEA (6489) Golevka (Chesley et al. 2003). However, the resolved thermal flux from an NEA, which is held to be responsible for the acceleration, has never been observed.

It is important to point out that improved fundamental understanding of the Yarkovsky force will enhance our ability to predict high precision orbits of small NEAs, thereby improving our understanding of the asteroid impact hazard on Earth. For example, the NEA (99942) Apophis will pass close to Earth in 2029, but if it passes through small, ~600 m "keyholes" it would subsequently hit the Earth (*e.g.* in 2036 or 2037). Currently the uncertainty in the predicted orbit from Yarkovsky is larger than the size of the keyholes (Giorgini et al. 2008). Therefore improving our ability to characterise the Yarkovsky effect would allow us to determine whether the solution of a trajectory leading to a collision can be removed.

The YORP effect (Rubincam 2000) is analogous to the Yarkovsky effect, as it is also driven by asymmetric thermal radiation reaction forces, but now producing a net torque instead of a force. It is at the origin of the change of spin axis and/or frequency of small asteroids and has been directly measured recently for three NEAs (*e.g.* Lowry et al. 2007). Walsh et al. (2008) showed that YORP spin-up of an asteroid can lead to the formation of a binary and may explain the large fraction (15 %) of such systems in both the NEA and main belt populations.

The measurements made by Marco Polo will constrain all the main parameters involved in the Yarkovsky and YORP models, which can then be compared with the results from future observational campaigns for the asteroid.

2.2.2.10 Ground truth

For the first time, a complete characterization of a primitive object, at both microscale thanks to the sample and macroscale thanks to observations at the asteroid, will be performed.

The data obtained from the ground on the target asteroid (and on the asteroids with the same compositional characteristics) will be compared with the much more detailed observations obtained with Marco Polo allowing us to obtain a ground-truth on the telescopic data. This procedure will permit the calibration of the data reduction algorithms providing a check on the depth to which the interpretation can be pushed. A significant improvement in our knowledge of asteroids can be obtained through the interpretation of ground-based observations of a large number of objects which will never be explored by a space mission.

Moreover, an asteroid sample return mission will provide, for the first time, detailed laboratory analysis of a sample from a known source, for which we have "ground truth" measurements made at the asteroid, and Earth-based remote observations. This allows us to identify links between each of these observation regimes that can be applied to the wider asteroid population and meteorite collections:

- The degree of alteration and contamination of meteorite samples from atmospheric entry and exposure can be assessed by comparison with an unaffected sample,
- Laboratory reflectance spectra of individual components from a returned sample of a primitive NEA can be compared with telescopic spectra,
- The level of space weathering that each component has experienced can also be determined mineralogically and geochemically (*e.g.* noble gas studies), by comparison with the mineralogy and chemistry of known meteorite types,
- Physical measurements (*e.g.* size, shape, spin properties, thermal inertia) from spatially resolved in-situ observations can be compared with those inferred from unresolved Earth-based observations.

Only on the basis of such analysis will it be possible to apply the knowledge obtained from meteorites to the vast amount of information available from asteroid observations.

3   Scientific requirements

3.1   Introduction

This section links the science objectives presented in the previous section to detailed science requirements. The detailed science requirements for the Marco Polo mission were compiled by the Science Study Team at the very beginning of the study phase in the Science Requirements Document [SCI-RD]. The SCI-RD was used by the Study Manager to produce the Mission Requirements Document that contains the technical requirements of the mission. It was provided to the industrial study teams and forms the ultimate basis for the mission design.

This section links the top-level scientific objectives to quantifiable science requirements. Constraints and requirements on the technical elements of the mission, in particular the capabilities of the sampling mechanism and the scientific payload, will be derived. A justification is given for each individual science requirement in the context of the science objectives outlined in the previous section.

The main goal of the mission is

> *To return a sample from a near-Earth asteroid belonging to a primitive class*

that will allow the analysis of asteroid material in ground-based laboratories to study the formation of the solar system and its planets, characterisation of a near-Earth asteroid as a representative of a primitive solar-system body, and contribute to the field of astrobiology.

In addition, scientific information shall be collected to provide the context of the sample.

3.2   Structuring the mission

The scientific measurements at the asteroid are structured in three phases: 'global characterisation', 'local characterisation', and 'sample context measurements':

- 'Global characterisation' means to measure the properties of the whole NEA, on a global scale;
- 'Local characterisation' is the characterisation of up to 5 dedicated areas which are identified as potential sampling sites (see requirement SR-10 below);
- 'Sample context measurements' are measurements being performed at the actual sampling site.

Table 5 gives an overview of the required orders of resolution for the different phases. The rationale for the required resolution will be given in the later sub-sections.

Table 5: Resolution requirements for global characterisation, local characterisation, and context measurements.

	Spatial resolution for imaging in the visual	Spatial resolution for VIS/IR spectrometer	Spatial resolution for mid-IR instrument
Global characterisation	Order of dm	Order of m	Order of 10 m
Local characterisation	Order of mm	Order of dm	Order of dm
Context measurements	Hundred μm	-	-

3.3   Target selection

As outlined in Section 2, the main goal is to return a sample from a primitive object. As defined in Section 2.1, a *primitive asteroid* is considered to be a low-albedo object of spectral class C, D, P or T including sub-classes, according to the taxonomic classification by Barucci et al. (1987) and Bus and Binzel (2002a, b). In addition to knowing the spectral class of the object, enough information should be available about it from ground-based observations to allow a safe mission design. This will limit the size of the asteroid – if too small, these parameters cannot be characterised from the ground. In particular, the rotation period and the orientation of the rotation axis should be known; otherwise planning of landing operations will be difficult. If the object rotates too fast, it may have ejected its regolith, making it difficult to approach the object's surface

safely and to perform the sampling. If it rotates too slowly, it will be more difficult to obtain global coverage when mapping the object.

Taking all these points into account, the following detailed requirements were derived:

TS-10: Target type: The target shall be a near-Earth asteroid of spectral class C or D. Subclasses of C as well as B or T are acceptable. Note, however, that a scientific selection of the final target should take place at a later stage.

TS-20: Target size: There is no strong scientific requirement for a minimum target size. However, the target should be of a size such that:

   i) It should have sufficient gravity to allow the determination of the gravity field to an accuracy good enough to provide some constraint on the internal structure (e.g. determine the J2 coefficient to 10 %).

   ii) It is bright enough for fundamental properties (size, shape, albedo, rotation) to be estimated from ground-based observations.

As no precise numbers can currently be given for the above points, a limit for the absolute visual magnitude of H ≤ 21 shall be assumed, corresponding to a diameter D ≥ 340 m for a representative primitive body assuming a visual geometric albedo of 0.06.

TS-30: To allow mapping of the whole NEA in illumination in a reasonable amount of time, the maximum rotation period should not exceed 5 days.

TS-40: Minimum rotation period: The rotation period shall be greater than the limit for tidal disruption of non-cohesive bodies (~2.5 hours) to ensure the possibility of the presence of regolith for sample collection.

Taking all of the above into account, a number of asteroids were selected as potential targets. From the over 6000 known NEAs, only about 10 % have been assigned a taxonomical classification, and only a fraction of these are of the spectral classes considered here. To further constrain the list of possible targets, the Δv necessary to rendezvous with the asteroid and return to Earth was determined using a simple Hohmann-transfer and inclination change. While this is not representative for the optimized transfer Δv, it does allow a first-order estimate of the reachable targets. Setting a Δv limit to a reasonable upper limit for the mission (about 10 km/s) and also considering the factors such as the size and rotation rate constraints as listed above, about 15 asteroids were found to be suitable candidate targets. Performing optimization analyses including launch window effects, four asteroids were chosen. For a short list of feasible targets, see Table 6. After iterations during the initial phase of the industry system studies, the asteroid 1999 JU3 was selected as the baseline, as it leads to the optimum mission profile.

Table 6: Possible Marco Polo mission targets.

Number	Prelim. Designation	Taxonomic class	Estimated diameter in km (*)	Rotation period in hours
162173	1999 JU3	Cg	0.92	7.7
162998	2001 SK162	T	1.52	68
65679	1989 UQ	C	0.76	7.73
	2001 SG286	D	0.35	*tbd*

(*) calculated from H assuming an albedo of 0.06.

Section 2.1.3.1 outlines numerical studies which were performed to determine the origin of an NEA. This exercise was done for the baseline target of Marco Polo, namely 1999 JU3 and can easily be done for other potential targets. It is estimated that 1999 JU3 has about an 8 % chance of coming from the 3:1 mean motion resonance with Jupiter at 2.5 AU, and 92 % chance of coming from the inner main belt through the *v6*[4] secular resonance.

---

[4] The v6 secular resonance occurs when the precession frequency of the longitude of perihelion of the asteroid's orbit is equal to the sixth secular frequency of the planetary system. The latter is related to the mean precession frequency of Saturn's longitude of perihelion, but it is also relevant in the secular oscillation of the eccentricity of Jupiter.

Thus, while 1999 JU3 is a C-class object which is the dominant class in the outer belt, its current orbit is more likely to be reached from the inner belt (Michel and Delbo 2009). This is consistent with the result by Bottke et al. (2007) that the Baptistina family is mainly composed of C-class bodies. According to these authors, most of the current NEA population is dominated by objects that belonged to this family formed 200 Myr ago at 2.26 AU, in a region close to the *ν6* resonance, and have been sent to NEA orbits through diffusion mechanism such as the 3:1 or *ν6* resonances. According to these dynamical estimates, 1999 JU3 may be linked to this family. In that case, its age would already be constrained and a comparison with craters observed during the mission would allow checking this scenario. Having the possibility to link an object to a potential source region is a great asset, also for the sample analysis, that will be exploited whatever the target will finally be.

3.4   Sample requirements

Section 2.2.1, Table 2, lists the measurements that can be done for a given available sample mass. For verification of the results and the investigation of heterogeneity, multiple analyses by multiple laboratory facilities will be performed. This results in the sample having to be split into several pieces, each of which must fulfil the minimum mass requirements.

To increase the relevance of the mission for exobiological research, the potential for analysis of organics must be available. Referring to Table 2, this results in a minimum returned sample mass of about 10 g. Taking into account the need to share samples between laboratories and the need to retain a fraction of the sample for future experiments and advances in technology, the resulting requirement concerning sample mass reads

SA-040: The sampling device shall have the capability to acquire a minimum mass of tens of grams and shall return them to Earth.

This requirement refers to the technical capabilities of the sampling device. If, for example, the asteroid surface only allows sampling of a few grams, this is acceptable, as the surface properties cannot be predicted with high enough accuracy to always guarantee sampling tens of grams.

If the surface properties of the landing site allow, a good mix between small dust particles and larger particles should be returned. The interiors of the larger particles are protected from space weathering effects (Section 2.2.2.7). Solar radiation, cosmic rays, and, to a lesser extent, micrometeoroids, continuously bombard the asteroid surface. This will produce changes in the optical properties of the surface by vaporizing and sputtering material. More important for the later ground-based analysis they can also implant ions and modify the ionisation state of atoms in the material. However, the penetration depth of typical solar cosmic rays is only a few micrometres (galactic cosmic rays penetrate up to metres, but the flux and effects are almost negligible over the expected lifetimes of the NEA surface). If particles of sizes in the order of tens of millimetres up to several centimetres were returned, these could be cut apart and their inner volume will be free of these effects. This results in the following detailed requirement:

SA-060: The sampling device shall have the capability to acquire a selection of cm-sized fragments, plus a large number (ca. 10^4) of small (hundreds of μm-sized to mm-sized) particles.

Obviously, if the asteroid has an inhomogeneous surface like Itokawa (see Figure 21), which contains both very rough areas and smooth areas, then careful sample site selection is required.

An overview of the asteroid surface terrain will be obtained as part of the global characterisation. To allow a decision to be made on where to take the sample, the following requirement was formulated:

SA-10: It shall be possible to characterise up to 5 potential sampling sites before the actual sampling. "Characterise" means:

> *(a) Determine the particle size distribution of the regolith down to scales of the order of a millimetre;*
>
> *(b) Determine the rough mineralogical composition on scales of the order of a decimetre;*
>
> *(c) Determine the thermal skin depth indicative of regolith properties.*
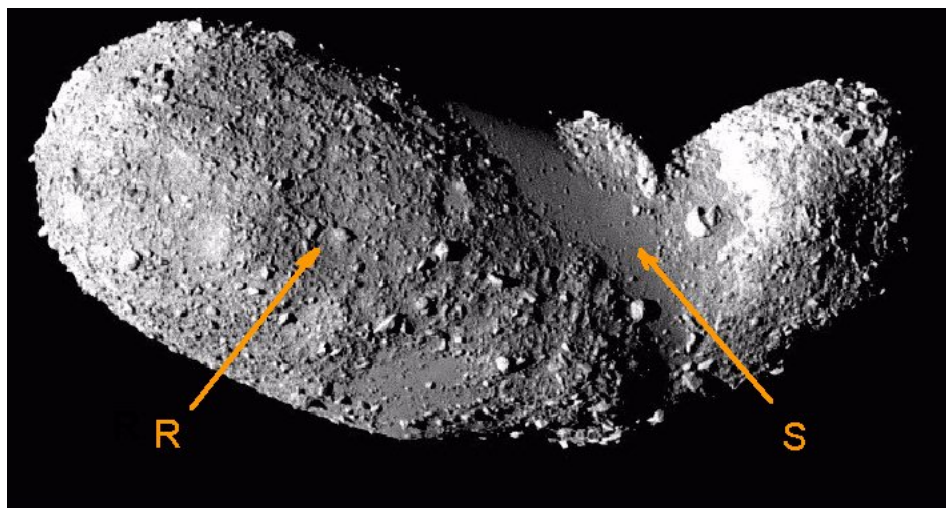
Figure 21: Asteroid Itokawa, showing smooth areas (S) and rough areas (R) (image courtesy: JAXA).

SA-020: It shall be possible to perform multiple sampling attempts (up to 3).

Items (a), (b), (c) of requirement SA-10 are detailed in Section 3.8 on 'local characterisation'. According to SA-020, if the first sampling attempt fails, two more attempts will be possible.

Another requirement for the selection of the sampling site is

SA-070: Highest priority for sampling shall be given to a target area that, from the global and local characterization of the NEA, appears to contain the most primitive material.

This requirement results in the need for both global and local characterisation. A 'primitive' surface area would be one which was only recently exposed to solar irradiation. This can be achieved by analyzing the morphology of the complete surface (*e.g.* age determination via crater counts), by measurements of the thermal inertia using near- and mid-IR observations to deduce the state of the surface regolith, and by mineralogical studies via near-IR spectrometry.

Shortly after sample acquisition, the sample will be transferred into a sample container and stored in the ERC. Any modification and contamination of the sample after this stage must be avoided.

Thermal modifications: The dynamical approach to study the source region of asteroids (Section 2.1.3) allows us to estimate how much time the asteroid may have spent at a perihelion distance smaller than a given value. 1999 JU3 may have spent about 8 Myr at a perihelion distance smaller than 1 AU, and 1.4 Myr at a perihelion distance smaller than 0.5 AU. Combined with a thermal model, these estimates allow us to calculate the temperature level the body may have reached on its surface or at a given depth. For instance, assuming a thermal inertia of 700 $J\ m^{-2}\ s^{-0.5}\ K^{-1}$ (Campins et al. 2009), the current temperature of 1999 JU3 is about 360 K at the surface and 300 K at 3 cm depth. Then, using the previous dynamical estimates, the probability that part of its surface were heated to temperatures above 450 K (350 K at the subsurface) is 50 % and this probability drops rapidly with increasing temperature (Michel and Delbo 2009). From these estimates, we can conclude that a sample taken from the depth of only 3 cm or even at the surface of 1999 JU3 should not have experienced extremely high temperatures. This is even more likely when considering that surface material is subject to motion, decreasing the exposure time to solar heat compared to the total time spent by the body at a given distance.

Taking this into account and assuming that the sample should not be heated excessively after sampling to avoid volatile components to evaporate, the following requirement for the maximum thermal temperature has been defined:

SA-050: After collection, the maximum temperature reached by the sample should not exceed +40 °C for long durations. For short durations of less than 1 minute, a temperature of up to +80 °C is acceptable.

The reason for distinguishing between long-term and short-term temperatures is the fact that directly after the sampling the sample mechanism may heat up quickly if exposed to the Sun (which would be difficult to

exclude from an engineering point of view). Comparing the temperatures with the possible thermal history of the material on the asteroid surface, a short-term exposure to 80 °C seems acceptable.

Contamination: Ideally, no atoms, molecules, or dust particles should get in contact with the sample after sample collection, both during the transport to Earth and later when on ground and handled in the laboratories. Extremely clean environments will be required when handling the sample. To derive quantifiable requirements, the accuracy with which the sample can be analysed using current measurement techniques was assessed. The contamination level for different sample constituents should be below the measurement accuracy. This results in the following requirements:

SA-090: During collection and storage (departure from NEA, cruise, Earth re-entry, ground retrieval and transfer to curation facilities) the sample shall be maintained free of organic and particulate contamination. The number of contaminating molecules deposited on the asteroid surface by the propulsion system shall be lower than 10^{14} cm^{-2} (goal 10^{13} cm^{-2}).

As a result of this requirement, special care will be taken in the design of the propulsion system. A mono-propellant system would result in the lowest contamination. However, current studies indicate that even with bi-propellant systems the contamination requirements can be fulfilled. However, thrusting towards the asteroid surface during the last phase of the approach should be avoided.

The following requirements address dust, liquid particles, and humidity:

SA-100: After being placed in the sample container, the sample shall not be contaminated by dust or liquid particles larger than 1 μm.

SA-110: Until the sample arrives in the curation facility, it shall be kept free of moisture from the atmosphere such that less than 0.1 ppm terrestrial water is present in the sample.

It will never be possible to fully avoid contamination. To distinguish between sample material and residual contamination, witness plates will be foreseen. This is addressed in the following requirements:

SA-120: The possible contaminants (e.g. propellant, S/C outgassing, etc.) shall be tracked in-situ (e.g. by using witness plates).

SA-140: During the complete manufacturing process of the spacecraft, special procedures shall be in place to keep all parts of the spacecraft clean to a level to be specified.

3.5   Ground-based laboratory facilities

The following lists the principal measurement capabilities of current laboratory instrumentation that will provide the results necessary to achieve the scientific objectives as given in the previous section. No quantifiable requirements need to be given, as the ground-based laboratories are not part of any items to be delivered. When the sample returns, the best available instruments will be used for analysis. Still, the following bullets give some feeling for the achievable results.

- The bulk elemental composition of the sample shall be measured both with a scanning electron microscope equipped with energy dispersive X-ray (SEM-EDX) spectrometry and using proton induced X-ray emission (PIXE) with elemental detectability of ≤ppm up to 10 nm depth and with a surface resolution of 1 μm.
- The bulk mineralogical composition of the sample shall be measured using the synchrotron X-ray fluorescence technique (XRF) with a resolution of ~1 μm.
- The bulk isotopic composition of the sample shall be measured with various mass spectrometry systems (NG-MS, GS-MS, ICPMS, TIMS) with an analytical precision down to ±10^{-5}.
- The isotopic composition of specific components shall be measured with SIMS and LA-ICPMS with a detectibility level down to ppb and a spatial resolution down to 100 nm.
- The bulk density of all fragments in the sample shall be measured with a gas-pycnometer with an accuracy of 0.25%.
- The bulk porosity shall be measured with gas (Hydrogen, Helium, etc.) porosimeter with an accuracy of 1 %.

- The reflectance spectrum shall be measured with UV-VIS-NIR spectrometry in the wavelength range from 300 nm to about 2.5 μm with a mean spectral resolution λ/Δλ of order of 200.
- The transmittance spectrum shall be measured with Fourier-transform infrared (FTIR) spectrometry in the wavelength range from 10000 cm^{-1} to 600 cm^{-1} with infrared microscope at spatial accuracy of 1 μm (synchrotron infrared source).
- The magnetic susceptibility shall be measured with superconductivity susceptometry with an accuracy of 1% relative to the iron content.
- The texture shall be measured with synchrotron X-ray tomography with a spatial resolution of 0.1 μm.
- The age of various mineral components shall be measured by various in-situ (*e.g.* SIMS, LA-ICPMS) and bulk measurements (*e.g.* TIMS, MC-ICPMS, NG-NS) with a precision and accuracy of $<10^6$ years on materials approximately $4.5 \cdot 10^9$ years old.
- The contents of organic compounds shall be measured with X-ray absorption near the edge structure (XANES) with a surface resolution of 1 mm and a detectability limit of 0.01 monolayer or with two-step laser desorption ionization mass spectrometry (L^{2}DMS) with 0.1 ppm detectability level with a surface resolution of 3 μm.
- The light element stable isotopic composition of individual organic compounds will be performed on nanomole amounts of individual compounds with analytical precisions of 0.1 to 1 ‰ (5 ‰ for D/H).
- The effect of space weathering by exposing parts of the sample to high-dose radiation shall be measured with the nano-secondary ion-mass spectroscopy (nanoSIMS) technique with a surface resolution of 50 nm and ppb-level of detectibility.

3.6   Requirements on the curation facility

As the curation facility is a 'deliverable' which must be ready at the latest when the sample is being returned to the Earth, requirements as for a space-based instrument have to be defined mainly addressing its cleanliness properties. The requirements as for the space element are repeated, but normally with more stringent numbers. The reason for this is because at least some particles are expected to be cut apart in the curation facility, exposing previously uncontaminated areas which will no longer be protected by the outer surface. The following requirements need to be fulfilled:

CU-010: The curation facility shall maintain the sample free of organic and particulate contamination. The number of contaminating molecules and particulates deposited on the sample surface during an expected stay time of 2 years shall be lower than 10^{13} cm^{-2} (goal 10^{12} cm^{-2}) and lower than 1 particle of size 1 μm on 1 cm^2, respectively.

CU-020: After arrival in the curation facility and extraction from the sample container, the sample shall be kept and processed in an environment equivalent to ISO class 4 (ISO 14644-1).

CU-030: After arrival in the curation facility, the sample shall be kept free of moisture from the atmosphere such that less than 0.01 ppm terrestrial water is present in the sample after an assumed stay time of 2 years.

CU-040: It should be possible to manipulate sample volumes from $5 \cdot 10^{-7}$ to 4 cm^3.

CU-050: The sample shall be classified through preliminary characterization according to its size and morphology (accuracy at least 0.5 μm), weight (accuracy 1% in the nanogram - gram range), and mineralogical phase (accuracy at least 1 % vol).

As it will never be possible to fully avoid contamination, the remaining contaminants should at least be tracked. This is addressed in the following requirement:

CU-060: The possible contaminants shall be tracked and monitored in-situ (e.g. using witness plates).

To ensure that later generations of scientists can make use of equipment which is not available yet at the time of return of the mission, the sample has to be available for a long time period and the SCI-RD gives the following requirement. The timescale is in line with ESA's Planetary Science Archive (PSA) lifetime.

CU-070: Undistributed parts of the sample shall be stored for 50 years in clean conditions.

3.7 Global characterisation requirements

Only a very small number of asteroids have been observed by spacecraft, most during fly-bys (most recently: asteroid Steins by Rosetta in 2008) and only two from an orbiting or hovering spacecraft (Eros by NEAR-Shoemaker, Itokawa by Hayabusa). There are significant differences from one location to another on the same object, as well as between asteroids, even though two of them (Eros and Itokawa) are of the same taxonomic class. Thus, to place a returned sample in context, the global characterisation of the target asteroid is of utmost importance.

Several properties need to be characterised to understand where the sample comes from and to place it in a geological context. Estimates must be made of the mass of the object, its porosity (thus its shape needs to be determined accurately), and its age. To characterise the surface properties of the asteroid – important to reconstruct the history of the sample – the detailed characteristics of the regolith have to be known. These can be obtained by measuring the thermal inertia and the mineral composition. To understand whether the sample is a typical representative of the complete asteroid or is just relevant for one geological region on the asteroid's surface, the properties of the complete object need to be determined.

Breaking this down further, the following items should be studied:

The surface topography will allow the collisional history of the asteroid to be deduced. For instance, is it a contact binary, as suggested for Itokawa (Fujiwara et al. 2006), or a monolithic object? The distribution of crater size versus frequency allows an estimation of the age of the surface, as done *e.g.* for asteroid Steins from the Rosetta fly-by images (Keller et al. 2009) or for Itokawa by using images from Hayabusa (Michel et al. 2009). To allow an accurate age determination, it is important to observe craters down to at least one metre in diameter. This results in a resolution requirement of the order of decimetres as given in Table 5 and is reflected in the SCI-RD as follows:

GR-010: The complete surface of the NEA shall be imaged in at least 3 different colours, in the visible range with a spatial resolution of the order of decimetres, and with local solar elevation angle between 30 and 60° (Note: it is acknowledged that depending on the rotation axis of the asteroid there may be areas which cannot be imaged due to illumination constraints).

GR-035: The spatial resolution of the relative 3-D topography (i.e. in relative coordinates) should be determined to an accuracy of the order of decimetres.

Imaging in at least 3 different colours will allow a first assessment of the geological properties of the target surface to be obtained (*e.g.* as for (951) Gaspra by Chapman et al. 1996). The illumination requirement was given to ensure that shadows are neither too long (which would 'hide' some of the surface) nor too short (which would not allow the determination of the local topography with proper accuracy). This will influence the selection of the orbit of the spacecraft.

It is assumed that the variation of mineralogical properties is not as large as variations in local topography. A typical ratio that is often used in instrument design is a factor of ten – thus, the resolution requirement for the near-IR measurements is 'of the order of metres'. While most mineralogical features in asteroid spectra are fairly broad, in particular, the lines indicating aqueous alteration are quite shallow. To clearly resolve them, a spectral resolution of $\lambda/\Delta\lambda$ in the order of 200 should be achieved. The final requirement in the SCI-RD reads:

GR-020: The complete surface of the NEA shall be imaged in the visible and near-IR wavelength range from 0.4 to 3.3 μm and with a mean spectral resolution $\lambda/\Delta\lambda$ on the order of 200 and a spatial resolution of the order of metres to characterise the mineral properties of the surface (Note: it is acknowledged that depending on the rotation axis of the asteroid there may be areas which cannot be imaged due to illumination constraints).

As mentioned above, the mass and density of the complete asteroid should be determined to a reasonable accuracy. The mass is needed both for engineering reasons to allow accurate navigation when landing the spacecraft, but also to determine the bulk density of the asteroid and thus constrain the collisional history. A reasonable goal is 1 % accuracy for the mass – which constrains the accuracy required for the shape determination, such that an accurate estimate of the bulk density can be obtained. Factoring in all dependencies, we arrive at the following:

GR-030: A shape model of the NEA shall be obtained with an accuracy of typically 1 m in height and spatial resolution with respect to the centre of mass, in both illuminated and un-illuminated regions.

GR-040: The mass of the NEA shall be determined with an accuracy of about 1 %.

The last two requirements will drive the resolution of the camera system and the laser altimeter, and the details of the radio science investigation.

The surface temperature, which depends predominantly on the structure of the surface material, will vary on the same scale as the topographic variations. However, the mean thermal properties can be derived for larger spatial units, resulting in a less stringent resolution requirement for mid-IR measurements. Thus, resolution requirements for mid-IR measurements are in the order of 10 meters. The detailed requirement reads

GR-060: The complete surface of the NEA shall be imaged in the mid-IR with a spatial resolution of the order of 10 m or better with a spectral resolution $\lambda/\Delta\lambda$ of the order of 200 to determine the wavelength-dependent emissivity, and hence identify mineral features in the range $8 - 16 \mu m$ (goal $5 - 25 \mu m$) and deduce the surface temperature distribution.

With slightly lower priority, a mapping of the neutral particle environment around the asteroid is required. Measuring the neutral particles that are released from the surface of the asteroid as a result of the exposure to the space environment will allow the study of the erosion processes and the relevance of space weathering on the asteroid surface. This will constrain the regolith properties on the surface and help in understanding the effect of space weathering on the returned sample. The related requirement is

GR-070: The flux, speed, direction and mass of atomic/molecular particles escaping from the surface should be measured to detect products of solar wind sputtering or other active release processes. The energy range from 0.01 to 1 keV shall be covered with an energy resolution of about 25 % and an angular resolution of 5° x 5°; the particles with energies <0.01 keV shall be measured with $m/\Delta m$ of about 50.

3.8   Local characterisation requirements

It is assumed that Marco Polo will perform the local characterisation of up to 5 potential sampling sites. The main goals of this local characterisation are to increase the measurement accuracy for dedicated areas by an order of magnitude. This means to *e.g.* increase the special accuracy of measurements in the visible range to a resolution of millimetres, to allow the precise determination of the regolith particle size distribution. As for the global characterisation, this should be done in three colour filters to get a first idea of the composition of the material:

LR-010: An area of the size of the expected landing accuracy around the potential sampling sites shall be imaged in the visible in at least three colour filters, with a spatial resolution of the order of millimetres.

As for the global characterisation, it is important to determine the mineralogical composition of the surface area. This is done via near-IR spectroscopy:

LR-015: An area of the size of the expected landing accuracy shall be imaged in the near-IR wavelength range to characterise the mineral properties of the surface with mean spectral resolution of $\lambda/\Delta\lambda$ of the order of 200 and a spatial resolution of the order of decimetres to characterise the mineral properties of the surface.

LR-020: An area of the size of the expected landing accuracy around any of the potential sampling sites shall be imaged in the mid-IR with a spatial resolution of decimetres and a mean spectral resolution of $\lambda/\Delta\lambda$ of the order of 200 to determine the wavelength dependent emissivity, and hence identify mineral features in the range $8 - 16 \mu m$ (goal $5 - 25 \mu m$) and deduce the surface temperature distribution.

As in the 'global characterisation' phase, monitoring the released neutral particles from the surface is important. From the shorter distance the expected flux will be much higher, allowing a better understanding of the area under study at the cost of coverage. This section repeats requirement GR-070:

LR-030: (As GR-070) The flux, speed, direction and mass of atomic/molecular particles escaping from the surface should be measured.   The energy range from 0.01 to 1 keV shall be covered with an energy resolution of about 25 % and spatial resolution at surface about 10 m; the particles at energy <0.01 keV shall be measured with $m/\Delta m$ of about 50.

3.9   Sample context requirements

The sample context requirements are defined as measurements obtained just before and after the sampling. They should cover a larger area than the actual sampling area (defined as the area covered by the sampling mechanism) to see any effects of the sampling on the surroundings. An area of roughly five times the sampling area – *i.e.* about twice the diameter of the sampling device – should be covered. The minimum measurement that must be performed is imaging. Other measurements would be beneficial, *e.g.* determining the bulk chemical composition via an APXS, however currently the duration of the landing on the surface is not long enough to allow these measurements.

Images must be taken before the sampling to study the structure (*i.e.* the arrangement of larger and smaller particles and dust). This allows distinguishing between a homogeneously mixed regolith and areas of larger particles or dust on a small scale. The structural property of the surface will likely be destroyed during the sample acquisition. In order to get a good coverage of small fragments, the resolution of the image should be better than a millimetre.

Images of the sampling site after the sample collection will allow an estimate of the friction coefficient of the regolith from observations of slumping of material. Areas that are not covered by material falling into the sampling hole may show possible layering of the regolith material.

These images can be obtained by a Close-Up Camera (CUC). Since the depth of field of a camera is restricted and expected to be much less than what is visible to the camera, it will need a focussing mechanism. A number of images with different focus positions must be taken.

To obtain colour information, images in at least three different filter bands should be taken.

The detailed requirements in the SCI-RD read:

SC-010: The regolith particle size distribution of the actual sampling site shall be measured before and after sampling to sizes as small as 100 μm (goal: 15 μm) in an area about 5 times larger than the area sampled by the sampling device.

The goal of 15 μm resolution extends the range of scales to study the texture of the regolith particles, considering that the typical size of structures on individual fragments like scratch marks or boundaries of mineral grains are of the order of several tens of microns. However, in the current design of the spacecraft the CUC would be located at the bottom side of the spacecraft and within a typical distance of several tens of centimetres up to 1.5 metres to the asteroid surface.

SC-040: An additional "local characterisation" shall be performed after the sample collection (i.e. fulfil LR-010 to LR-030 again).

It is assumed that the landing will be performed using optical navigation. A navigation camera will regularly take images when the spacecraft approaches the asteroid. The surroundings of the sampling area will be imaged with a resolution between that of the local characterisation campaign and the images taken by the CUC, and covering an area smaller than that covered during the local characterisation, but larger than the CUC images. It is thus desirable to have these images available for analysing the surroundings of the sampling area, leading to the following requirement.

SC-050: The images taken by the navigation camera (if any) during the descent should be made available to scientists upon request.

3.10   Other requirements

Appropriate calibration is essential for interpretation of the measurements of the scientific instruments on the spacecraft. Typically, all instruments undergo an extensive laboratory calibration before being launched into space. However, certain environmental conditions may not be reproducible on the ground, *e.g.* vacuum or the precise temperature environment. Also, the instrument characteristics may change during the launch phase. Thus a re-calibration of the instruments in flight is important. Typical calibration targets would be standard stars like Vega (for flux and spectral calibration of cameras and spectrometers) or extended surfaces, *e.g.* the Moon. Some of the Apollo landing areas on the Moon are the best space calibration targets because samples

with well-known spectral characteristics have been returned from them to ground-based laboratories. Alternatively, the instruments can be operated during planetary fly-bys to obtain calibration data. Also, these fly-bys will serve as a test for the instruments and it is considered of high importance to operate the instruments at those times. This leads to the following requirements in the SCI-RD:

OR-010: It shall be possible to calibrate the colour response of the instruments, by providing a calibration target (if mission analysis foresees a lunar flyby, imaging of the Apollo 16 landing site should be allowed).

OR-040: If the mission scenario foresees any planetary flyby, it shall be possible to switch on all payload instruments for testing.

It is required that more than one sampling attempt can be performed. This means that a way to verify whether a sample was taken has to be in place. This could be *e.g.* a system of break wires or a small camera inside the sample canister.

OR-020: After sample collection, a device or method shall allow verification that a suitable sample has been collected, giving a rough estimate of the volume or mass of the sample.

It is currently not required that the stratigraphy of the sample is maintained, as it is deemed too challenging from an engineering perspective. However, a physical deformation of the sample upon return to the Earth – *e.g.* by the landing shock – should be avoided. Based on literature studies, we assume that the possibly porous or fragile agglomerates should not be exposed to g-loads larger than 800 g:

OR-030: The sample shall not be exposed to a shock load higher than 800 g.

The SCI-RD also lists some additional requirements, which are not repeated here due to their lower importance. The reader is referred directly to the SCI-RD for those.

4   Model payload complement

This chapter describes the model payload complement to demonstrate that the science requirements can be satisfied within the nominal mission profile. This suite of scientific instruments, listed in Table 7, accomplishes all scientific goals as specified in the SCI-RD. Further details provided in the rest of this section describe specific examples of instruments that meet the requirements. An AO for the actual flight experiments will be published in 2010, which will solicit proposals from the entire science community.

The instrument designs use heritage from previous (Smart-1, Rosetta, MarsExpress, VenusExpress) and implemented (BepiColombo) space missions to the largest possible extent. All instruments have been supported throughout the mission study phase by DOI (Declaration of Interest) studies. In addition, breadboarding activities were initiated to mature and verify the technical design.

Table 7: Overview of the nominal payload complement and main resource budgets

	Wide Angle Camera (WAC)	Narrow Angle Camera (NAC)	Close-Up Camera (CUC)	Laser Altimeter
Weight [kg]	2.0	8.92	0.82	4.0
Dimensions [mm³]	237x172x115	520x380x197 250x170x120	364x78x68	150x100x100
Power [W] average	11.5	13.5	12.5	22
Data volume single measurement	67 Mbit	67 Mbit	67 Mbit	80 bit/shot

	Visible Near Infrared spectrometer (VisNIR)	Mid-Infrared spectrometer (MidIR)	Radio Science Experiment (RSE)	Neutral Particle Analyser (NPA)
Weight [kg]	3.6	3.0	Contained in the resources of the radio subsystem	2.2
Dimensions [mm³]	270x110x90 150x180x82	160x220x370	Contained in the resources of the radio subsystem	200x200x100
Power [W] average	18	2		11
Data volume single measurement	0.45 Mbit	360 Mbit	Data recorded in the ground station in real time	0.72 kbit

4.1 Sample analysis

The analytical techniques used on the ground to study the returned sample are divided according to scientific information that can be gained: bulk properties, mineral properties, isotopic composition, age dating, and chemical composition. An overview of analytical techniques and example instrument locations in Europe is presented in Table 8. This is not an exhaustive list but shows that within Europe the expertise for analyzing extra-terrestrial material is available. The analytical instrumentation is also available in laboratories not yet dealing with extra-terrestrial material.

Table 8: Overview of analytical techniques and examples of instrument locations in Europe and some facilities in the US and Japan.

Measurement	Instrument	Example Lab
Bulk Properties		
Bulk Mineralogy	X-ray Diffraction	NHM, London (UK), UPC Barcelona (S), DES Florence (I); UpU, Uppsala (SE); MSL, AarU, Aarhus (DK)
	Mössbauer Spectrometer	NHM, London (UK); UpU, Uppsala (SE); NHMS, Stockholm (SE); MSL, AarU, Aarhus (DK)
Bulk Chemical and Isotopic Composition	ICPMS	EES, OU (UK); ES, Oxford (UK); CRPG Nancy (F); Inst. Mineralogie Münster, (D),
	Elemental Analyser	PSSRI, OU (UK); DES, Florence (I); IGS Bern (CH); DES, Gothenburg (SE)
	Noble Gas MS	MPI Mainz (D); CRPG Nancy (F); ETH Zurich (CH); SEAES Manchester (UK); DESP, Kyushu (Japan); others
	INAA	IG, UCLA (USA); Lawrence Berkeley National Laboratory (USA)
	Laser Fluorination MS	PSSRI, OU (UK), CEREGE, Aix-en-Provence (F)
	X-Ray Spectrometer	UH, Helsinki (FI); UmU, Umea (SE); MSL, AarU, Aarhus (DK)
	Mass Spectrometer	NHMS, Stockholm (SE)
	EDXRF	UpU, Uppsala (SE)
Bulk Spectral Properties	UV-Vis-IR Spectrometer	RELAB, Brown Univ, (USA); NASA Ames (USA), INAF Naples & Catania (I), Univ. Lecce (I), UPC, Barcelona (S), Inst. Chem. Leiden (NL), NHMS, Stockholm (SE)
	VIS-SWIR:	FGI, Masala (FI)
Bulk Density & Porosity	Pycnometers	Vatican Observatory
	XRMT	UH, Helsinki (FI)
Magnetic Susceptibility	Susceptometer	CEREGE, Aix en Provence (F); MNA Siena (I)
	S-SQUID-M	UH, Helsinki (FI)
Mineral Properties		
Mineralogy	TEM	MN, Berlin (D), DES, Siena (I), Dep. Phys, Glasgow (UK); DEPS New Mexico (USA), others
	X-Ray Microscope	NHM, London (UK)
	Raman	INAF, Catania (I); PSSRI, OU (UK); IAS, Paris (F); IGS Bern (CH); UpU, Uppsala (SE)
	FTIR Microscope	INAF Naples (I), ES, OU (UK); ESR, Geneva (CH); IAS Paris (F); numerous others
Mineral Composition	EMPA	NHM London (UK), DES Florence (I); UpU, Uppsala (SE), numerous others

	ASEM	Everywhere
	Synchrotron-XRS etc	ESRF Geneva (CH); Diamond, Oxford (UK)
	TOF-SIMS	SEAES, Manchester; Inst. Mineralogie, Münster (D)
	SIMS	ES, Edinburgh (UK); MPI Mainz (D); CRPG, Nancy (F)
	NanoSIMS	PSSRI, OU (UK); MPI, Mainz (D); MNH, Paris (F); MSL, AarU, Aarhus (DK)
	Laser Ablation ICPMS	ES Oxford (UK); Mineralogie, Munster (D); ES, Lyon (F); numerous others
Isotopic Composition and Age Dating		
Stable, short and long-lived radionuclide isotopic ratios	SIMS	ES, Edinburgh (UK); MPI, Mainz (D); CRPG, Nancy (F)
	Laser Ablation ICPMS	ES Oxford (UK); Mineralogie, Munster (D); ES, Lyon (F); numerous others
	MC-ICPMS	ES, Oxford (UK); ESE, IC (UK); Mineralogie, Munster (D); ENS, Lyon (F); DES Pisa (I); DES Zurich (CH); DES Osaka (Japan); NHMD, Copenhagen (DK); others
	TIMS	ES, Bristol (UK); ENS, Lyon (F); NHMD, Copenhagen (DK); others
Stable and short-lived radionuclide ratios	NanoSIMS	PSSRI, OU (UK); MPI, Mainz (D); MNH, Paris (F)
Stable, cosmogenic, short and long-lived radionuclide isotopic ratios	Noble Gas MS	MPI Mainz (D); CRPG Nancy (F); ETH Zurich (CH); SEAES Manchester (UK); others
Stable and cosmogenic nuclide ratios	GS-MS	PSSRI, OU (UK); CRPG Nancy (F); Inst. Mineralogie Münster (D); others
	Accelerator MS	AAMS, Arizona (USA); AMS, Purdue (USA)
Chemical Composition		
Soluble Organic Inventory	GC MS	PSSRI, OU (UK); ESE, IC (UK); DC Antwerp (B), numerous others
	LC-MS	PSSRI, OU (UK), DCB Arizona (USA);
Soluble Organic Isotopic Compositions	IR-GC-MS	PSSRI, OU (UK), DCB Arizona (USA)
	IR-LC-MS	Life Sci, Oxford (UK), DCB Arizona (USA)
Insoluble Organic Composition & Structure	Elemental Analyser MS	PSSRI, OU (UK), IGS Bern (CH);
	Pyrolysis GC-MS	PSSRI, OU (UK); ESE, IC (UK); Inst. M. Chemistry, Paris (F) ; others
	NMR	Inst. M. Chemistry, Paris (F); Inst. Chemistry, Leiden (NL); UmU, Umea (SE)
	Circular Birefringence	Univ Barcelona (ES)
	TEM	MN, Berlin (D); DES Siena (I), Phys, Glasgow (UK); others
	Raman	INAF, Catania (I); PSSRI, OU (UK); IAS, Paris (F); numerous others
	FTIR	INAF Naples Catania (I), ES, OU (UK); ESRF Geneva (CH); IAS Paris (F); DC Antwerp (B), numerous
	XANES	ESRF Grenoble (F)
	TOF-SIMS	SEAES Manchester (UK); Inst. Mineralogie Münster (D)
	NanoSIMS	PSSRI, OU (UK); MPI Mainz (D), MNH Paris (F)

4.2   Narrow Angle Camera (NAC)

The asteroid is intrinsically a dark object, and in the determination of the performances of the instrument an average geometric albedo of 0.06 is assumed. The low contrast resulting from the low albedo makes it difficult to obtain high contrast images that are necessary to study the regolith properties well. A high contrast image can be obtained only if the optical contrast performance of the camera, including the residual diffraction contribution, is very high.

Optical designs with central obscuration are well known for their loss of contrast in extended object images and for their straylight problems. Therefore, for the NAC, an unobstructed and unvignetted optical design concept is very much preferred. Moreover, one of the main scientific objectives of the NAC is the generation of the Digital Terrain Model (DTM) of specific regions, which is based on matching of the windows obtained in different images of the same areas. The central obstruction reduces the matching capabilities and consequently the vertical accuracy, since it degrades the point spread function (PSF) sharpness and decreases the modulation transfer function (MTF).

4.2.1 Instrument Concept

The NAC optical design is based on an off-axis TMA (three mirror anastigmatic) configuration which follows the heritage of the OSIRIS cameras for the Rosetta mission, that are working in-flight, very well satisfying the original specifications, see Figure 22.

The NAC design is based on a focal ratio of 8 and a focal length of 660 mm, in order to provide the spatial resolution set in the scientific requirements. The diffraction limit has been calculated at 650 nm which is the middle of the spectral range coverage requested, in order to have an encircled energy greater than 70% all over the FOV and in the entire spectral range of interest for the camera. The NAC layout guarantees good aberration balancing over the full FOV of the instrument, an MTF greater than 52% and distortion less than 1.5%.

According to preliminary calculations the optical design provides a good S/N ratio and it is not necessary to have a panchromatic filter covering the entire spectral range. Following the scientific requirements one may think of one filter with broad-band coverage of 100 nm, and up to 7 filters with bandwidths of 5-10 nm. Their central wavelengths will be selected according to specific scientific simulations. The filters will be fixed in front of the detector.

The requirement to observe very close to the surface, i.e. at 200 m, is very demanding in terms of focus depth, which cannot be satisfied without introducing a mechanism moving at least one optical element in the camera. Furthermore, the focal plane position is sensitive to very small variations of the distance of surface elements which requires the use of autofocusing through an appropriate sensing device.

The NAC is designed around a detector of 2048 x 2048 pixels with pixel size of 10 μm to guarantee a pixel scale of 3 cm over the field of view of 1.7° x 1.7° when imaging the surface at 2 km distance. An array solution is preferred over linear detectors in order to allow snapshot image acquisition, which appears less critical with respect to requirements on pointing and stability, and reducing the number of images for a surface mosaic.

The image sensor is based on a Hybrid Active Pixel Sensor (APS) that uses CMOS readout technology. Its characteristics/capabilities of low power consumption, high radiation tolerance and very high Quantum Efficiency (QE) ensure a high performance of the camera system, even for short exposure times of the order of milliseconds, as may be required in the Marco Polo mission.
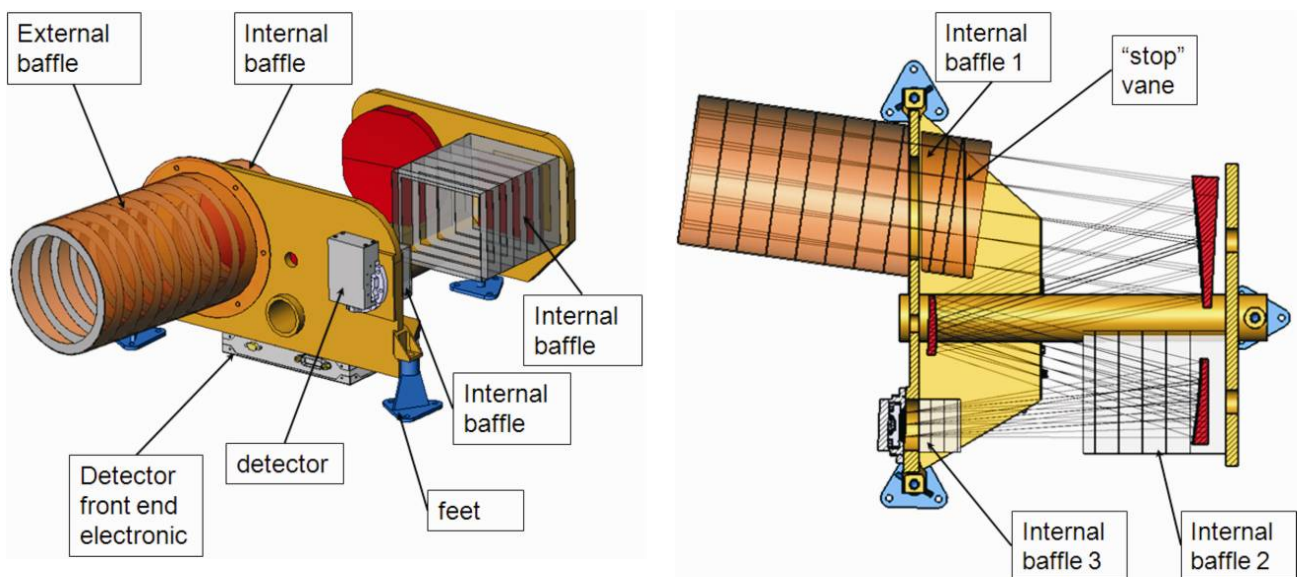
Figure 22: Conceptual drawing of the NAC.

The baseline for the command and data management is an integrated approach for the NAC and WAC into a single Command and Data Processing Unit (CDPU). The instrument is complemented by a general electronics package (for voltage, power, harness) that serves both the NAC and the WAC.

4.2.2   Operation requirements

The NAC optomechanics plus detector is fixed nadir pointing. The front end electronics is to be placed close to the detector system. Maintenance of the operating temperature range of the detector system and optomechanics is critical for camera operations and performance quality. Active control may be required (including DPU and general electronics). Knowledge of accurate alignment with the WAC is required, that with other imaging and spectroscopic instruments, in particular with the laser altimeter, is highly desirable. Laser ranging for focus distance estimation during NAC imaging at close distances should be available (otherwise on-board autonomous – but time consuming – NAC focusing sequence will be applied).

The NAC will be used for:

– nadir pointing during global mapping of the target
– nadir and off-nadir pointing (0-60 deg) for the DTM application of the target
– limb pointing for special applications like shape model details and activity search
– any pointing direction for in-flight calibrations and special applications at the target (satellite imaging)

NAC operations are done in quasi-continuous mode and snapshot mode at the target. Full orbit operations must be possible.

Default operations are by timeline; in exceptional cases (commissioning, in-flight problems, special science applications) commanding and data transmission in interactive mode may be required.

4.3   Wide Angle Camera (WAC)

The WAC is a small aperture camera for the visible wavelength range providing wide angle low resolution images of the target (or other fields), see Figure 23. Single bandpass imaging is sufficient for the WAC applications.
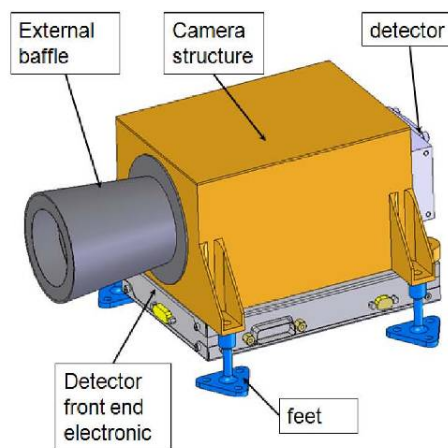
Figure 23: Conceptual drawing of the WAC.

4.3.1   Instrument concept

The WAC has a compact dioptric design with a 105 mm focal length; the focal ratio is kept as low as possible, but compatible with the scientific and the mechanical constraints, in order to achieve a wide field of view and high sensitivity. The lenses for this camera have to be small, simple, and efficient. The fewest number of lens elements is chosen. All optical surfaces are spherical or flat. A modified double Gaussian design is adopted, paying attention to lateral and axial color balancing, and keeping distortions as low as possible. The WAC will have a fixed focus set-up that supports sharp imaging (70 percent encircled energy per pixel) from infinity to about 200m above the surface. The encircled energy versus field position is always

above 70 percent per pixel and the modulated transfer function MTF is essentially above 70 percent over the field of view, indicating a camera optics of high contrast and high spatial resolution.

The field of view will be of 11.2°. An object of diameter of about 950m is fully covered in the field of view at 5 km from the surface (in order to support the task for shape reconstruction of the body and to search for a possible satellite at larger distances). Filter optics is not required though possible to be included (through a glass substrate in the light path); limitation of the transmission range of the WAC optics may have advantages for the global MTF of the camera. According to SNR simulations the WAC may be suitable to image the laser spot on the ground.

The same detector system is used for the NAC and CUC design. The mechanical structure accommodates the optics components, the external baffle, the detector, and the front end electronic. The electronic box and the external baffle are thermally decoupled from the camera structure in order to reduce the thermal load on the camera itself.

4.3.2   Operation requirements

The WAC optomechanics plus detector is fixed nadir-pointing. The front end electronics is to be placed close to the detector system. Maintenance of the operating temperature range of the detector system and optomechanics is critical for camera operations and performance quality. Active control may be required (including DPU and general electronics). Knowledge of accurate alignment with the WAC is required, that with other imaging and spectroscopic instruments, in particular with the laser altimeter, is highly desirable,

The WAC will be used for:

– nadir pointing for body shape imaging and rotation monitoring;
– limb pointing for special applications like shape model details and activity search;
– any pointing direction for in-flight calibrations and special applications at the target (satellite search) and for navigation purposes.

WAC operations are performed in quasi-continuous mode and snapshot mode at the target. Full orbit operations must be possible.

Default operations are by timeline; in exceptional cases (commissioning, in-flight problems, special science and navigation applications) commanding and data transmission in interactive mode may be required.

4.4   Close-Up Camera (CUC)

The CUC is assumed to be accommodated at the bottom side of the Marco Polo spacecraft looking downwards to the sampling area (*i.e.* fixed-mounted and nadir pointing, with the sampling area and the sampling tool included located centrally in the CUC field of view).

4.4.1   Instrument concept

The CUC camera consists of a rectangular shaped camera-head box (with a short straylight baffle, a folding mirror, the lens system with the focusing drive, and the detector), the detector electronics box and the external harness between CUC detector electronics and camera head and the main electronics of the camera system.

The CUC is a compact imaging device for the 400-900 μm wavelength range designed for microscopic resolution (better than 100 μm).

The CUC uses the CDPU and general electronics devices foreseen for the WAC/NAC camera system (the latter is assumed not to be in operation while the S/C is on the surface for sample collection).

The instrument consists essentially of three key components, i.e. (1) optics, (2) a multi-colour illumination device (so far solar illumination is assumed; the illumination device has still to be designed in the course of the industry study) and (3) a hybrid APS detector with readout electronics (similar to those used with the WAC and NAC). Furthermore, due to the intrinsically small depth of field of microscopic designs, a

focusing device is needed. The current design uses a linear translations stage that moves the lens with respect to the focal plane.

An optional illumination device could be added in case sunlight illumination turns out to be inadequate or puts unacceptable constraints for the landing scenario. The illumination device would consist of 4 arrays of light emitting diodes covering the R, G, B and near IR bands. In addition to enabling the characterization of heterogeneity of the asteroid surface, these colours will allow near true-colour reconstruction to be performed.

4.4.2   Operation requirements

The CUC will operate before and after each sampling operation. Prior to the acquisition sequence, the camera will be focused. This will be achieved automatically by acquiring several images at different focus distances, and using an algorithm that determines the best focus position based on image contrast. Alternatively, compatibly with the available data volume, the whole set of images taken at different focus positions could be relayed to Earth, so that a 3D reconstruction of the sampling site could be performed. Each data set will consist of 5 images, one for each LED channel, and one without illumination, in order to subtract the background scattered contribution. WAC and NAC are assumed to be out of operation while the CUC images are taken at the surface of the asteroid.

Default operations are by timeline; in exceptional cases (commissioning, in-flight problems, special science and focussing applications) commanding and data transmission in interactive mode may be required.
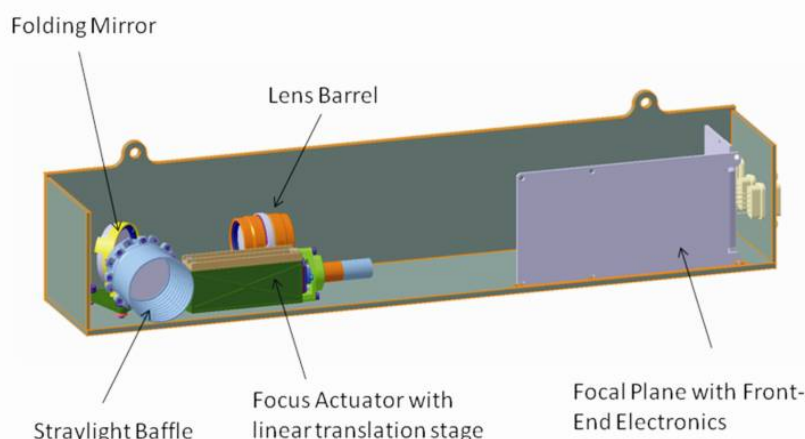
Figure 24: Conceptual drawing of the Close-Up Camera.

4.4.3   Heritage

- Rosetta Lander Imaging System.
- ROKVISS imaging system (on the International Space Station)
- ExoMars-PanCam-HRC (in development)
- Geochemistry Instrument Package Facility - Micro Rover Camera (ESA technology programme)

4.5   Laser Altimeter

The instrument will measure the two-way travel time of a laser pulse travelling from the instrument to the surface and back. A topographic profile along the ground track of the spacecraft will be produced. By interpolation, a global shape model will be derived. By measurements of pulse amplitude and shape, the reflectivity of the surface, as well as slope and surface roughness (within the footprint of the laser) can be modelled.

An optional scanning mechanism to increase the instrument field-of-view perpendicular to the spacecraft track is envisaged.

The scanner is a rotating circular wedge prism, which sits in front of a combined transmitting and receiving optics. The free aperture of this scanner is 4 cm or 2.5 cm, the rotation speed is low.

4.5.1   Instrument concept

As optical receiver systems are standard for space applications, the proper choice of the optical system is not critical. In contrast, the choice of an appropriate laser drives the complexity of the instrument.

The Marco Polo laser altimeter is based on the BELA (BepiColombo Laser Altimeter) wherever possible. While BELA differs from the Marco Polo laser altimeter in terms of performance and operation requirements, the basic principle is the same and requires the same laser hardware parts, laboratories, procedures, ground support equipment *etc*. which are all established and used in the BELA programme.

The laser box comprises two laser lines in cold-redundancy configuration. The same applies to the laser electronics, the digital processing unit and the power converters.

Two different instrument configurations are considered:

"MARCO I" is a classical laser altimeter like BELA with performance parameters specifically designed for the mission. This would reduce size, total mass, and required power compared to BELA. We therefore do not anticipate any major changes to the detector and onboard-software *etc*.

"MARCO II" is a laser altimeter based on single-photon counting. The detector is a silicon APS, operated as a photon-counting device, which requires only a few (< 10) signal photons for a detection event and consequently a very small laser. Such laser systems are now becoming operational in terrestrial airborne applications, and have been studied by a DLR-led consortium under ESA contract in 2002: Laser Altimeter for Planetary Exploration. Such a new system would have dramatically reduced size, mass, and power requirements. However, besides the development and space-qualification of the detector, a new pulse detection and processing scheme must be developed.
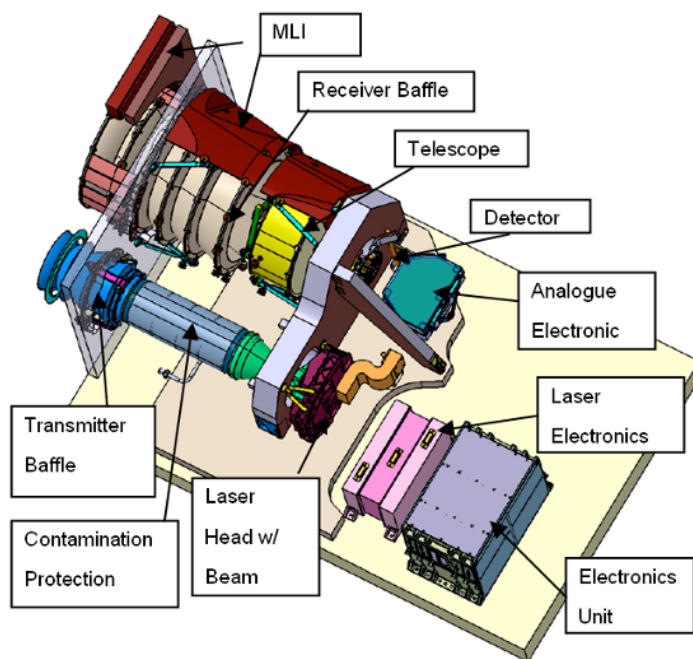
Figure 25: Sketch of the BELA laser altimeter.

4.5.2   Orbit, operations and pointing requirements

The instrument will operate during approach to the asteroid and during the spacecraft orbit phase. It will typically fire at a rate of 1 Hz, which ensures a seamless ground pattern in along-track direction.

Nighttime observations and daytime observations (which have to overcome the solar background noise) are equally possible. The pointing shall be accurate to within the size of the laser footprint. The instrument

should also be capable of 2-way (offline) ranging measurements to terrestrial laser stations for instrument alignment calibration, performance tests, and also for supporting the tracking of the spacecraft.

The divergence of the laser beam is 200 µrad, which results in a laser spot diameter of 1 m at a range of 5 km. At lower ranges, the footprint decreases below 1 m and the pulse repetition rate will be increased in order to obtain the seamless along-track spacing, which results in a finer grid spacing, *e.g.* 0.1 m from 1 km range.

4.6   Visible/near-IR spectrometer

A visible-near-infrared imaging spectrometer is an important instrument to characterize the surface mineralogy and to map the complete surface of the target.

4.6.1   Instrument concept

The instrument MAPIS (Marco Polo Imaging Spectrometer) is a classical slit imaging spectrometer in the spectral range 0.4-3.3 µm with a mean spectral resolution of about 200. It is composed of a refractive telescope imaging the scene at the entrance slit of the spectrometer. The spectrometer includes a collimator, a low groove density grating, an objective and the focal plane. Both collimator and objective are pure conical off-axis mirrors. A shutter is placed in front of the entrance slit to subtract the background images. Due to the low groove density of the grating, a sorting order filter is placed in front of the detector. Its variable pass band along the spectrum not only rejects unwanted orders, but also reduces background radiation seen by each pixel.

On a 2-D detector, this kind of imaging spectrometers records a 1-D image and a full spectrum for each point of the 1-D image. Either the relative displacement of the S/C with respect to the asteroid or a scanning system is needed to recover the second spatial dimension. In order to simplify complex S/C balancing modes, a scanning device is proposed.

Internal spectral calibration system using Fabry-Perot, allows checking the spectral registration before each session. The scanning system is used to point the calibration device.

External calibration by pointing at stars and the Moon is foreseen after launch. It is assumed that a DC-DC converter is provided by the instrument main electronics. The proximity electronics is based on an ASIC and a FPGA minimizing its mass and volume. The instrument and the detector shall be cooled by means of a radiator. The typical detector temperature will be 150 K.

MAPIS depth of focus is sufficient to allow observation during this phase without degradation of the performances. Therefore MAPIS can observe at all operation phases (FAR, GLO, LOC).
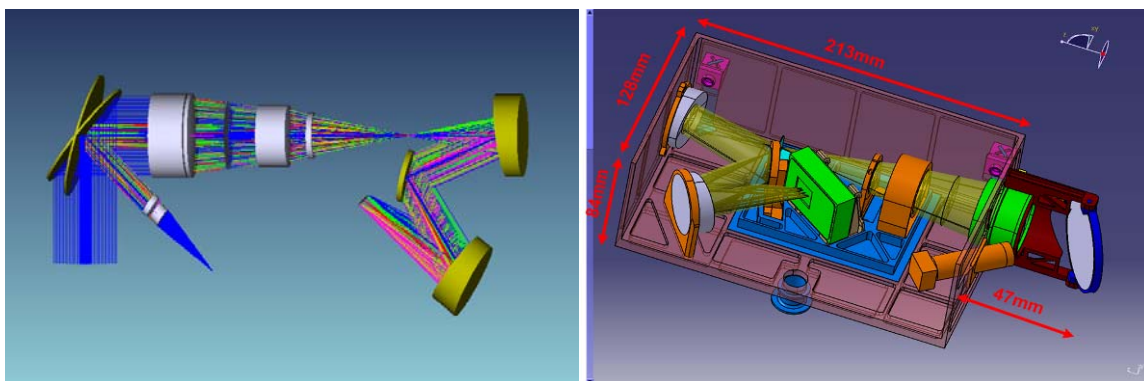
Figure 26: A concept for the optical head and mechanical design.

Figure 27 shows the key components of the proposed design of the instrument. The instrument (A) is electrically and mechanically linked to the proximity electronics (B). The proximity electronics drives and provides electrical power to the detector. The proximity electronics (B) is electrically linked to the main electronics (D) via SpaceWire. The main electronics provides stabilized voltages to proximity electronics and formats data. The cooling system (C) is electrically linked to the proximity electronics (B). The cooling

system (C) is thermally linked to the instrument (A) and the S/C thermal well (E). The main electronics (D) is electrically linked and data linked to the S/C (E) via a SpaceWire link.
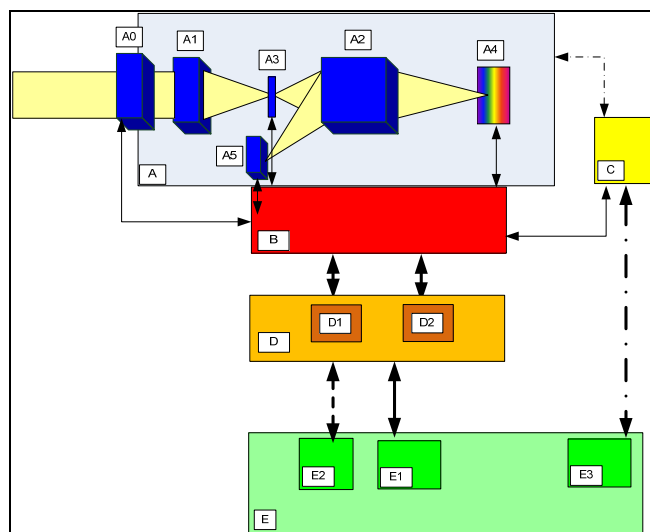
Figure 27: Instrument sketch and interfaces.

4.6.2   Heritage

The heritage comes from: MarsExpress, Rosetta, VenusExpress, BepiColombo for development of visible, infrared, and imaging spectrometers. Strong contributions come also from ExoMars and Hayabusa mission payloads. All MAPIS subsystems have been developed and used in previous planetary exploration programs.

4.7   Mid-IR spectrometer

The instrument is an imaging Fourier transform mapping spectrometer utilising a beam-shearing interferometer to generate a set of spatially resolved interferograms that are imaged onto a detector array. This allows spectral image cubes of the target body to be measured. The instrument covers the key spectral range of 400 to 2000 cm^{-1} (5-25 μm wavelength) with a maximum programmable resolution of 10 cm^{-1}. The extended spectral range is vital, as it includes important diagnostic mineral absorption bands as well as the thermal continuum due to the full diurnal temperature range of the object.

4.7.1   Instrument concept

The proposed instrument is the latest in a series of interferometers designed by F. Reininger of SpiLab, first breadboarded at JPL, and with later versions developed at SpiLab incorporating actively cooled optics and detectors, and then a flight like version assembled and tested in Oxford with passively cooled optics and detectors. The instrument uses a mid-infrared beam splitter and all reflective optics to image the interferogram onto a 640x480 micro-bolometer array, rather than using a traditional moving mirror arrangement. The mirrors are fabricated from aluminium alloy and are incorporated into their mounts. This leads to a highly reliable, compact, low mass and low power instrument with no moving parts except a rotary scan/calibration mirror assembly. The scan mirror is essential to allow measurements of the asteroid, of dark space, and of a low-power miniature black body target to maintain radiometric calibration during operation. The rotation axis of this scanning mirror is oriented so that a single mechanism can perform this calibration as well as scan the field of view across the asteroid.
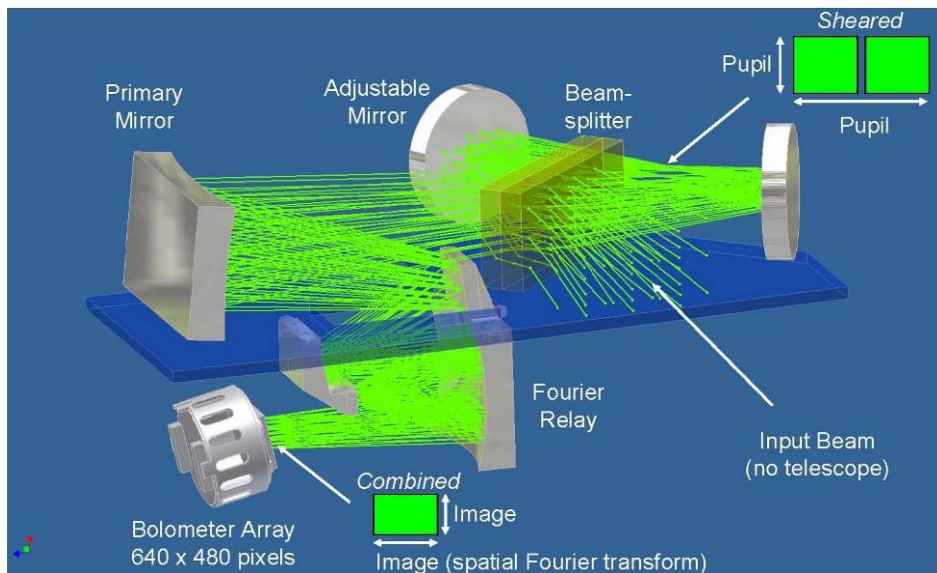
Figure 28: An optical layout of the mid-IR spectrometer breadboard. The dimensions are 160x220x370 mm³.

4.7.2   Orbit operations

The image cube generated by the instrument is illustrated in Figure 29. The asteroid is mapped by scanning the 480 cross track pixels across the surface. To maximise signal to noise, the measurements along the 640 pixel axis do not correspond to the same point on the target. Instead these must be scanned to assemble the interferogram of each single point.
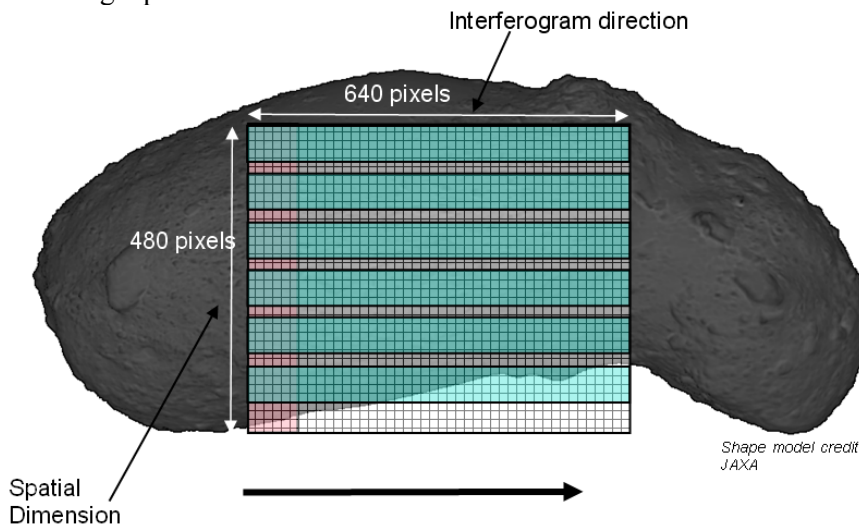
Figure 29: Scanning scheme for the mid-IR spectrometer.

The instrument is ideally suited to a "pushbroom" measurement approach in which the motion of the spacecraft around the target body provides the scanning to build up the interferograms. For most of the potential Marco Polo targets, however, the drift of the field of view due to the target rotation is comparable with that caused by the spacecraft motion. For the approach to be acceptable the orbit direction would have to be aligned with the rotation so that the cross track motion is less than about 10 % of the along track. The "pushbroom" approach remains a potential operating mode for some targets under consideration and could potentially reduce power consumption.

4.8   Neutral Particle Analyser (NPA)

Detecting and characterizing neutral atoms in the energy range of interest, <1 eV to 1.0 keV, in an environment of photon, electron and ion fluxes, requires 1) highly effective suppression of photons, electrons, ions and 2) two sensors for particles above and below 10 eV.

4.8.1 Instrument concept

Figure 30 shows the basic concept of the instrument. The incoming radiation made by neutrals, ions and photons impinges upon an aperture. The ions and electrons are deflected by electrostatic lens before the entrance. The neutral particles pass through an entrance of about 1 cm^2 divided for detecting both low energies and higher energies separately.

For low-energy particle detection and mass analysis, the neutral particles pass through a carbon nanotube system (C1) that ionizes the particles (Modi et al., 2003). The ionized particles cross an electronic gate (C2) that provides the start signal to the Time-of-Flight system (ToF - an example of such time tagging characterization is given in Brock et al. 2000). Then the particles are accelerated up to more than 1 keV and deflected by an electrostatic system (C3) and are detected by a MCP detector (C4) giving the stop signal. The ToF provides information about mass (since the spread in energy is assumed to be negligible).
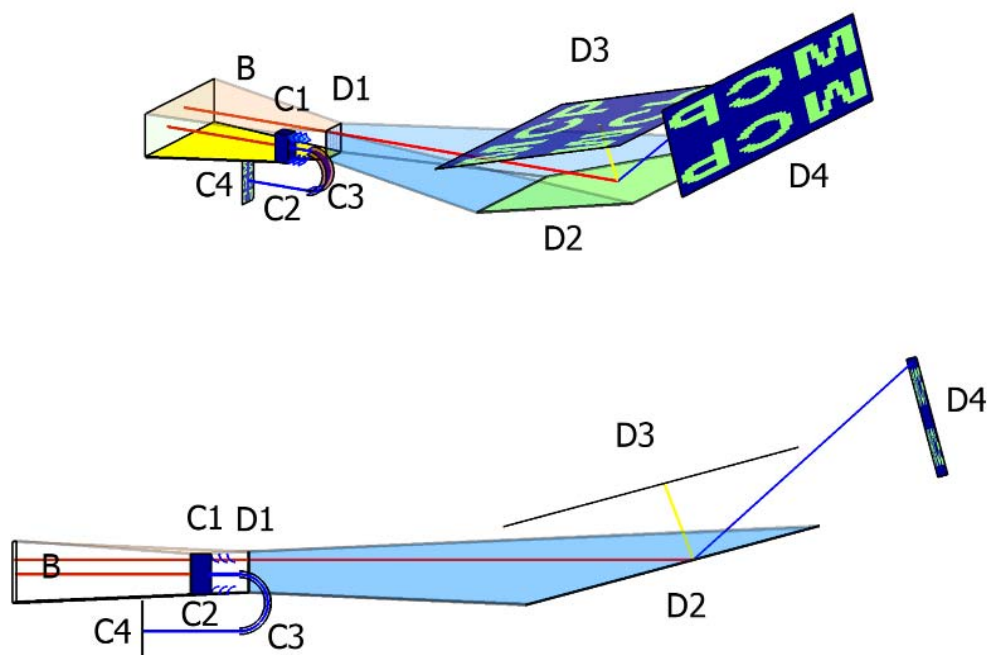
Figure 30: NPA basic concept.

In summary the NPA sensor consists of the following subsystems:

- A: Cover (not shown); B: Parallel plate collimator, biased with +5 kV and –5 kV;
- Mass spectrometer: C1: nanotube for ionizing lower energy particles, C2: electronic gate, C3: ESA, C4: MCP, C5: 2D Anode system (not shown).
- The particle (red line) enters from the left side (B), gets ionized (blue line) passing through C1, accelerated by C2, deflected by C3, and finally detected by C4.
- High energy detector: D1 two nanogrids and the shuttering system, D2: Conversion Surface; D3 MCP electron detector; D4: MCP ion detector; D5: 2D Anode system (not shown).
- The particle (red line) enters from the left side (B), passes through D1, hits D2, releasing electrons (yellow line) detected by D3. The particle is deviated and ionized (blue line). Finally, the ion is detected by D4.

For detecting particle between 0.02 – 1 keV, the neutrals pass through a double grating system (with slits of nanometric dimension) (D1) (Orsini et al. 2009) that provides photon suppression. A shuttering system allows the movement of the two gratings with respect to each other in order to permit the neutrals to enter the sensor only when the slits are aligned (open gate), which defines the start time. Then the neutrals fly into a ToF chamber and are converted into ions by using the technique of neutral-ion conversion surface (D2) (Wurz, 2000). The ionization efficiency is sufficient at the lowest particle energies and even increases for higher energies. When particles impact at the conversion surface electrons are released, even at low impact energies (Wieser et al., 2005). An electrostatic system accelerates the released electrons keeping them well

aligned to the original projection to the surface impacting point and pushing them toward the MCP detector, which also has position sensing capability (D3). The MCP will provide the stop signal for the ToF measurement as well as the angular direction of the velocity of the registered neutral particle. The atom, converted to an ion by the conversion surface, will be accelerated and detected by an MCP (D4) that will provide an additional stop signal. Moreover, for increasing the geometrical factor, the detector can be used in open-gate mode. In this way the ToF can be identified using as start the first MCP signal. However, the energy resolution will be lower, due to the indetermination in the energy and recoil angle after the impact on the conversion surface.

4.8.2   Interfaces and physical resource requirements

The FOV of the two detection systems is $5° × 30°$. The higher energy distribution will be analyzed with an angular resolution of $5° x 2.5°$ (high angular resolution mode) or $5° x 5°$ (low angular resolution mode). The FOV will be oriented towards the target surface. Hence, the spatial resolution on the NEA surface can be computed via the angular resolution and the distance between the spacecraft and the NEA.

Taking into account the instrument elements, the estimate of the high energy detector geometrical factor is in the range $4·10^{-4}$ - $2·10^{-5}$ cm^2 sr, and the mass spectrometer efficiency of about 0.14 counts$·s^{-1}·cm^{-3}$.

These sensor characteristics permit a detection of the estimated particle release. In fact, if the estimated particle flux due to IS from an NEA is 10^7 $cm^{-2} s^{-1}$ (Plainaki et al. 2009), more than 1200 counts are estimated in the high energy sensor for 1 minute of integration time. The estimated gas density is, at least, of the order of 10^2 cm^{-3} close to the surface. In this case, for a 1-minute integration time, about 1000 counts in the low energy sensor are expected. All the NPA operations will be controlled by an FPGA based microcontroller (Sensor Control Unit - SCU).

Additional requirement for GASP: Gas detection could be affected signal background due to spacecraft and thrusters outgassing. The first disturbance will be excluded thanks to the possibility to discriminate particles at different relative velocities (environmental particles and particles of spacecraft origin). The thrusters-emitted gas may significantly affect measurements during specific time periods. For this reason, NPA must be located far from the thrusters.

4.8.3   Heritage

ENA sensors already flown, in the energy range tens eV and few keV, are IMAGE/LENA, MEX/ASPERA-3/NPD, VEX/ARPERA-4/NPD, Chandrayaan-1/CENA, IBEX-Hi. The present concept is based on the SERENA-ELENA design (Orsini et al. 2009), to be on board BepiColombo/MPO because of its better angular resolution and UV noise suppression.

Many mass spectrometers have been flown in past space missions. The proposed design is based on the heritage of BepiColombo/SERENA-STROFIO (Orsini et al. 2009) for the ionization source and on BepiColombo/SERENA-PICAM (Orsini et al. 2009) for the electronic gating system, while electrostatic analyzers have been extensively studied in the frame of the CLUSTER/CIS instrument (Di Lellis et al. 1993; Rème et al., 1997).

4.9   Radio Science Experiment (RSE)

The precise determination of the mass of the target asteroid must be considered as a high priority of the mission not only for scientific reasons but also for allowing navigation at close distances to the body.

Mass determination or gravity field determination by radiometry is an established method. These experiments have been included in missions to or flyby at small bodies, like NEAR at Mathilde and Eros, Mars Express at Phobos and Rosetta at Lutetia in 2010 or at the nucleus of P/Churyumov-Gerasimenko in 2014/15. Although it may be possible to determine the mass to an accuracy of the order of 1 %, the higher harmonics of the gravity field will be very challenging.

4.9.1   Instrument concept

No extra hardware is provided by the experiment team, the observations are done by using the on-board radio subsystem which consists of

- transponder (redundant)
- Amplifiers (to be specified by the industry for mission requirements)
- Radio Frequency Distribution Unit (RFDU) which connects all (redundant) receivers and transmitters at various frequencies with the available antennas
- High Gain Antenna (size to be specified in order to meet required link budgets)
- Low Gain Antennas for near-Earth phases after launch or emergency operations

The operational radio link is a two-way coherent radio X/X. A hydrogen maser in the ground station is used as the frequency standard for generation/reception of the uplink/downlink signal. A transponder system working in the X/X band would also be used for spacecraft operations and communications.

An optional X/Ka band system for an improved Doppler signal compared to X/X only and for the correction of the plasma noise in combination with X/X could be envisaged, requiring a second radio science frequency band.
The following receiving and transmitting frequencies are common:

- X-band uplink (at approx. 7100 MHz)
- X-band downlink (at approx. 8400 MHz)
- Ka-band downlink (at approx. 32000 MHz)

The satellite radio subsystem shall then be capable of using a transponder for the X/X or X/Ka-band for both RSE and spacecraft operations and communications.

The transponder ratios of the coherent radio links shall be constant with the following numerical values:

- X-band transponder ratio: $k_X = 880/749$
- Ka-band transponder ratio: $k_{Ka} = 3344/749$

for the X-band uplink in the 7100 MHz frequency band.

4.9.2   Interfaces and physical resource requirements

No additional hardware is provided by the experiment team. The on-board radio subsystem as described above shall be used for the operations. The current scenario for the radio science phase is to slowly go down over ~ 60 days from a 5 km to a 2.5 km radius orbit. Radio science analysis showed that the level of uncertainty that can be reached after 60 days is the following: the mass will be known by 2.1 %, the J_2 by 5.1 % and C_{22} by 4.8 %. If an X/Ka link can be accommodated, an extra X/Ka transponder capability is available by industry and may be estimated to be 1.5 kg in mass at most.

4.10   Possible complementary instruments

This chapter comprises all instruments which have been identified as important to achieve the mission scientific goals or which may address other scientific questions beyond the key science objectives. These instruments are only recommended for implementation if the resource budgets of the spacecraft system allow doing so. Under no circumstances these instruments shall constrain the sampling procedure or other operational sequences throughout the mission.

The lander package including its payload is considered as a single self-standing item. The Alpha Particle Analyser, the Thermal Sensor and the Regolith Microscope/IR spectrometer must be in direct contact with the surface during data acquisition. Since an additional deployment device is currently not envisaged, these instruments have to be integrated into the landing feet. The Asteroid Charge Experiment (ACE) will also perform measurements while the spacecraft is orbiting the asteroid.

Table 9: Overview of complementary instruments.

	Asteroid Charge Experiment (ACE)	Alpha Particle X-ray Analyser (APXS)	Thermal Sensor	Regoltih Microscope / IR spectrometer	Lander
Weight [kg]	1.465	0.35	0.24	0.18	16.2
Volume [mm]	Various sensors	52($\varnothing$) x84 160x80x10	20x20x40 (e-box)	26 ($\varnothing$) x 158	
Power [W] average	1.5	1.5	0.5	1.2	na
Data volume single measurement	170 bit/s	192 kbit	100 bit	21 Mbits	

4.10.1 Lander package

Lander-based exploration has played an important role in the history of solar system science. In-situ information on the object at micro-scale is only accessible by the scientific payload onboard a lander. The instrument package will have the means to characterise physical properties (*e.g.* electrical, magnetic, thermal) of the landing site, as well as its surface and subsurface fine structure and composition (elemental, mineralogical, molecular). Complementary data from a lander science package can address questions such as: Are the returned soils and rocks representative of the bulk of the parent body? What are the macroscopic physical properties of the terrain from which the samples have been extracted?

A Marco Polo lander package study was performed to define a surface package that i) would accomplish *context science* by complementing the remote sensing observations from the main spacecraft and the sample analyses to provide ground truth information on materials down to the microscopic scale, ii) would accomplish *stand-alone science* that only a landed package can do such as geophysics and iii) could serve as *a 'scouting' vehicle* to guide the sampling site selection of the main spacecraft [MASCOT-SCIRD].

The study started out with a preliminary assessment of lander type, landing mode, mobility options and their impact on minimum achievable mass and volume. Differentiation was made between legged landers ('landing in a defined orientation'), landing packages ('landing with uncontrolled orientation') and the number of achievable landing sites (single vs. multiple) and thus the degree of mobility. The analysis showed that a legged lander in the mass range of 70 kg - 100 kg with full mobility, a weeks-long lifetime and ~14 kg P/L is feasible, given the weak gravity of potential target NEAs. Reducing size and capability, a legged lander of 30 – 40 kg was then conceived by giving up mobility, reducing lifetime and by cutting the P/L to ~10 kg. Finally, a mobile package version with a self-righting mechanism (MASCOT – XS) and 3 kg of P/L was found feasible for a total mass of 10-15 kg. The constraints imposed by the overall Marco Polo mission mandate this to be the baseline for MASCOT.

As a result of the study a MASCOT – XS lander with approximately 3 kg of P/L would have a total dry mass of ~10 kg, with subsystem maturity margins applied (including for the instruments) but without an additional system margin – see Table 10. Overall, the total mass of the MASCOT system would be ~16 kg which includes a system margin of 20 % on top of the subsystem maturity margin and MASCOT-related items remaining on the main spacecraft (*e.g.* antenna, transceiver, launch locks, push-off mechanism).

MASCOT-XS has a prismatic shape, Figure 31, to ensure that it can lay on two sides after landing on the NEAs surface and the self-righting and mobility system can interact with the terrain. This flat shell/disk concept offers the best P/L ratio and robustness for the uncontrolled landing. However, the design of the lander could change once a final P/L is defined, because it is strongly influenced by each instrument mass, volume and viewing requirements. Overall dimensions currently are 446 mm x 394 mm x 195 mm.

A model P/L was assumed for MASCOT sizing. During the Marco Polo mission studies, several instruments had been proposed for contact science at the NEA. The model instrument suite should focus on providing ground truth for an organic-rich, possibly aqueously altered C-class NEA for both the orbital observations and the laboratory analyses of the returned sample. Priority is given to non destructive sample analyses (chemistry and mineralogy), and/or macroscopic physical properties (*e.g.* terrain or internal structure) which are out of reach or cannot be acquired from orbital measurements alone.

Table 10: MASCOT XS mass break down

Element 1	MASCOT-XS							
					Target Spacecraft Mass at Launch		12,00	kg
					ABOVE MASS TARGET BY:		-4,23	kg
	Input Mass	Input Margin	Dry mass contributions	Without Margin	Margin %	kg	Total kg	% of Total
EL			Structure	1,06 kg	10,00	0,11	1,17	11,32
EL			Thermal Control	0,43 kg	11,16	0,05	0,48	4,62
EL			Mechanisms	0,49 kg	16,44	0,08	0,56	5,46
EL			Communications	1,09 kg	8,90	0,10	1,19	11,48
EL			Data Handling	0,40 kg	20,00	0,08	0,48	4,64
EL			Power	1,20 kg	13,33	0,16	1,36	13,15
DI	1,10	20,00	Harness	1,10 kg	20,00	0,22	1,32	12,77
DI	3,15	20,00	Instruments	3,15 kg	20,00	0,63	3,78	36,56
			Total Dry(excl.adapter)	**8,92**			**10,34**	**kg**
			System margin (excl.adapter)		**20,00 %**		**2,07**	**kg**
			Total Dry with margin (excl.adapter)				**12,41**	**kg**
			Other contributions					
EL			Mothership parts	3,08 kg	24,00	0,74	3,82	36,94
			Total wet mass				**16,23**	**kg**

Three scientific instruments could be accommodated on MASCOT comprising a camera system of ~ 0.3 kg mass and a microscopic spectral imaging system of ~ 0.7 kg. For a 3 kg overall P/L, 2 kg would then remain for an analytical instrument that could be a mass spectrometer, a XRD/XRF *or* a bi-static radar. Four further small sensors, an inclinometer, accelerometer, thermal sensor and an electric charge sensor, are proposed to be part of the model P/L to monitor some of the lander's engineering states and the NEA surface physical properties. They have a combined mass of ~ 0.15 kg.
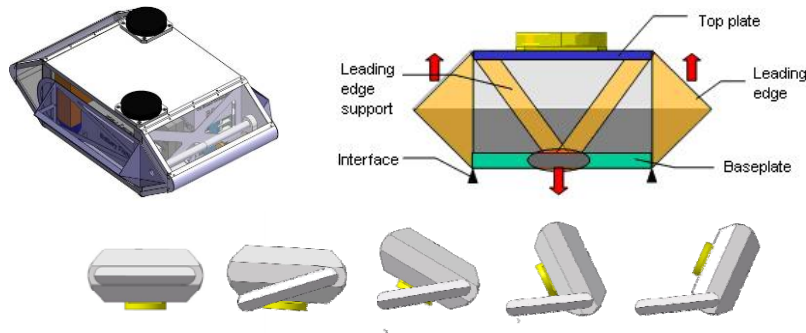
Figure 31: MASCOT - XS (top, left); Structural design (top, right); Self-righting sequence (bottom).

Upon separation from the main spacecraft at low altitude and low relative velocity to the NEA, the lander will undergo a ballistic descent and reach the surface with less than about 0.2 m s^{-1}, in a random attitude, followed by a bouncing and settling phase. MASCOT is equipped with a self-righting mechanism, both to enable a correct measuring position for the instruments and to offer mobility ('hopping'), see Figure 31 (bottom). Control of torque and speed of the lever rotation mechanism will allow for switching from self-righting to turning the MASCOT main body fast enough to lift off the surface of the NEA for a ballistic flight.

A detailed study on the thermal design of the lander was performed, see the DOI report [MASCOT-DOI].

4.10.2 Asteroid Charge Experiment (ACE)

This instrument package characterises the electrical environment at the asteroid through electric field and electron flux measurements, and assesses electrostatic effects at the time of sample collection.

4.10.2.1 Electric field measurement

The displacement current sensor is simply two small conducting plates connected to a logarithmic current amplifier. The displacement current, proportional to the asteroid electric field, is proportional to the detector surface area, whereas local plasma currents will only be related to the cross-sectional area. Two sensors of

differing geometry, but identical horizontal cross-sectional area, can therefore be used to remove the effects of local plasma currents and measure the displacement current only.

The displacement current sensor will be studied in parallel to the cylindrical electrodes as a complementary technique for asteroid electric field measurement.

4.10.2.2 CPEM

The CPEM (Circularly Polarized ElectroMagnetic waves) instrument, based on the Improved Plasma Analyser developed at UCL/MSSL, will consist of a top hat electron spectrometer measuring in the energy range 3 - 5000 eV with electrostatic deflector plates to increase its field of view to ±45º. The analyser will have a wide field of view (360º x 45º) to enable simultaneous sampling of both the solar wind as well as the asteroid.

4.10.2.3 PenRad

To assess the radiation dose on the collected sample, particularly at the time of collection of the exposed sample, but also during the return phase, a simple radiation sensor is proposed. A prototype was built at MSSL to study highly energetic electrons using an MCP. The proposed sensor will be a simplified low resource miniaturized system based on penetrating radiation seen by the MCP and a solid state detector, measuring both electrons and ions in the energy range 1-50 MeV.

4.10.3   Alpha Particle X-ray Spectrometer (APXS)

The Rosetta-Philae APXS system is described here as a typical instrument concept. The arrangement of the Rosetta detectors and alpha sources is strictly concentric. The X-ray detector is in the centre of the front side. Six alpha sources (total of ca. 30 mCi = 1.1 GBq of Curium-244) are placed on a circle around the centre of the sensor head at a movable holding device. On the outer periphery of the aperture, six alpha detectors are located concentrically to the alpha sources. The alpha detectors have a thickness of 300 μm, which makes them also sensitive to charged background particles. Therefore, they are operated with lower than usual voltages so that they are not fully depleted (volume reduction). This decreases the sensitivity to cosmic or solar energetic particles.

The sensor head is mounted within the foot of the lander. The nominal working distance between detectors and sample is ~30 mm (standard geometry) and is defined by a cylindrical apron. The end is surrounded by a ring that moves inward when it is brought in contact with the surface and opens two protective doors. The rear of the doors serves as a calibration target when in closed position. The nominal diameter of the surface sample is 25 mm.

4.10.4   Temperature sensor

In-situ temperature sensors will provide a ground-truth measurement at the NEA surface for the temperature distribution derived from remote sensing IR spectrometry. Sensors placed on small probes can measure the near surface temperature gradient, constraining the regolith properties used in the thermal modelling.

A suite of thermal sensors can be mounted in the feet of the spacecraft, with some sensors on a thin needle-like structure penetrating the first few centimetre of the regolith. The current design comprises 2 units per foot. Another possible mounting location is the sampling tool. The actual accommodation has to be explored during the development of that facility. The temperature measurements also provide monitoring of the working condition of the sampling head. It is planned to place 3 sensors at this location. Platinum Resistance Thermometers cover the temperature range from -200 to +600 °C. For example the "PT100" sensor would be a good candidate for an application on an asteroid. The total weight including sensors, cabling and electronic box is 240 g. While the sensors themselves have a size of a few mm only the electronic box will be in the order of 20x20x40 mm.

4.10.5   Regolith microscope and IR spectrometer

Remote spectroscopic imaging of the surface, even at high resolution during local characterisation, provides an average spectrum from all regolith particles in the FOV. In-situ spectroscopy can provide information on

individual regolith particles to investigate the mineralogy and spectral diversity. Microscopy can yield information on the size distribution and texture or grains at higher resolution (but over a smaller area) to complement the CUC imaging. A combined microscope and IR spectrometer is proposed, based on the WatSen instrument developed for deployment on Mars.

Attenuated total reflection (ATR) spectroscopy is a powerful technique for studying the absorption IR spectra of a variety of materials. Because spectral reflectance features are almost always dependent on surface properties (flat or uneven, rough or smooth, *etc.*), the signal generated must be from a representative grain surface. This is best achieved by placing the sensor in direct contact with the surface of the grain; the most appropriate sensor type to achieve this measurement is an ATR sensor. It is based on the phenomenon of total internal reflection, occurring when electromagnetic waves in a transparent dielectric medium impinge onto the surface of an absorbing medium with a lower index of refraction and with an angle of incidence above the critical angle. An evanescent wave is excited which propagates a certain distance (penetration depth) into the sample. Some of the energy of the evanescent wave is absorbed by the sample at particular wavelengths and this affects the signal received by the detector. In addition to a light source and the ATR probe itself, a spectral separation technique (spectrometer) is needed to obtain a useful spectrum.

An ATR spectroscopy system based on a linear variable filter spectrometer and a linear sensor array is very competitive with regards to robustness, physical size, power consumption and performance. In particular it is possible to implement this concept with no moving parts. It is also possible to use a sensor technology that has no or very moderate requirements for cooling (thermoelectric), further reducing the complexity and power consumption of the system.

An integrated optical microscope images the previously spectroscopically investigated surface with a resolution of about 8 μm. This delivers additional information on the grain size distribution and optical properties of individual regolith grains.

5   Mission design

This chapter describes the overall Marco Polo mission profile and the design of the space segment. It was studied by three European industrial consortia from September 2008 to September 2009, leading to the design options A, B and C presented below..

This scenario has been developed with the primary goal of maximizing the science return while coping with the technical and programmatics constraints of the Cosmic-Vision programme [CV]. Towards this goal, it builds on a comprehensive set of engineering and programmatics requirements, respectively described in the Mission Requirements Document [MRD] and the Requirements and Interfaces Document [RID]. These are derived from the science requirements and the payload interfaces (chapters 3 and 4).

All trade-offs and analyses assumed European capabilities but the collaboration scheme is open and international collaboration may be sought for. Section 5.1 gives an outlook of the high-level mission trade-offs leading to the selected baseline mission architecture. Chapter 5.1.2 describes the selected design features common to options A, B and C while Sections 5.1.3, 5.1.4 and 5.1.5 separately describe the elements specific to each design option. Section 5.1.4 (option B) and 5.1.5 (option C) mainly point out design differences with Section 5.1.3 (option A) in order to avoid repetitions but the options are presented in a random order.

All these studies benefited from Hayabusa heritage (e.g. NEA descent and landing GNC and Earth re-entry).

5.1   High-level trade-offs

An extensive trade-off involving cost, operational and development risk, technology readiness, science return as well as mass feasibility as primary criteria was performed at mission architecture level as well as for the key capabilities: asteroid descent, touchdown/landing, sampling and Earth re-entry.

5.1.1 Mission architecture

The space segment of an asteroid sample return mission involves various functions: interplanetary outbound and inbound transfer, asteroid orbiting, descent, sampling, re-ascent and Earth re-entry. Combining them all yields more than 50 different architectures. However, preliminary screening shows that a reduced set of options are meaningful in the cost-constrained environment of Cosmic Vision while taking into account collaboration opportunities. These architectures were analysed for four primary asteroid candidate targets: 1999 JU3 (Cg-type), 1989 UQ (Ch), 2001 SK162 (T) and 2001 SG286 (D) with both electric and chemical propulsion.

Following this, it was determined that a single spacecraft and a separate re-entry capsule, to the target 1999 JU3, relying on chemical propulsion, led to very promising launch mass margins while being the most cost-efficient mission scenario and was thus selected as a baseline. Preliminary analysis suggests that the concentration of bi-propellant-induced contaminants on the asteroid surface is within the scientific requirements. Nevertheless, an additional mono-propellant system for close-to-surface operations is kept as an option. Further activities are planned to determine whether it is required or not (Table 15). Chemical-based transfers to 1989 UQ [CDF FR] and 2001 SK162 also seem to give access to a mass-feasible mission profile (Table 11). It is also expected that the analysis of data from current sky surveys and upcoming ones, such as Pan-STARRS and LSST, will discover many more NEAs. Among those it is hoped that many will be of primitive nature and may turn out to have adequate physical properties and to be easily accessible with similar mission constraints. In order to confirm that, these candidate NEAs need to be observable on time shortly after their discovery with more powerful observatories so as to infer their spectral and physical characteristics. Gaia will in addition survey asteroids in such a way that it can directly provide physical and spectral information about not yet classified NEAs.

Target	Launch date	Escape declination (degrees)	Escape V_{inf} (km·s^{-1})	Out/inbound Δv (m·s^{-1}) incl. margins	Re-entry velocity (km·s^{-1})	Mission duration (years)
1989 UQ	September 2017	0	3.45	963	11.9	6.2
2001 SK$_{162}$	July 2018	-3.4	2.7	1200	12.7	7.3
1999 JU$_3$	December 2018	0	3.2	1394	11.9	5

Table 11: Examples of trajectory parameters to alternative potential targets (upper two rows) and to the baseline target. All scenarios involve a direct escape by Soyuz-Fregat upper stage, chemical propulsion-based spacecraft and asteroid stay times > 10 months.

5.1.1.1 Descent, touchdown/landing and sampling strategy

The sampling strategy is a central element of the Marco Polo mission and the resulting sample acquisition, transfer and containment system can be seen as the "backbone" of the spacecraft design. A detailed trade-off of various sampling tool-transfer system combinations coupled with the top-level concepts presented in Figure 32 was performed.

Sampling strategy	Duration of surface operations	Sampling tool location	Dedicated landing system	
1. Short-term landing	10-20 minutes	Separate transfer system	YES + down-thrust	
2. Short-term landing	10-20 minutes	Landing legs	YES + down-thrust	
3. Long-term landing	Hours/days	Separate dextrous transfer system	YES + anchoring	
4. Touch and go	< 5 seconds	Landing legs	YES	
5. Touch and go	< 5 seconds	Horn or tip of long boom	NO, control required	
6. Hover and go	> 5-10 minutes	Tip of long boom	NO, fine control required	
7. Hover and go	> 1-2 minutes	Harpoon with winch/tether retrieval	NO, control required	

Figure 32: Sampling strategy concepts

Option 3 was discarded due to higher cost and technical risk due to the need to anchor on a relatively unknown surface. Preliminary analysis showed that options 5 and 6 led to a high development risk for ESA while option 7 yields a higher technical risk. Leg-based landing (e.g. Philae) or touch and go lead to the lowest technology development risk and thus cost can be better controlled. It has the highest chance of success in order to collect tens of grams of material and gives access to a wider range of sampling tools and sample transfer techniques, including robust volumetric sample collection techniques and deterministic transfer mechanisms, which have been matured through various programmes (Figure 33) such as the Comet Nucleus Sample Return (CNSR), Philae, Beagle 2 or ExoMars and generic ESA technology activities. Options 1 and 4 were finally selected. Option 5 was used for Hayabusa and is considered for follow-up missions by JAXA to limit the risk associated with the large solar arrays, resulting from the use of solar electric propulsion.

Figure 33: Sample simulant material collected in various tests based on the coring method. Fine powder mixed with cm-sized fragments on the left and in the centre, and hard core on the right.

The use of landing legs also decreases the technical risk by decoupling touchdown and sampling operations, which also allows simpler testing. The higher maturity of these capabilities in Europe is a key asset given that all technologies must reach a Technology Readiness Level (TRL) 5 by the beginning of 2012 for M-class missions. In this context high landing accuracy is an asset as the spacecraft clearance with respect to the surface is lower than for other options. Yet, data from NEAR and Hayabusa show that large safe surface areas exist, even in the case of the particularly hazardous surface of Itokawa as illustrated on Figure 34, based on measurements made by Hayabusa. As a starting requirement and in order to give access to a large

part of such a surface a landing accuracy of ~ 5 m was thus targeted during the assessment study. Discussions with scientists however suggest that it is highly likely that safe sampling sites as big as tens of meters can be found on a kilometre-sized asteroid. Thus a landing accuracy in the order of tens of meters would still allow fully meet the mission objectives with an acceptable risk level. Furthermore it is worth noticing that both Hayabusa and NEAR actually landed on an asteroid although they were not designed for that and Hayabusa reached its sampling site with a touchdown accuracy in the order of 30 meters.
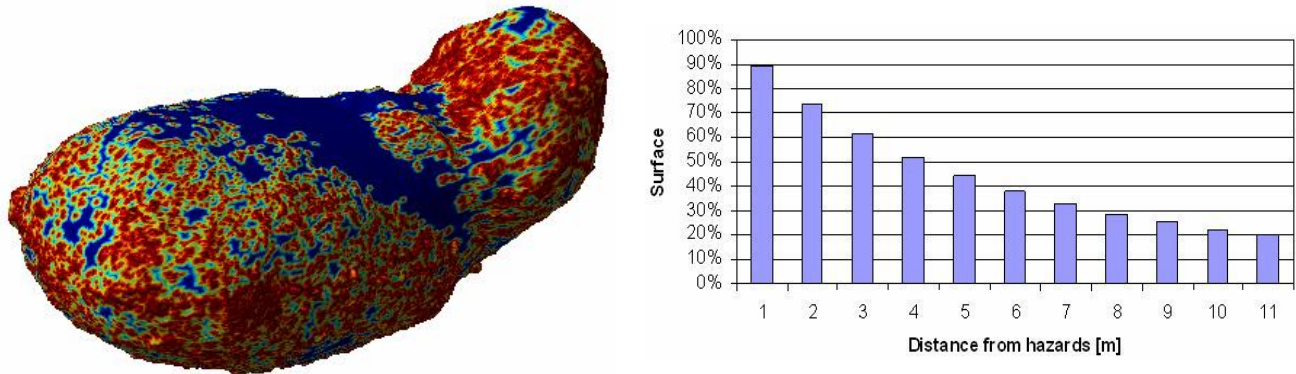
Figure 34: Itokawa surface accessibility. Hazardous areas (in red) → distance from hazards ~ 0m, safe areas (in blue) → distance from hazards > 10 m. Hazards defined as a slope of 10 degrees over 1 m distance. For example, 10 m landing accuracy gives access to ~ 20% of the Itokawa surface.

5.1.1.2   Earth re-entry

Finally, a direct Earth re-entry is baselined. Landing shocks can be mitigated via parachutes or impact absorption material. Since Marco Polo is classified as unrestricted sample return for planetary protection [PP] and because it yields a lower capsule mass, a parachute-based approach was selected.

5.1.2   Baseline mission scenario, analysis and environment

5.1.2.1   Baseline mission scenario and analysis

The baseline mission is launched by Soyuz-Fregat 2-1b from Kourou on a direct escape trajectory to 1999 JU3 in November/December 2018 with a backup one year later. The spacecraft rendezvous with the NEA in February 2022, both in the baseline and backup scenario. The spacecraft departs from the asteroid in July 2023 and returns to Earth in December 2024 and releases the re-entry capsule which undertakes a re-entry at V_{entry} ~ 11.9 km$\cdot$s^{-1}.

Mission features are summarized in Table 12. The asteroid proximity operations last for about 17 months. The first ~7 months are dedicated to global science observations and hazard mapping. Up to five potential sampling sites are then characterized at high resolution. After a successful sampling rehearsal the spacecraft attempts to sample up to tens of grams of surface material on the site which yields the best compromise between science return and risk-mitigation. If it is confirmed, via a reliable verification technique, that a scientifically meaningful sample has been collected, the sample is transferred to the re-entry capsule and sealed.

If not, the spacecraft can undertake two extra sampling attempts. The mission has to cope with a maximum distance to Earth and to Sun of respectively 2.4 AU and 1.4 AU during the stay at the asteroid. The minimum distance to the Sun is 0.95 AU. A solar conjunction occurs during the stay at the asteroid when the Sun-Earth-Spacecraft angle is lower than 5 and 3 degrees for respectively 30 and 10 days in January/February 2023 during which the spacecraft can be temporarily inserted on a safe position.
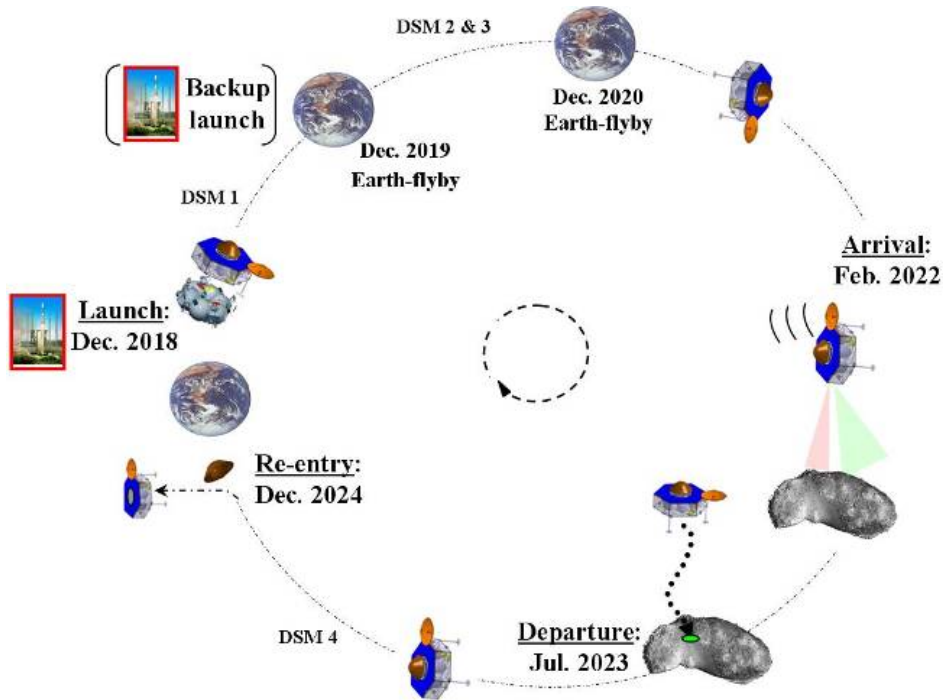
Figure 35: Marco Polo mission concept overview.

1. Earth at launch, Dec. 2018	**4.** Arrival at 1999 JU3, Feb. 2022
2. Earth swing-by 1, Dec. 2019 (backup launch)	**5.** Departure from 1999 JU3, Jul. 2023
3. Earth swign-by 2, Dec. 2020 (backup swing-by 1)	**6.** Arrival at Earth, Dec. 2024
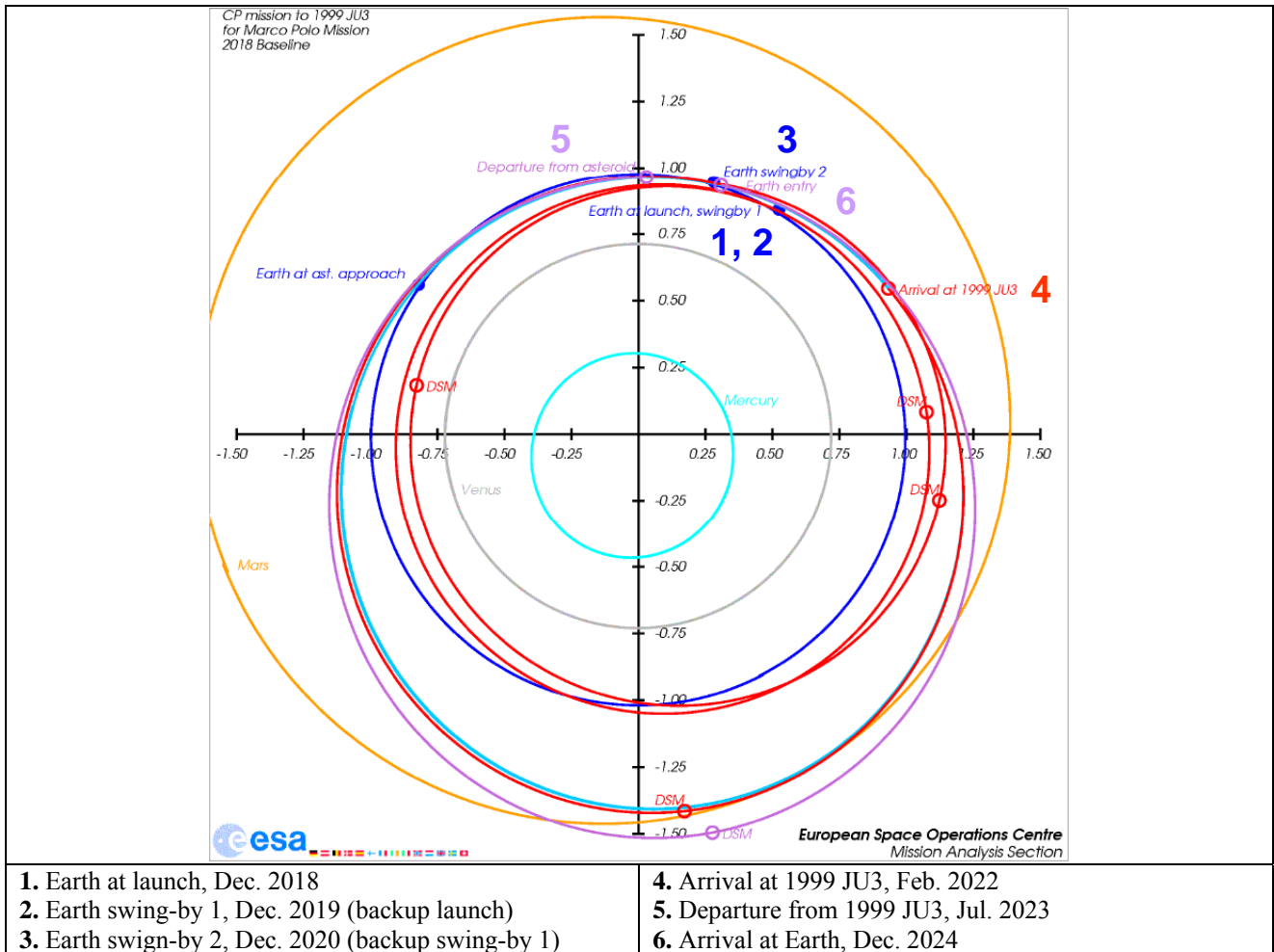
Figure 36: 1999 JU3 reference mission transfer. Trajectory in red: outbound transfer, in purple: inbound transfer, in dark blue: Earth, in light blue: 1999 JU3 (outer) and Mercury (inner), in yellow: Mars orbit, in grey: Venus.

Table 12: Typical mission key parameters (Slight variations exist over the launch window, most conservative numbers are shown in the table below).

		Value	Unit	Comment
Launch vehicle performance		**1629**	**kg**	Backup launch (baseline: 1661 kg)
Earth escape declination		0	deg	
Hyperbolic escape velocity		3.2	km·s^{-1}	
Transfer	Outbound	861	m·s^{-1}	Incl. arrival manoeuvre ~ 135 m·s^{-1}
	Inbound	533	m·s^{-1}	
	Total	**1394**	**m·s^{-1}**	Baseline launch, incl. margins
Navigation	LV dispersion correction	25	m·s^{-1}	
	Outbound/inbound cruise	45	m·s^{-1}	
	Asteroid approach	25	m·s^{-1}	
Asteroid proximity operations		< 100-150	m·s^{-1}	Orbit maintenance/changes, descent, sampling (hold-on thrust), ascent
Spacecraft deflection		20	m·s^{-1}	~ 4 hours before re-entry
Re-entry velocity		**11.9**	**km·s^{-1}**	120 km altitude, prograde re-entry
Landing site		Woomera test Range		Australia, night re-entry

The model payload suite is defined in Section 4: NAC, WAC, CUC, Visible-NIR spectrometer, Mid-IR spectrometer, laser altimeter, and NPA. Section 6 provides a summary of mission and science operations.

5.1.2.2   Asteroid environment

Upon arrival the science Narrow Angle Camera (star trackers as back-up) will be used for far detection of the asteroid to refine the ephemeris and plan adequately the asteroid arrival manoeuvre. 1999 JU3 has not been characterized in high details but some information derived from recent observation campaigns (Abe et al. 2008) help to constrain its physical properties (Table 13) which were used in the frame of this study for the analysis of proximity operations [MED]. The thermal environment of 1999 JU3 (Section 2.2.2.8) and the minimum/maximum Sun/Earth distances were used for the sizing and operational scheme of the thermal, power and communication systems. The radiation dose never exceeds 10 krad behind 4 mm Aluminium for the 6 year mission which allows using standard space-qualified components.

Table 13: Left: Simulation of 1999 JU3 in the camera field of view 50000 km (5 days) before nominal arrival (17th February 2022) with a shape similar to Itokawa - Right: 1999 JU3 range of physical properties (Various orientation of the rotation axis were considered including tumbling) assumed for orbital and GNC (Guidance, Navigation and Control) analysis.

Rotation period (h)	Albedo	Diameter (m), sphere	2:1:1 Ellipsoid dimensions (m^3)	Density (kg/m^3)	Mass (kg)
7.67	0.063	880	1396:698:698	1100	3.9E+11
				1500	5.4E+11
		1080	1714:857:857	1100	7.3E+11
				1500	9.9E+11

5.1.2.3   Proximity operations

During proximity operations, various types of orbits, trajectories and/or positions were defined to conduct science operations (Section 6.3.1) and for the sampling operation itself:

- Far formation flying at ~ 20 km distance (far initial observations),
- Control-free terminator orbit (radio science) with an orbit radius starting at 4.5 km and slowly going down to 2.5 km to increase measurement accuracy, or alternatively a GLO-type of orbit (see below) if the manoeuvre frequency is acceptable for radio science in this case,
- Controlled 2.5 km radius polar orbit (GLO: global characterization) with ascending nodes at 09:00 or 21:00 (local time), or alternatively formation flying at 2 km altitude,
- Hovering at 200 m altitude (LOC: local characterization), fixed above the surface of the five selected sampling sites,
- Descent, sampling, ascent and safe position.

Simulations show that global and local characterization orbits/positions can be maintained (Figure 37) at moderate delta-V (GLO: < 3 m.s^{-1} over 4 months, LOC: < 1 m.s^{-1} over 30 minutes) and operational cost. The spacecraft design is compliant with the payload pointing and scanning requirements during the LOC phase.

Orbit evolution in blue over a period of 2 months.
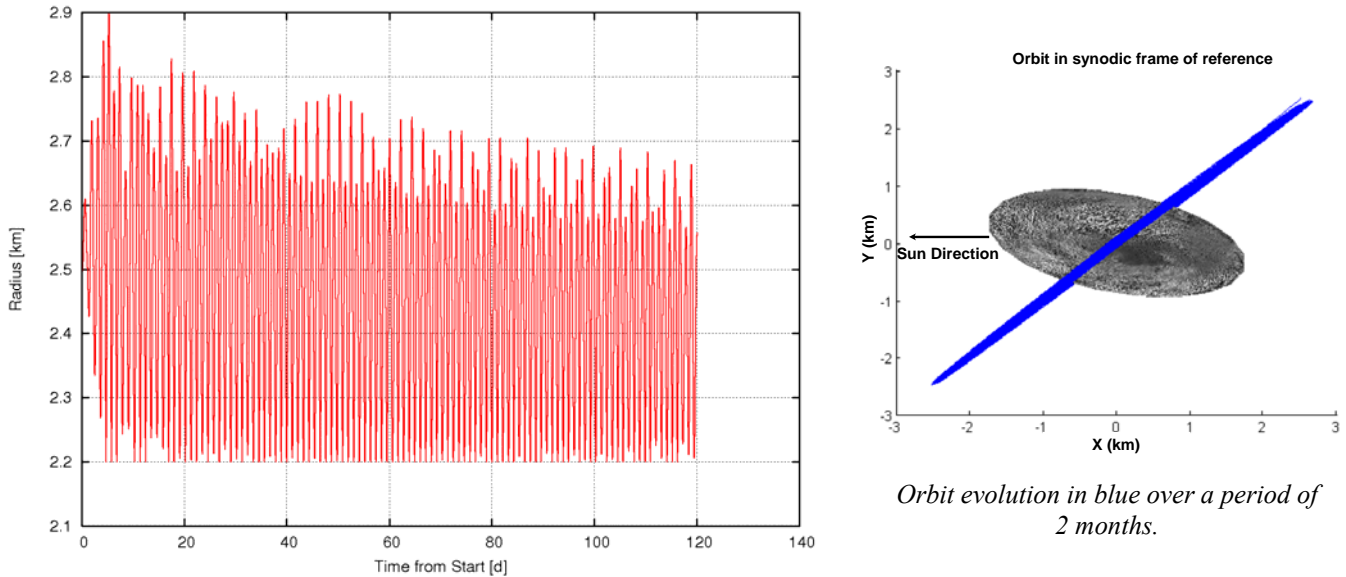
Figure 37: Left: radius of the "controlled global characterisation orbit" (Vertical axis in km) vs Time (Horizontal axis in days) – Right: Example of a visual 3-D representation of orbital plane evolution.

No local topographical data, not even at coarse resolution, will be available until the spacecraft reaches its destination making it difficult to infer any rock, crater or hazard distribution. Yet, high resolution pictures of the surface of Eros and Itokawa and data such as on Figure 34 suggest that many large-sized areas are adequate for landing on bodies in the 100 m size range. Nevertheless, in order to minimize the risk relating to the a-priori unknown asteroid surface environment, a metric landing accuracy is sought for during the assessment study and a spacecraft clearance with respect to the surface of 50 cm is assumed. It is to be noted that such a high landing accuracy is not driven by science even though this would also be an asset..
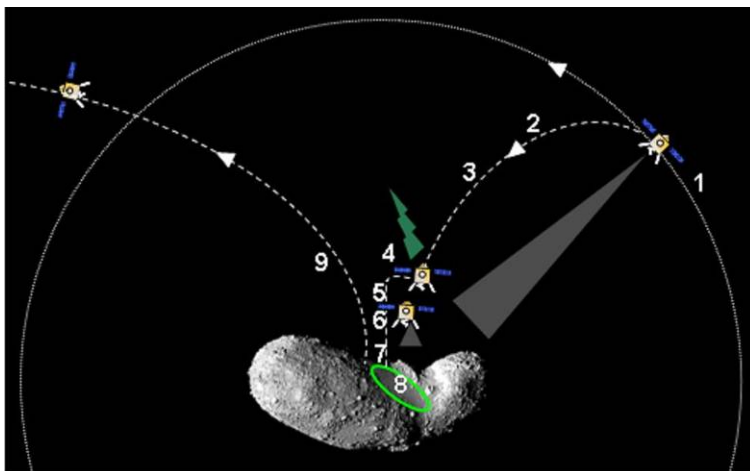
1. Controlled 2.5 km radius orbit (construction of landmark database)
2. Initial descent phase
3. Possible hovering points
4. Hovering at few 100 meters altitude. Last contact with ground
5. Autonomous landing site-relative navigation descent phase
6. Possible hovering points
7. Propulsion-free descent (start at few meters or tens of meters altitude)
8. Touchdown/sampling operations
9. Ascent to safe position

Figure 38: Generic descent and sampling strategy. Actual trajectory and sequence depends on design option.

The selected sampling strategy therefore requires accurate descent navigation. Figure 38 illustrates the typical descent, sampling and ascent strategy. The detailed events and trajectories depend on the design options and are presented in the relevant chapters. As hazards can be identified at high resolution from orbit (typically 2 km altitude), real-time autonomous re-targeting of the landing/touchdown site during descent is not required. Subsequently, the landing site can be pre-defined by the ground prior to the descent. Of course, the spacecraft has the ability to detect anomalies and perform an abort or correction manoeuvre during descent. Preliminary simulations suggest that a landing accuracy as good as ~ 3-5 m and touchdown

velocities better than 20 cm$\cdot$s^{-1} (vertical) and 5 cm$\cdot$s^{-1} (horizontal) can be achieved (Figure 39) by using a vision-based closed-loop navigation and control chain.
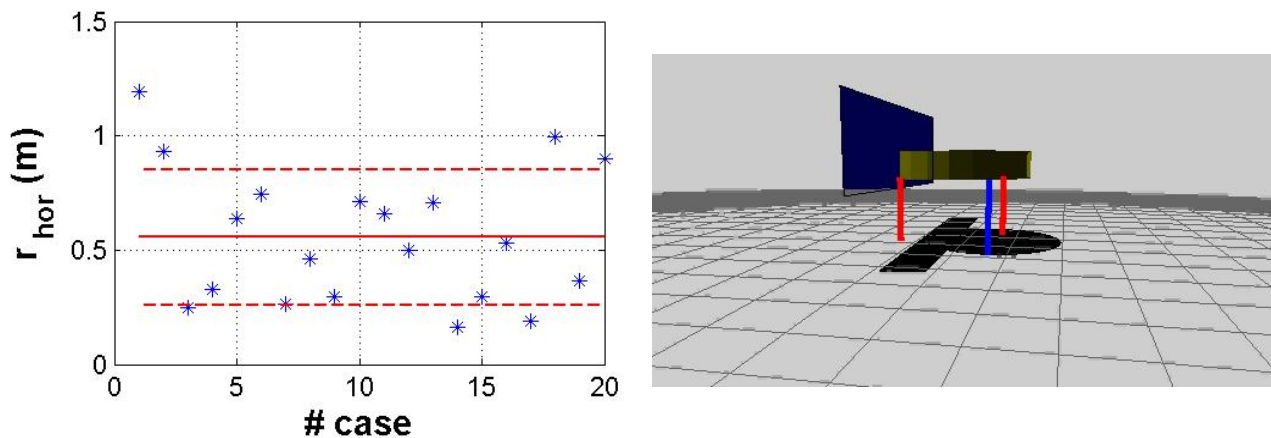
Figure 39: Left: Option B Monte Carlo analysis of the lateral position error (r_{hor}) at landing (Vertical axis in meters) for a limited number of cases (Horizontal axis) – Right – 6 degree of freedom touchdown dynamic simulations.

During descent, this approach makes use of a database of landmarks whose position is accurately known to perform absolute navigation (control of the position), a set of a-priori unknown landmarks for relative navigation (control of the velocity) and possibly a digital elevation model if attitude is also controlled via the vision-based system. The landmark database and the local shape model (*i.e.* around the sampling site) will have been constructed a priori from orbit and during the local characterization phase via the science and navigation camera. The ascent operation follows a more classical approach using a pre-determined thrust impulse to take-off and coarse sun sensors to re-acquire sun-pointing attitude. The touchdown and/or the resting position itself (*i.e.* bounces have stopped) can be detected via the onboard accelerometers, the multi-head altimeters or small contact sensors in the landing feet. 6-degree of freedom dynamic simulations have been performed for both touch and go and short-term landing (with down-thrust) options showing that the 3-legged spacecraft can safely perform the sampling operations (Figure 39, lower right) even in worst-case touchdown conditions (lateral/vertical velocities and relative attitude). Due to the highly perturbed environment and near-to-surface manoeuvres (especially descent and landing), the robustness of the Failure, Detection, Isolation and Recovery (FDIR) strategy and the associated collision avoidance and safe modes is key to ensure mission safety. It will build on the Rosetta experience for the orbital operations and a robust altimeter FDIR sensor as well as the GNC camera for the descent phase.

5.1.2.4   Earth re-entry

Upon return to Earth the ERC is ejected 4 hours before re-entry via an ejection device spinning the capsule up to 5 rpm. The main spacecraft performs then a deflection manoeuvre to ensure Earth collision avoidance (perigee > 150 km). The capsule overall descent trajectory is shown on Figure 40. At 10 km altitude (Mach ~ 0.3) the back shield is jettisoned releasing a ring-folded parachute. Landing velocity is 5-10 m$\cdot$s^{-1}, ensuring landing shock loads lower than 200 g for the sensitive equipment such as battery, UHF beacons or sample canister seal.

List of events (right figure)	**1.** Earth Reentry Capsule separation ($T_0 - 4$ hours)	**a.** Hypersonic phase (M>5)
	2. T_0: Re-entry interface ~ 120 km	**b.** Supersonic phase (1.2<M<5)
	3. $T_0 + 40$ s: Peak heat flux	**c.** Transonic phase (0.8<M<1.2)
	4. $T_0 + $~100 s: Transonic dynamic instability	**d.** Ballistic subsonic phase (M<0.8)
	5. $T_0 + 200$ s: parachute opening (~ 10 km)	**e.** Subsonic phase under parachute (M<0.3)
	6. $T_0 + 1800$ s: landing	
	7. Landing → $T_0 +$ few hours: search & recovery	

Figure 40: Left: Earth re-entry hyperbolic incoming trajectory in inertial frame (red: main spacecraft Earth avoidance trajectory, blue: re-entry capsule trajectory) – Right: Re-entry sequence of events

5.1.3 Main spacecraft design option A

5.1.3.1 Configuration, structures and propulsion

Figure 41: Spacecraft design option A configuration of main spacecraft

The spacecraft is hexagon-shaped, features a maximum diameter of 3.7 m, a height of 2.8 m in the launcher fairing and the solar arrays span 8 m when fully deployed from tip to tip. It builds around a 937 mm diameter central cylinder-based structure, completed by shear walls, top/bottom and closure panels. The sample acquisition and transfer system is located inside the central cylinder, allowing access to the top panel-mounted re-entry capsule, sharing space with the radiators. Two deployable solar panels with a total area of ~10 m^2 are needed to meet the power requirement. Instruments share an optical bench on the nadir-pointing side panel. Four propellant tanks are equatorially mounted on the bottom panel. The spacecraft is controlled by 4x22 N and 16x10 N thrusters.

5.1.3.2   Mechanisms and robotics

The spacecraft performs a short-term landing (option 1 of Figure 32) relying on 800 mm length landing legs. Honeycomb crushable material is used to dissipate the energy at landing. This ensures a clearance of 500 mm at the last sampling attempt. The spacecraft is held on the surface and bounces are minimized via a 20 N down-thrust, triggered at landing and running throughout the whole landing/sampling operation of ~ 10 minutes. The sample is acquired via a rotating corer, also used as a sample canister, deployed and transferred to the ERC via a 3 dof articulated arm (Figure 42). An active shutter ensures that material is retained inside after collection while a movable lightweight surface allows verifying success of the sample collection operation. Even though the sampling tool is essentially designed for regolith type of material with compressive strength up to 100 kPa, simulations show that it may also collect materials featuring a compressive strength up to 1 to 2 MPa within the allocated time. The articulated arm also allows sealing of the sample canister, closing of the ERC backcover and easy grabbing of a simple backup tool (e.g. sticky pad).
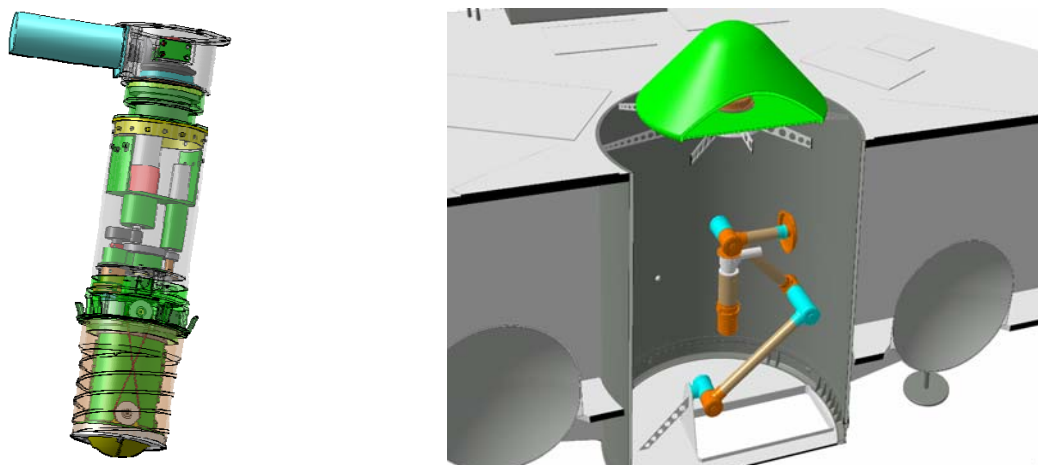
Figure 42: Option A sampling tool (left) and transfer system (right)

5.1.3.3   GNC and AOCS

A classical ESA approach (*i.e.* Rosetta) is envisaged for the interplanetary transfer. For descent and sampling, the spacecraft requires a navigation camera (redundant) located on the bottom panel as well as a radar altimeter (redundant) to derive direct altitude measurement but also used as a robust FDIR sensor in order to safely navigate relatively to the landing site. An additional navigation camera is located on the payload optical bench in order to construct the landmark database from orbit which is later on used during descent a number of times to be correlated to descent images and ensure position accuracy. The camera will also build a local shape model around the sampling site to derive relative attitude information during descent. In order to increase robustness, three other inclined radar altimeters may be used, providing direct attitude at landing. Control is performed via four reaction wheels and the RCS thrusters. Descent starts from the 2.5 km radius orbit and makes use of a simple hyperbolic transfer arc to go down to 500 m. At ~500 m altitude, navigation relative to the landing site starts and a ~1 hour hovering allows locking the spacecraft above the sampling site and the last contact with the ground for the "go" decision. From then on, the descent is vertical and the spacecraft is fully autonomous for approximately 1 hour. Due to the unknown position of the landing site, the spacecraft runs on battery until ascent and recovery of Sun-pointing attitude.

5.1.3.4   Power, thermal, data handling and telecommunications

Power is generated by the solar arrays able to provide up to 910 W in the sizing case (GLO with 45 degree sun aspect angle) and a 74 Ah battery, mostly used during descent and sampling operations. 65 W output Travelling-Wave Tube Amplifiers (TWTA) are used to amplify the signal from the X-band transponders which communicate through a 1.3 m high gain antenna with the ESA 35 m ground stations. Data rates between 45 and 111 kbps are achieved, depending on the mission phase. All required 400 Gbits science data can be downlinked. A steerable medium gain antenna is used for safe mode and minimum housekeeping data transmission during descent. Low Gain Antennas (LGA) are used for Low-Earth Orbit (LEO) operations. A

LEON 2 processor is capable of accommodating all tasks to be done onboard the spacecraft. Data can be stored in a 1200 GBit flash memory. The large processing load from the navigation cameras is taken care of by a dedicated and optimized proximity image processing unit. The thermal environment is regulated via 1.7 m^2 radiators mounted on the top panel, Multi-Layer Insulation (MLI) and heaters. Directional radiators of parabolic shape are envisaged to reject the heat from the low-temperature instruments if needed and to minimize the incoming heat flux from the Sun and the asteroid.

5.1.4 Main spacecraft design option B

5.1.4.1 Configuration, structures and propulsion

The spacecraft is square-shaped, features a maximum diameter of 2.5 m, a height of 2.65 m in the launcher fairing and the solar arrays span 8.45 m from tip to tip when fully deployed. It builds around a central cylinder-based structure, completed by shear walls, top/bottom and closure panels. The sample acquisition and transfer system is located at the bottom of the spacecraft with a direct access to the re-entry capsule also located on this panel. The front heat shield is facing the inner part of the spacecraft throughout the mission until the spacecraft returns to Earth. The capsule is then rotated by 180° via a motorized mechanism (Figure 44) before ejection. Two rotating solar panel wings of 3.2 m^2 each provide the required power and allow having the same asteroid-pointing attitude during orbital and most of the descent operations while running on solar power. The 3 m^2 radiators are mounted on the side panels. The payload is mounted on the bottom panel. The propulsion system consists of four bi-propellant tanks, a 425 N main engine and 4 $\cdot$ 20 N thrusters. For low-altitude manoeuvres around the asteroid a mono-propellant tank and 16 $\cdot$ 10 N thrusters are used.
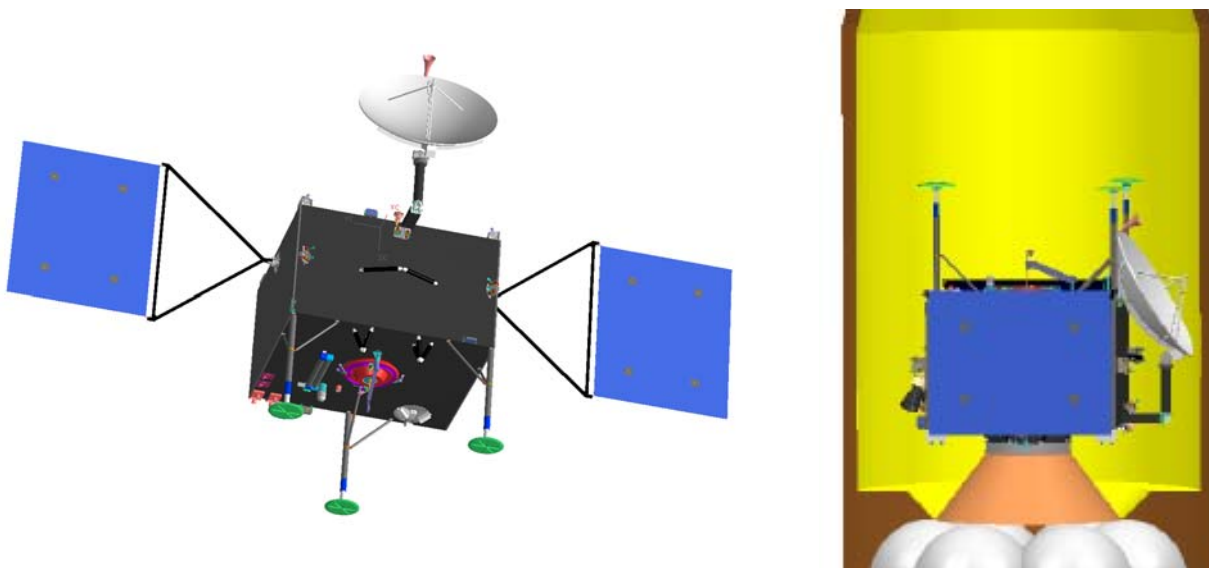
Figure 43: Spacecraft design option B configuration of main spacecraft

5.1.4.2 Mechanisms and robotics

The spacecraft also performs a short-term landing and it thus held on the surface by the thrusters for ~ 10 to 20 minutes. A rotating corer, mounted on a 1 dof (degree of freedom) articulated arm, is used for sampling operations. A 2 dof articulated arm then grabs it and performs the final transfer to the ERC and closes the backcover. The legs, also using crushable material to absorb energy at landing are 1150 mm long to provide clearance to the 2 dof articulated transfer system and the hold-down thrust is 40 N in order to provide ~16 N at the last sampling attempt in blow-down mode. In the worst case situations (*e.g.* one spacecraft leg hits a 50 cm rock) the spacecraft may require an incremental thrust when the second and third leg touches the surface instead of providing 16 N already when the first leg makes contact.
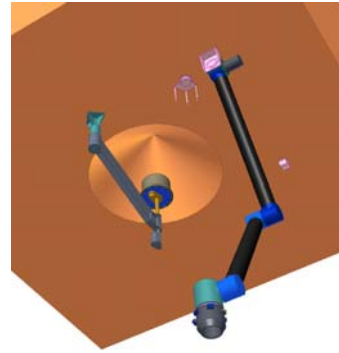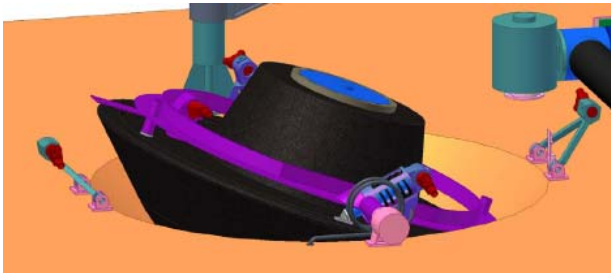
Figure 44: Option B capsule rotation sequence (left), sampling tool and transfer arms (right).

5.1.4.3   GNC and AOCS

One navigation camera (+ redundant) is sufficient to build the landmark database from orbit. The mid-descent phase follows a radial trajectory and starts from a high feature-detection gate (GLO orbit) where navigation relative to the terrain is already engaged. The above mentioned camera and and a long-range laser altimeter (redundant) are used for this purpose. At a low-gate (~100 m) short range multi-head altimeters providing direct attitude with respect to the local terrain are activated. Then close-descent (shown on Figure 45) starts and culminates in the sampling operation. The spacecraft descends towards the centre of mass down to ~50 meters above the surface. Below that, it descends along the local vertical. A number of hovering are included throughout the sequence when ground contacts can be made. At the beginning of the final vertical descent (~15 m altitude), navigation switches from absolute to relative navigation mode (using a-priori unknown landmarks) due to the possible absence of known features in the camera field of view. Two inclined cameras are used additionally. They will allow tracking a-priori unknown landmarks in a much wider area in case none are available in the field of view of the nadir-pointing cameras in the last 15 m of the descent. This approach increases robustness for the control of the lateral velocity.
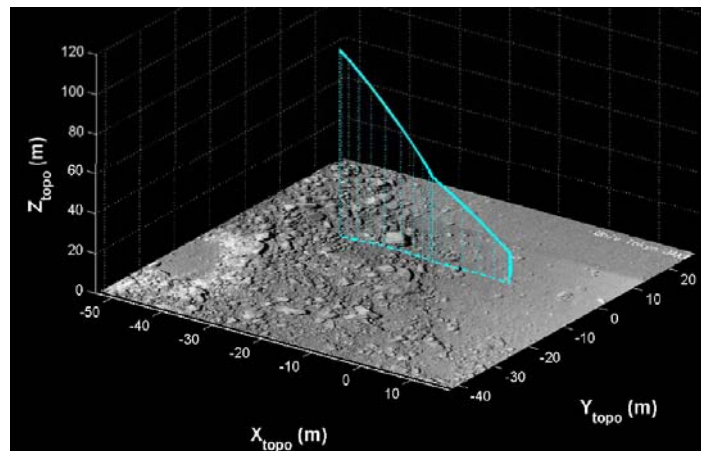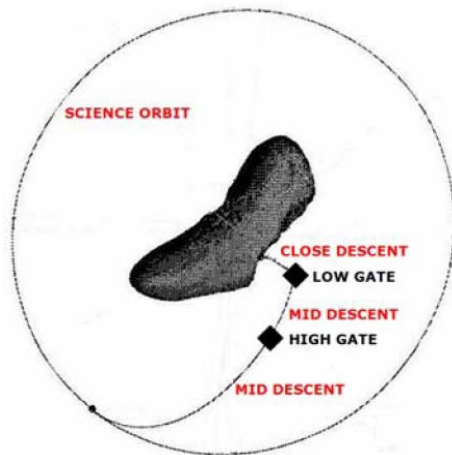
Figure 45: Option B global (left) and close (right) descent strategy. For a description, see the text.

5.1.4.4   Power, thermal, data handling and telecommunications

The power, thermal, data handling and communication architectures and strategies are similar to option A. However the design makes use of rotating solar arrays able to provide 644 W in the sizing case (GLO) and the battery capacity is 72 Ah. The TWTAs output power is 120 W and an antenna of 1.6 m can be accommodated. Data rates between 87 and 175 kbps are achieved. All required 400 Gbits science data can be downlinked. The flash memory has a capacity of 132 GBit. The MGA is however fixed and co-aligned with the HGA. The radiator area is 1.5 m^2.

5.1.5 Main spacecraft design option C

5.1.5.1 Configuration, structures and propulsion

The spacecraft is octagon-shaped, features a maximum diameter of 3.26 m, a height of 2.25 m in the launcher fairing and the solar arrays span 5.58 m from tip to tip when fully deployed. It builds around a central cone-based structure of 1194 mm base diameter, completed by 8 shear walls, top/bottom and 8 closure panels. The landing feet are used to collect the sample while the landing legs and the inner volume of the central tube ensure the sample transfer function to the ERC, located at the centre of the top panel. Five deployable (non-movable) solar panel wings totalizing an area of 7.5 m^2 are accommodated on one of the side panels. They provide the required power and allow having the same asteroid-pointing attitude during orbital and most of the descent operations while running on solar power. The radiators are mounted on the side panels. The payload is mounted on the bottom panel. The propulsion system consists of six propellant tanks, 16 x 4 N and 4 x 22 N thrusters.
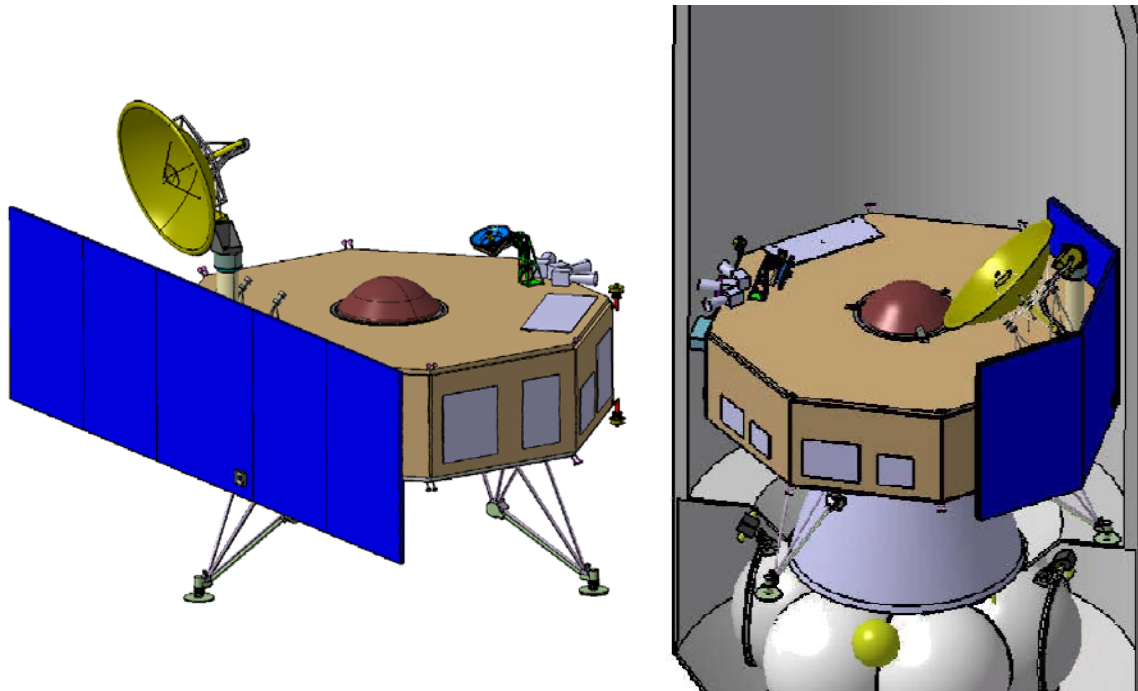
Figure 46: Spacecraft design option C configuration of main spacecraft

5.1.5.2 Mechanisms and robotics

The spacecraft stays in contact with the ground for a few seconds only, removing the need for down-thrust and energy-absorbing legs. The sampling tool is a square-shaped mechanical pusher triggered by the touchdown action and a spring-based mechanism integrated in the landing pads. A shutter is also used to retain the material. After sampling, the leg is retracted and transfers the sampling tool forward to a recovery system consisting of a sample container transferred to the ERC as a whole via a 2 dof elevator. Mounting two extra sampling tools on the other two legs allows using two recurrent landing legs and sampling tools, with an additional but limited cost. This solution is thus considered as a baseline in this design option.
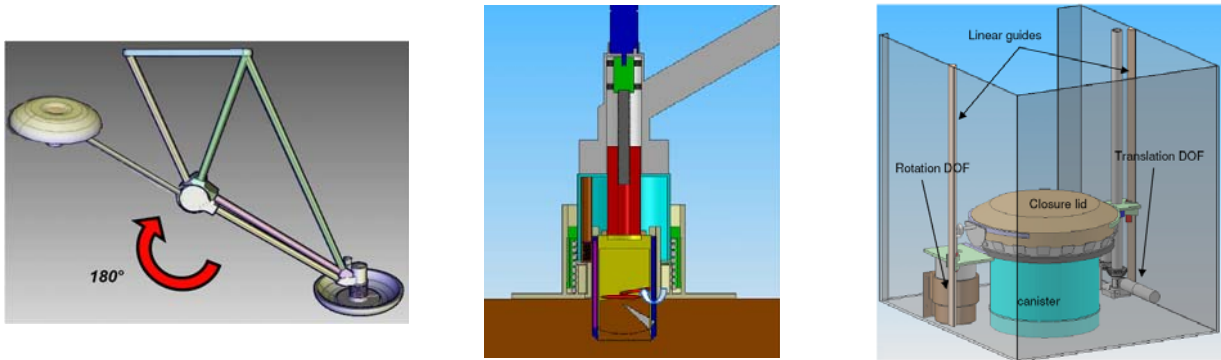
Figure 47: Option C landing leg (left) integrating the sampling tool (centre) and sample container recovery system (right)

5.1.5.3 GNC and AOCS

The GNC and AOCS system, functions and strategy are somewhat similar to option B in the sense that the navigation relatively to the asteroid surface using vision-based navigation already starts from the GLO orbit. At typically 400 to 500 m a stationary phase is planned of ~ one hour, as in option A, so as to enable the last ground check before descent. One navigation camera (+ redundant) on the bottom panel is deemed sufficient in the envisaged configuration to build the landmark database and to be used as a relative navigation sensor during descent. A dedicated GNC multi-beam laser is used as an attitude sensor in order to align the spacecraft with the local surface for the final descent and sampling phase (*e.g.* last tens of meters).

5.1.5.4 Power, thermal, data handling and telecommunications

The power, thermal, data handling and communication architectures and strategies are similar to option A. The solar arrays are also deployable but non-rotating and provide 555 W in the sizing case (GLO) and the battery capacity is 144 Ah. The communication equipment is identical to option A. All required 400 Gbits science data can be downlinked. The flash memory has a capacity of 436 GBit. The radiator area is 2.1 m^2.

5.1.6 ERC design options A, B and C

The architecture of the ERC design options A, B and C (Figure 48) is similar, making use of a subsonic parachute, deployed via release of the back heat shield. An o-ring based sealing is used to prevent contamination of the sample inside the capsule by Earth contaminants. UHF beacons (via a patch antenna) emit 5 days for recovery operations. The battery, UHF beacons, antenna and sample sealing system are designed to withstand the 200 g load at landing.

The flight path angle varies between -8 and -13 degrees depending on the option. The 45° half-cone angle, backshell shape and capsule centring are such as to provide stability throughout transonic regime (Figure 49, right), as it was for example demonstrated for the Hayabusa capsule via drop tests. If next study phases show that stability cannot be guaranteed supersonic parachutes might have to be considered. This is currently assumed for option A. Option A, B and C yield a maximum heat flux and peak of ~ 15 – 17 MW$\cdot$m^{-2} and 250 MJ$\cdot$m^{-2} (including margins) which were used to select and size the thermal protection system. An in-development European lightweight ablative material and Norcoat Liege cover respectively front and back shield of options A and B while option C uses high-density carbon phenolic for the front shield, all ensuring a maximum temperature of 150 °C of the capsule front structure made of Aluminium. Additional crushable material can be accommodated if required by possibly sensitive equipment. Preliminary analysis shows that it may not be necessary. A thermal insulation barrier (e.g. MLI) can also be inserted behind the cold structure should the post-landing steady-state temperature go beyond the 40 °C sample temperature requirement. This is however unlikely for this scenario as landing occurs at 04h00m local time and the retrieval operation is likely to take place within 1 hour after landing (*e.g.* Stardust was recovered within 20 minutes).
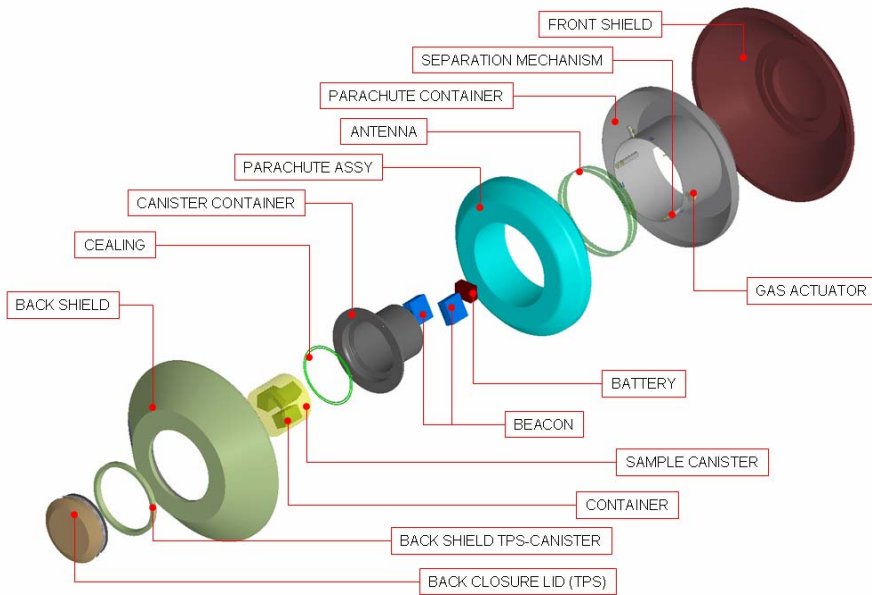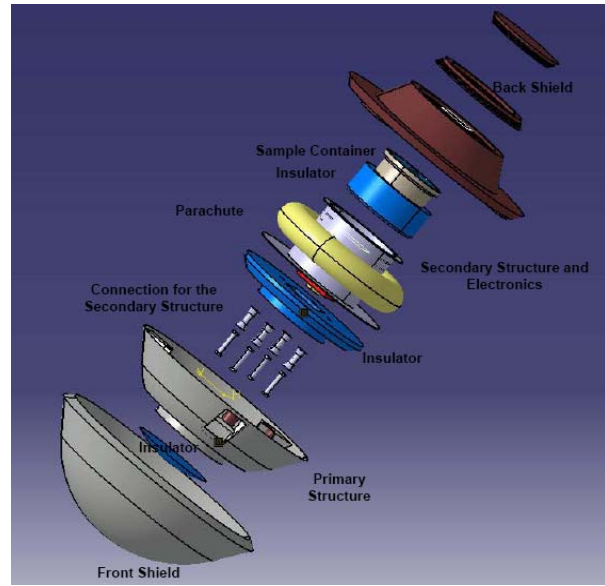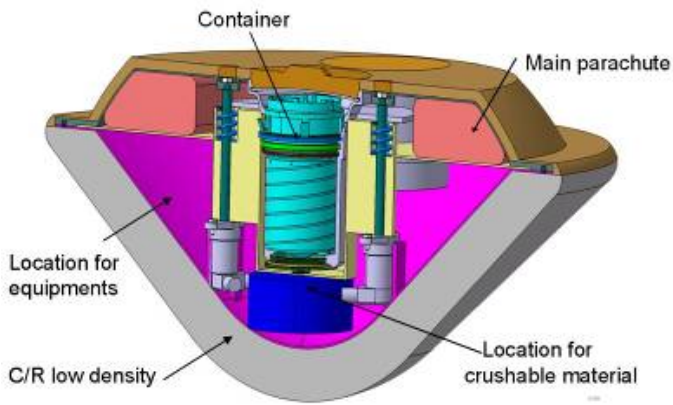
SUB-SYSTEM	Mass, kg		
	Option A	Option B	Option C
Structure	8.1	4.7	5.2
Internal thermal insulation/crushable material	0.1	0.1	0.0
Parachute deployment mechanism	0.7	1.0	1.4
Parachute assembly	4.8	0.8	8.2
Avionics, beacons & antenna	1.7	1.3	3.5
Battery	1.2	1.3	0.9
Harness	1.3	0.0	0.6
Sample container (+ sample)	1.3	4.6	3.6
ERC nominal mass without TPS	19.2	13.9	23.3
ERC total mass without TPS (incl. 20% SM)	23.0	16.7	28.0
Front shield TPS	5.4	4.2	35.4
Backshield TPS	1.8	4.0	5.4
Total ERC mass	30.2	24.9	68.8

Figure 48: Configuration and mass summary of the Earth Re-entry Capsule for Option A (top left), B (top right) and C (centre). SM: System Margin, TPS: Thermal Protection System

Capsule mass: 68 kg, diameter: 800 mm
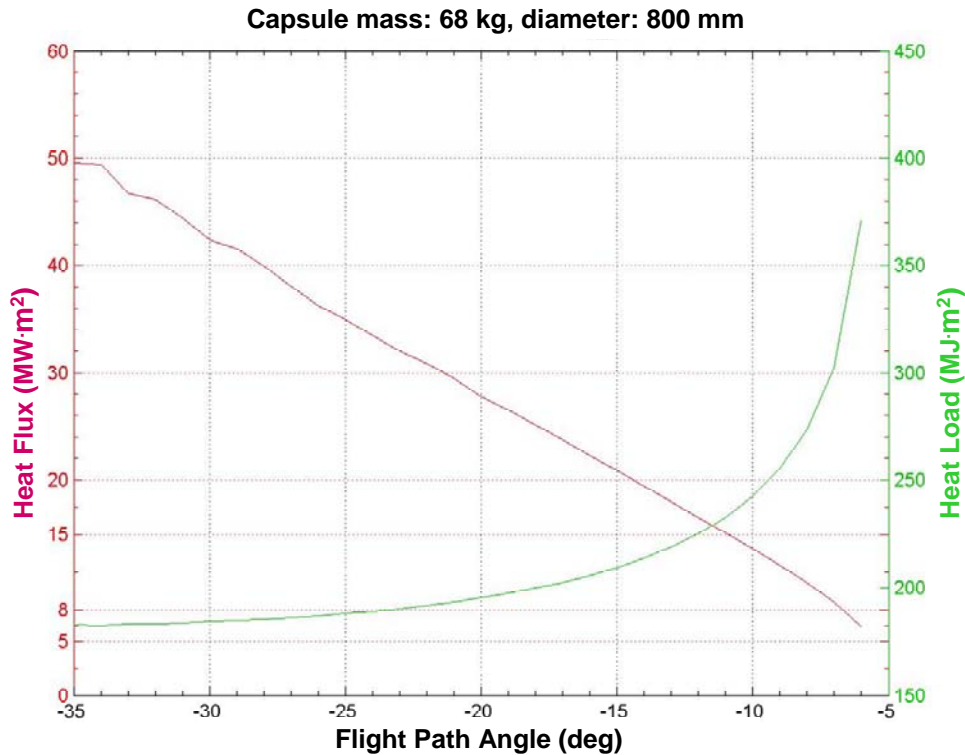
Figure 49: Typical resulting heat flux (red)/loads (green) vs the initial flight path angle at 120 km altitude. This data is shown for one of the design options but the variations of these data due to the slightly different mass and aerodynamics parameters across the design options do not affect the feasibility of the design.

5.2   Summary of the three Marco Polo design options

Mass budgets for the three design options are presented in Table 14. At subsystem level, maturity mass margins between 5 and 20% have been applied according to the equipment TRL status and a 20 % system margin has been applied on the nominal dry mass. Launch mass margins for all three design options are well within the requirements for an ESA assessment study and provide robustness against the launch vehicle performance uncertainties. It is recommended to keep these margins as long as possible.

A few remarks on the below budget should be made:

- A different optimization of the propulsion system in option B yields slightly higher delta-v but also higher launch vehicle performance.

- Option C requires 3 Close-up camera units. It also allows collecting 3 separated samples which are transferred via the landing legs, hence the higher science instrument and landing/touchdown system mass for this option.

- All industrial studies assumed the masses of the science instruments indicated below. This mass slightly increased at the very end of the instrument studies which explains the discrepancy with the mass of ~ 30 kg shown in Section 4. This clearly does not compromise the mass feasibility of the mission as the resulting increase of the total spacecraft wet mass for any option is limited to ~ 12 kg.

SUB-SYSTEM	Mass, kg		
	Option A	Option B	Option C
Structure	143.7	149.5	167.7
Thermal Control	27.3	30.5	37.0
Landing/touchdown system	6.5	14.8	35.3
Sampling, transfer and containment system	8.1	29.2	7.1
Capsule spin-ejection mechanism	6.0	10.2	12.2
Other mechanisms	28.7	12.7	23.3
Communications	28.7	29.5	32.0
Data Handling	23.3	24.8	33.0
AOCS	43.1	52.9	36.2
Propulsion	119.7	106.5	104.6
Power	87.9	74.2	69.7
Harness	50.0	42.0	37.2
Science instruments	22.9	22.9	24.2
Main spacecraft nominal dry mass	596	599	619
Main spacecraft total dry mass (incl. 20% SM)	715	719	743
Total dry mass (main spacecraft + ERC)	745	744	812
Pressurant mass	3	2	3
Propellant mass	643	606	644
Total wet mass (excl. adapter)	1391	1352	1456
Adapter mass	57	110	101
Launch mass (incl. adapter)	1448	1462	1557
Launch vehicle performance	1629	1719	1629
Launch mass margins (%)	11	15	4
Launch mass margins (kg)	181	256	72

Table 14: Mass budget summary (Launch vehicle adapter → Option A/C: customized, Option B: Standard 937).

5.3   Marco Polo required Technology development

The Marco Polo mission designs presented above are deemed to be feasible providing a timely and adequate technology development programme. During the assessment study, technologies were selected so as to have as much as heritage in Europe as possible and minimize development risk. The activities below are key to ensuring that Marco Polo enters implementation phase with the appropriate technology maturity (TRL 5 in 2012) and are proposed to be implemented either in the ESA Technology Research Programme (TRP) or in the Core Technology Programme (CTP).

Table 15: Marco Polo required and foreseen technology developments.

Marco Polo enabling and enhancing technology activities	Heritage (or activities ongoing for future missions: *e.g.* ExoMars, MoonNEXT)
Sample acquisition, transfer and containment system	Exomars, Philae, MSR activities
Low-gravity and high-clearance landing/touchdown system	Philae, Moon NEXT activities
Parachute system: canopy, packaging and deployment device	Huygens, Exomars
Autonomous GNC technology for proximity operations	MSR/MoonNEXT activities (VisNav, etc.), NEA GNC TRP activity
FDIR, altimetry and attitude measurement sensor *(need to be confirmed in future phases)*	ExoMars, ongoing Aurora activities
Delta-development of high-flux ablative TPS material	Ongoing TRP and previous ESA activities
Contamination assessment of bi/mono-propellant thrusters	Classical thrusters firing tests
Capsule dynamic stability	Huygens, ExoMars

6 Ground Segment

6.1 Overview

The ground segment will be set up similar to current planetary missions performed by ESA. The scientific instruments will be operated by the responsible PI teams via a Science Operations Centre (SOC) which is part of the Science Ground Segment (SGS) which coordinates the scientific input. The SGSs are located at ESAC, close to Madrid in Spain. The spacecraft operations, flight dynamics and ground station activities will be performed at the Operational Ground Segment (OGS) which includes the Mission Operations Centre (MOC). The OGS is located at ESOC in Darmstadt. Figure 50 shows an overview over the setup.
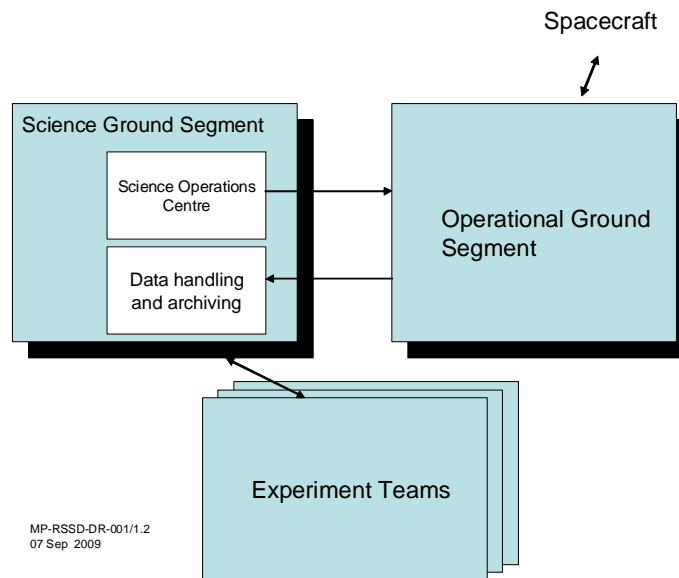
Figure 50: The Ground Segment consists of a Science Ground Segment and an Operational Ground Segment.

6.2 Mission operations

6.2.1 Operations schedule

The schedule of the spacecraft operations, starting in December 2018, is depicted in Table 16. Science operations at the asteroid are summarised in Section 6.3. The definition of the operations and the ground segment implementation phase, including test and validation, start ~ 5 years before launch. Detailed mission and science operations as well as capsule retrieval ground operations are described in details in the Mission Operations Assumptions Document [MOAD], the Science Operations Assumptions Document [SOAD], and the Capsule Recovery Assumptions Document [CRAD].

6.2.2 Operations concept

ESA/ESOC and possibly other involved Agencies will conduct the mission operations listed above and provide a ground segment including all required facilities, hardware, software, documentation, the respective validation, and trained staff.

Table 16: Baseline scenario operational activities schedule (backup mission is one year shorter with only one Earth fly-by). d: day, m: month, w: week, y: year, L: launch.

Mission Phase	Duration	Operations Support
LEOP	**L – 8h to L + 3d**	Real-time support. 2 ground stations. Solar panel deployments. Orbit tracking and first trajectory correction manoeuvre (DSM 1).
Commissioning Verification	**L + 3 d to L + 90 d**	Real-time support. S/C and instruments commissioning including HGA deployment/calibration. S/C system tests.
Outbound Cruise	**3 y + 9 m**	See sub-phases below
Initial Cruise	6 m	Daily passes. Intense operations during early cruise and then off-line operations support. System and element health checks.
Cruise to asteroid	2 y 9 m	Weekly passes. Off-line operations support (S/C, flight dynamics, ground segment maintenance).
Passive payload checkout	4 * 1 w	Daily passes. Offline checkout procedure for instruments.
Earth Flyby	2 * 1 m	Daily passes. Flyby navigation. Trajectory correction manoeuvres, Instrument calibration/check-out.
Deep Space Manoeuvres	DSM 2, 3, 4 x 1 m	Navigation/tracking campaign. Trajectory correction manoeuvres
Asteroid Preparation Phase	~1.5 y Overlaps with cruise	Asteroid operations procedures updated, tested and validated. Simulation campaigns. Team build-up for asteroid phase. Mission planning for asteroid phase.
Asteroid Approach	**2 m**	See sub-phases below
Asteroid Detection	5 w	ΔDOR. Increased pass frequency. Real-time support (S/C, flight dynamics, etc.) during manoeuvres. Intense system checks and detailed planning activities
Ephemeris Refinement	2 w	ΔDOR. Real-time operations support. Off-line flight dynamics support. Re-planning, data analysis, troubleshooting. Use of science camera or STR.
Insertion into 20 km from the asteroid	1 w	Real-time shift support for manoeuvres otherwise routine daytime support (spacecraft operations, flight dynamics, ground segment maintenance and support)
Asteroid Proximity operations phase	**18 m**	Daily communication passes with one station, except SAM. Mission planning/re-planning, intense flight dynamics activities. See sub-phases below. ▪ FAR: payload commissioning, operations coordinated by Science Ground Segment. ▪ RSE: Daily off-line control, instrument operations as commensurable with RSE. ▪ GLO, LOC and EGLO: Downlink of global and local characterization data + selection of 5 most suitable sampling sites, selection of the primary candidate. Digital elevation model and asteroid landmark database are built, used by flight dynamics teams, later implemented in the S/C navigation software. ▪ SAM/Sampling rehearsals: Two ground stations. Real-time operations. Analysis of descent/sampling flight data. Updates of onboard navigation software ▪ Solar conjunction: Limited tracking accuracy. Possibly used for science data downlink (not possible for Sun-Earth-asteroid angle < 3° → idle safe orbit, *TBC.*) ▪ Preparation for return cruise and escape: Real-time support
Inbound Cruise	**1 y + 2 m**	Similar to outbound cruise albeit no fly-by, no payload checkouts. Weekly passes
Near Earth Phase	**5 w**	▪ Final approach: navigation, ERC separation and Earth avoidance manoeuvres, navigation/tracking, intense preparation, real-time operations in critical phases ▪ Re-entry and capsule recovery: ERC tracking (UHF beacons, possibly airborne optical trajectory determination), calculation of landing site by flight dynamics, recovery by helicopter within 1 h, transport of sealed capsule to curation facility

The Marco Polo mission operations will consist of:

- Mission Planning: (24 hours to 1 week timeframe)
- Spacecraft control, following the flight operations plan and the short-term plan (including in particular deep space and asteroid orbit manoeuvres, sampling operations and Earth re-entry capsule separation.)
- Spacecraft status monitoring and off-line performance analysis
- Instrument status monitoring, control, implementation of the observation schedules and collection and data control of the instrument housekeeping telemetry following requests coming from the SGS.
- Orbit determination and control using tracking data and implementing orbit manoeuvres
- Off-line attitude determination and control based on the processed attitude sensors data in the spacecraft telemetry and by commanded updates of control parameters in the on-board attitude control system
- On-board software maintenance
- Capsule recovery operations (Woomera test range - Australia) and transport to curation facilities

The operational concept will make maximum sharing and reuse of manpower, facilities and tools of the Solar and Planetary Science family of missions (*e.g.* BepiColombo).

The spacecraft will spend most of its time at distances from the Earth where the two-way light-time delay in communications is in the order of up to 40 minutes. This requires the operational mission to be considered as "off-line" for which the on-board systems must be robust and have an advanced level of autonomy, in particular in case of on-board anomalies where the spacecraft should autonomously perform corrective actions. Only one ground station will be allocated for communications and precision orbit determination with the spacecraft during most of the commissioning, cruise and asteroid phases, except for critical events. Dual ground station coverage will be used when required for navigation during cruise and during the critical asteroid descent and sampling phase. During cruise the nominal coverage will be limited to a single pass per week while daily passes will be used during asteroid proximity operations.

6.2.2.1 Mission Planning, Spacecraft Monitoring and Control

All operations will be conducted by ESOC according to procedures contained in the flight operations plan. Nominal spacecraft control during the routine mission phase will be 'off-line'. All operations will be conducted by up-linking of a master schedule of commands for later execution on the spacecraft. Nominal science operations are coordinated by the SGS and command files for the instrument operations will be delivered to the OGS in regular intervals. Specifically, descent and sampling operations require presence of a team with expertise on the drill and sample transfer mechanisms as well as vision-based GNC. The minimum required ground reaction time is in line with the spacecraft autonomy periods as shown in Table 17.

Table 17: Ground reaction times.

Phase	Autonomy for mission safety
Launch and Early Orbit Phase (LEOP)	12 h
Cruise	2 weeks
Superior solar conjunction	50 days
Asteroid Proximity Phase (high orbits)	48 h
Low Asteroid Orbits and manoeuvres	48 h (to be confirmed)
Descent and sampling	1-3 h (to be confirmed)
Special manoeuvres (Deep Space Manoeuvres (DSM), flyby, asteroid insertion/escape, separation and Earth avoidance)	Coverage plan to be developed on a case by case basis taking into account navigation and telemetry/telecommand. (TM/TC)

6.2.2.2 Orbit and Attitude Control

The trajectory, attitude and coverage analyses required for mission preparation are carried out by mission analysis. The flight dynamics teams will support tasks such as:

- Orbit determination using two-way Ranging and two-way coherent Doppler data,
- Preparation of flybys and asteroid orbit insertion (Doppler, ranging and ΔDOR measurements),
- Trajectory/Manoeuvre optimisation, command generation, execution and monitoring, including those needed for the sampling/landing,

- Attitude Control System Monitoring,
- Antenna steering, commanding the navigation camera (used for spacecraft asteroid relative navigation)
- Capsule separation, capsule re-entry trajectory location analysis.

6.2.3   Operational Ground Segment infrastructure

The ESA/ESOC Operational Ground Segment (OGS) will consist of:

- The Ground stations and the communications nsetwork
- The Mission Control Centre (infrastructure and computer hardware)
- The Flight control software system (data processing and Flight Dynamics Software)
- Computer infrastructure (Mission Control System, simulator, *etc*.).

6.2.3.1   *Ground Stations and communications network*

All communications with Marco Polo are done via X-Band and will use the 35 m antenna in New Norcia (Figure 51) as a baseline. During periods of conflict with other missions New Norcia could be switched to the Cebreros or the DS3 station which can also be used when a second ground station is required. This network almost provides a ≥ 16 hours coverage of the spacecraft during critical periods. For LEOP activities, it will be supported by the 15 m antenna in Maspalomas. The use of the ground stations will be optimized to share coverage time with other missions. On the spacecraft, communications will be mostly made through the high gain antenna. For LEOP, low gain antenna will be used and a medium gain antenna is planned for safe mode and during asteroid descent to guarantee a minimum health status of the spacecraft during this critical phase (i.e. ~ 100 bps data rate). The Ground Facilities Control Centre monitors and remotely controls all the ground stations. They are also responsible for the TM/TC links to and from the ground stations.

Figure 51: ESA New Norcia (Australia) 35 m deep space antenna.

6.2.3.2   *The Mission Control Centre*

The flight control team, integrated into the Solar and Planetary Division at ESOC, will operate the mission from ESOC. The mission will be controlled from the mission operations centre, which consists of the main control room (see Figure 52) augmented by the flight dynamics room and dedicated control/support rooms. The main control room will be used for mission control during LEOP (and possibly during sampling operations at the asteroid). During cruise and the other asteroid operations the mission control will be conducted from a dedicated control room shared with other solar and planetary science missions. The control centre is equipped with workstations for different tasks of operational data processing and staffed by experts.

The mission operations are defined by the flight control team, experts in spacecraft control dedicated to the Marco Polo mission. The team is led by the spacecraft operations manager. At least one operations engineer is dedicated to instrument operations which are provided via the SGS.

Figure 52: ESOC Main Control Room.

6.2.3.3 *The Flight Control Software System and computer infrastructure*

The flight control system will be based on infrastructure development (SCOS 2000), using a distributed architecture for all spacecraft monitoring and control activities. It includes various facilities: telemetry reception and analysis, telecommand processing, uplink and verification capabilities, monitoring of instrument housekeeping telemetry, etc. The computer configuration will be derived from existing structures, for example: a multi-mission server to edit the flight operations plan, a mission dedicated computer system for mission planning (commands/instructions schedules for spacecraft and ground systems), the simulation computer, providing an image of the spacecraft system during ground segment verification, etc.

6.2.3.4 *Capsule recovery infrastructures and operations*

For Marco Polo, the capsule landing is assumed to take place in Woomera, South Australia on 03 December 2024 (longitude: 136.5 ºE, latitude: 31 ºS, altitude with respect to the geoid: 0.25 km). The currently estimated 3-σ landing uncertainty is given by an ellipse of 74.5 km along track by 23.4 km cross track. The capsule retrieval operations could be quite similar to those of Stardust (2005) and Hayabusa (foreseen in 2010) and Europe already has some experience in this field with Mirka (DLR) and the ARD (ESA).

The capsule is equipped with a UHF or VHF beacon that operates for 5 days after landing for contingency. If operations are nominal the detection (UHF/VHF beacons) and recovery (*e.g.* by helicopter) can however be done much faster which is beneficial to thermal control of the sample (< +40 ºC). For example, the Stardust capsule was recovered within 30 minutes after landing. Optionally, airborne observations with conventional cameras could help narrow down the landing location by triangulation but this is not mandatory. This was done for Stardust and the ATV re-entry. The capsule is then transported to a working area where the capsule is cleaned off before being further transferred to the curation facility where it is unsealed and the sample can be recovered.

The Woomera Test Range (WTR) hosts a wide spectrum of ground, air and space activities. The favourable desert climate, benign electromagnetic environment and flat easily accessible terrain for test object recovery are additional major assets of the WTR. Infrastructure or logistics such as radar tracking services, helicopters, *etc*. are readily available or can easily be rent so no new investment is required.

The following services for management and the actual capsule recovery are assumed to be provided by ESA:

- Technical interface to the project and working level interface to Woomera facility.
- Coordination with scientists for sealed container processing.
- Detailed planning of recovery operations, including manpower and transportation.
- Landing rehearsals in Europe and Woomera and actual landing in 2024.
- Flight dynamics services for re-entry site prediction.

Figure 53: Stardust re-entry observations (left); Stardust capsule at its landing site (bottom right) and during recovery operations (top right).

6.3 Science operations and data handling/archiving

The Science Ground Segment (SGS) combines the two tasks of science planning and operations and the handling of the returned data including long-term archiving. Detailed assumptions for the design of the Science Ground Segment are given in the 'Science Operations Assumptions Document' [SOAD] which outlines a first baseline mission scenario and puts down some first requirements on the SGS.

The SGS is assumed to be located at ESAC. It will collect science observation requests from the PI teams providing the instruments and produce a consistent operations plan together with the PI teams. It will handle the physical inputs and produce a final operational request file which will be given to the Mission Operations Centre for combination with spacecraft commands and uplink. The returned telemetry from the instruments will be pre-processed by the SGS and made available to the PI teams in an easy to read format. With the support of the PI teams, data products for the long-term archive following the standards of the PSA will be generated.

The following detailed functions will be provided to the PI teams by the SGS:
(a) Collection of the science observation requests from the PI teams
(b) Production of spacecraft pointing requests and a consolidated operational timeline for all on-board instruments
(c) Iteration of this timeline with the Mission Operations Centre
(d) Pre-processing of the received science data and provision to the PI teams
(e) Provide a science quick-look system
(f) With support of the PI teams, prepare data sets for ingestion into the long-term archive (the PSA)
(g) Validate the datasets, organise peer reviews, and ingest the data into the PSA

Ad (a): Just as on current planetary missions, the SGS will, together with the PI teams, produce a top-level plan of the observations which will have to be performed with the on-board instruments when the spacecraft is at the asteroid.

Ad (b) and (c): This encompasses both the scientific coordination of pointing and operations of the instruments, taking into account the resource constraints, and also the production of the actual computer-readable command files which will be sent to the Mission Operations Centre.

Ad (d) and (e): The scientific data from the instruments returns to ground in bits and bytes and is received at ESOC. The SGS will convert these data into PDS-labelled datasets and provide quick look visualisation tools for the PI teams.

Ad (f) and (g): As on all other current planetary missions, it is assumed that the Planetary Science Archive (PSA) will be the final long-term archive of the Marco Polo data. In addition to the actual science data, auxiliary data (spacecraft orbit and attitude data, relevant housekeeping, and more) will be stored in the PSA. The data in the PSA has to be self-explanatory, meaning that additional information on data formats and how to properly interpret them, needs to be provided. After producing these datasets together with the PI teams, the SGS will use their validation and verification tools to ingest the data into the PSA. For each dataset, a peer review will be performed to ensure the correctness of the dataset.

The PI teams are expected to provide science observation requests to the SGS and support the consolidation of the operational timelines. They have to provide input for the data processing pipelines and in particular work on the calibration of the data, where the expertise is in the PI teams. The PI team has to prepare the final long-term data archive products which will be made available to the scientific community via the PSA.
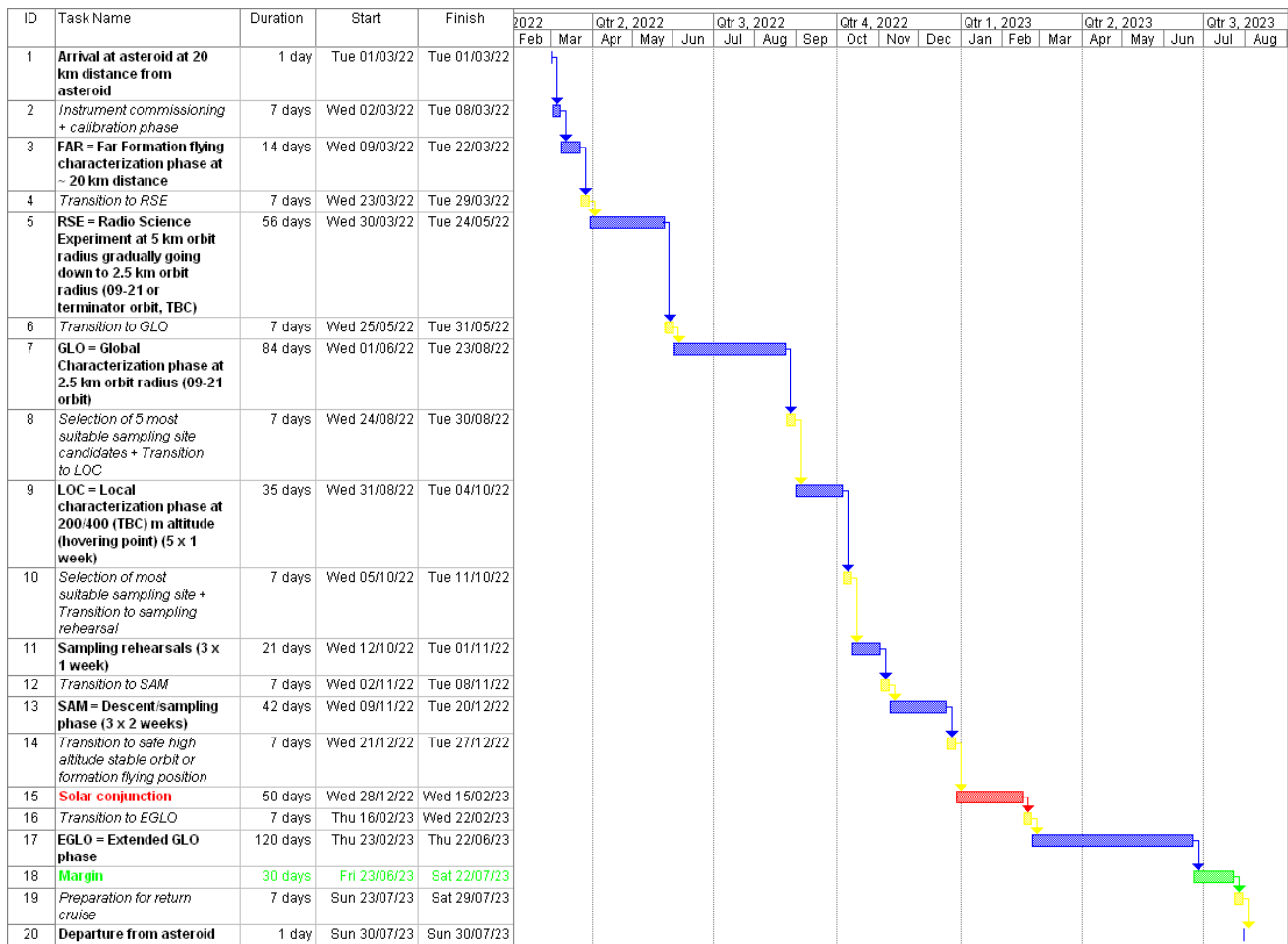
Figure 54: Reference science operations during the asteroid proximity operations phase. Note: The above scenario is very flexible and includes substantial margins. For example: the sampling phase (SAM) could also be shifted to early 2023, soon after the solar conjunction to extend the global characterisation phase (GLO).

6.4 Curation facility

A sample return receiving and curation facility is an essential asset for the preservation and distribution for analysis of the collected extraterrestrial sample and the long term archiving of such a valuable resource. It is foreseen to be requested via an AO process as a nationally-funded contribution. A terrestrial facility capable of receiving the sample returned from the Marco Polo mission must be designed to guarantee the most thorough analyses with the highest scientific return.

The facility has to provide secure and appropriate long term storage, preliminary characterization of the sample, the ability to prepare sub-samples for allocation in order to achieve the required effectiveness and collaborative outcomes for the whole international scientific community. Above all, the facility must guarantee to preserve the sample in its pristine condition, avoiding chemical and physical alteration of materials by the Earth environments in order to avoid false positive or misleading results.

It needs to provide a comprehensive and useful catalogue of the collection that enables individual researchers to identify the specimens to request for detailed laboratory investigation and to accurately record all activity on the sample, both within the facility and in the scientific community.

The facility also has a unique opportunity to act as a focal point for outreach activity associated with extraterrestrial materials.

6.4.1   Security

Experience from the Apollo lunar programme and meteorites indicate that extraterrestrial materials, particularly pristine returned samples, attract great interest from the general public. Such material represents great commercial value (*e.g.* Lunar meteorites achieve many thousands of Euros per gram), and therefore, given the need for access to the facility by scientists, the facility will require carefully considered security aspects. In addition, protection of the sample from extreme natural events is also required. However, no bio-containment of the sample is required as Marco Polo will only be a COSPAR designated "unrestricted" sample return mission.

6.4.2   Contamination control

Contamination is defined as molecular (chemical substances) and particulate (solid tiny particles of micrometre size), which has the potential to react with or become intimately mixed with the sample – with the potential for generating misleading analytical results. The levels of contamination that the sample will be exposed to must be controlled during all operational tasks involving the samples inside the curation facility:

- ERC handling;
- ERC storage;
- Sample handling:
- Sample storage;
- Sample characterization;
- Sample preparation and delivery for external studies and returns;
- Maintenance of curation facility.

Witness plates will be used to monitor contamination during each task of curation activity. These will be able to record particulates and volatile organics present during all stages of sample activity and storage. High temperature can change sample properties and induce desorption.

Materials and Environmental Properties: Considering the contamination issues and according to technical characteristics, the materials present in the sample handling areas must be strictly controlled. Materials should be clean room compatible (*i.e.* low particle shed) and in the case of the need to preserve the organic inventory of the sample, have low volatile organic content.

Materials in direct contact with the sample (handling, storage) should be restricted to the absolute minimum; at least until a sample aliquot has been designated for a specific analysis programme. Potential materials for storage and handling should be restricted to stainless steel and quartz (or glass). All the materials with which the sample come into contact have to be sterilised, cleaned and packaged according to approved procedures, and introduced to the storage area only through sterilised transfer locks.

The environmental requirements for the working area inside the curation facility are strictly related to its design. The anticipated facility can be summarised as (Class defined per ISO 14644-1):

- **Control room**, for control of environmental parameters, verification of procedures, control of operations and general viewing.
- **Entrance room** (ISO Class 7 clean room) - access of personnel and materials to the working area.
- **Exchange room** (ISO Class 6 clean room) - transit room for personnel and materials.

- **SRC handling room** (ISO class 6 clean room) – for partial disassembly of ERC to recover witness plates and sample container(s) and subsequent storage of ERC.
- **Laboratory room** (ISO Class 5), is the area where complex sample preparation is performed
- **Sample handling** (ISO Class 4 – purged with inert gas (see below)) – initial sample selection and sub-sampling and preliminary characterisation.
- **Storage room** (ISO Class 4 – purged with inert gas (see below)), is the core area where the parts of the sample are stored in their boxes and cabinets.

6.4.3   Sample storage

It is anticipated that the long-term storage of the sample will be strictly in environments with controlled atmosphere composed of inert gas (argon or nitrogen). Vacuum could be considered for the long-term storage of the fraction of material preserved for posterity.

Initial sample handling should also be performed under the same conditions as storage, as there could be multiple handling of the same fragment. Dry, filter gas purged storage areas linked to sample handling glove boxes (most probably by robotic mechanisms) are therefore required as the innermost part of the curation facility. Sample storage will be in numbered holders (for materials – see above), easily accessible by a remotely controlled robotic arm inside a storage cabinet, where many sample holders are packed. The robotic arm transfers the sample holder to the glove box for initial processing. This makes it possible to keep the sample always in a controlled and inert atmosphere in order to minimise contamination at least until its delivery to external laboratories.

The storage cabinets should be fabricated in stainless steel in order to allow clean surfaces compatible with the requirements for an ISO class 4 environment and to avoid any contamination from molecular outgassing. To this purpose, lateral apertures should allow better gas flow inside the entire cabinet volume. The storage cabinet should also allow an efficient packing of sample holders that allows robotic and remote operations for storing and retrieving parts of the sample.

6.4.4   Sample characterisation

It is anticipated that detailed study of the sample will be performed by the scientific community (building on successful programs following Apollo, Stardust and Genesis sample return missions). However, a preliminary characterisation of all the principal components (say down to 1 mm particle size) will need to be performed to provide sufficient information to understand the variation of material types present and to allocate appropriate sub-samples to the scientific community (*e.g.* in the first instance organic rich material may be prioritised for organic studies, low aqueous alteration for interstellar grain and early solar-system studies, *etc*.).

To provide this information a number of non-destructive and non-contaminating analytical tools will be required within the clean area of the sample curation facility:

- Optical microscopes - for recording colours, grain sizes, *etc*. of particles;
- FTIR microscope – for providing mineralogy and nature/abundance of organics on exposed surfaces.
- High precision balances – for measuring the sample masses;
- Laser Raman microscope – for providing more specific mineralogical and chemical information.

Additional analytical facilities will be required within the curation facility to support various aspects of the sample preparation and operation of the facility:

- Field Emission Scanning Electron Microscopy (FESEM) equipped with Energy Dispersive X-ray Spectroscopy (EDX) and Focused Ion Beam (FIB) systems – for recording morphology, size, mineralogy and composition of particles; for screening/quality control of prepared sub-samples, and assessment of particulate contamination on witness plates; for the preparation of location-specific electron-transparent wafers.
- GC-MS systems - for assessing organic contamination levels on witness plates and ERC;
- XPS – for assessing contamination levels on surfaces and cleaning procedures.

6.4.5   Sample preparation

Many of the analytical techniques employed by the scientific community demand special preparation of the sub-samples – *e.g.* polished sections, homogenised powders, electron transparent sections. In order to ensure optimum use of materials in the preparation of these sub-samples and minimizing contamination of the parent fragments, preparation of these specialised sub-samples must be performed within the curation facility. This will require clean room compatible splitting, cutting, polishing and microtoming equipment as well as the FIB-FESEM capability already listed above.

6.4.6   Sample documentation

Detailed descriptions of each fragment within the sample will be generated by the curation facility for distribution to the scientific community in order to facilitate sample requests. The facility will be required to document all activities for each part of the sample, including all movements and processes within the facility and to track and monitor usage and movement once allocated. The sample catalogue will be accessible through a web interface.

6.4.7   Other activities

In addition to the returned sample, the curation facility should also be responsible for documentation, curation and distribution of witness plates from the spacecraft and the sample curation facility itself as well as representative materials collected during the construction phase of the spacecraft and key systems (*e.g.* lubricants, fuels, materials in close proximity to the sample, *etc.*). Because of the potentially contaminating nature of these materials they will need to be stored and handled in an entirely separate, albeit lower specified, adjoining facility.

7   Management

This section summarizes the envisaged management approach for Marco Polo. It also serves as a starting point for writing the Marco Polo Science Management Plan (SMP). In this document the following topics are covered and described:

- The overall mission management within ESA
- The various steps from the end of the assessment study to the launch
- The overall procurement and model philosophy
- The major actors and teams involved in the Marco Polo project
- The payload-related aspects, in particular the set-up of the consortia, the various actors, the selection process and the data rights
- The overall project schedule

The procurement schedule and model philosophy described herein is provided for illustrative purposes only, as a result of the assessment study. The procurement approach is based on a fixed price contract instead of a cost reimbursement type of contract.

7.1   Project management

7.1.1   Overview

The science and project management will follow the current practises of ESA science missions. Following the approval of the Marco Polo mission in February 2010 ESA will release an Invitation to Tender (ITT) for the selection of two competitive industrial contractors for the competitive Definition Phase (Phase A/B1) for a typical duration of 16 months. This phase will specifically consider the payload design building on the concepts of Phase 0/A but accounting for the design of specific instruments rather than a model payload. To facilitate this, an Announcement of Opportunity (AO) will call for proposals for the payload instruments and the curation facility. This will be carried out in parallel with the Phase A/B1 ITT. The definition phase

(Phase A/B1) system study, starting in July 2010, will be led by a Study Manager (responsible for all technical aspects under ESA responsibility), a Study Scientist (responsible for all science aspects) and a Payload Manager (responsible for all payload interfaces), as during the assessment study (Phase 0/A). It will typically include two major reviews: the Preliminary Requirements Review (PRR), to be held by the mid-term of the study, and the Systems Requirements Review (SRR), which will close this phase. The Technology Development Activities (TDAs) will be initiated as soon as possible after the mission down-selection in February 2010. These activities will run in parallel to the definition phase and their intermediate results will be fed to the system study as necessary. Critical outputs from the TDAs that are ensuring the mission feasibility or its development schedule are expected to be available before the decision for the mission final adoption. At the PRR, the mission baseline should be well established and documented. It will be critically reviewed with the aim of confirming the feasibility of the overall mission concept. The SRR will close the definition phase by consolidating the overall mission concept for enabling start of the implementation phase, should the mission be finally adopted.

At the end of Definition Phase a scientific evaluation by ESA's scientific advisory bodies in early 2012 will provide a recommendation as to the final adoption of missions to go into Implementation Phase. This recommendation will be provided to the Science Programme Committee (SPC) for approval and the successful candidates will move into the Implementation Phase (Phase B2/C/D/E1) and a Prime industry contract will be selected via a further ITT. The final industrial organization will be completed in phase B2, mostly through a process of competitive selection, by taking into account geographical distribution requirements.

At the start of this phase a project team will be formed in the Project Department (SRE-P) at ESTEC in the Netherlands. This team is lead by a Project Manager, who has the overall technical responsibility for implementing the mission. He/she will be supported by the Project Scientist who keeps the responsibility for all science-related aspects. The ESA Project team will conduct a preliminary design review, a critical design review and a flight acceptance review. To support the project team in this and other tasks, a Marco Polo Science Working Team (SWT) will be formed, made up of PIs and the Project Scientist along with support from components of the Operational and Science Ground Segments. This SWT will form the primary scientific voice of Marco Polo, chaired by the Project Scientist.

After successful commissioning of the instruments shortly after the launch, the responsibility of the Project Manager will be handed over to the Mission Manager who is located in the Solar System Science Operations Division (SRE-OS) at ESAC in Spain. The Project Scientist will continue his/her task.

7.1.2   Management of operations

ESA will be responsible for the launch, checkout, and operations of the spacecraft. ESA will establish an Operational Ground Segment (OGS, formerly called Mission Operations Centre) and a Science Ground Segment (SGS). The OGS will be located at ESOC, the SGS at ESAC.

ESOC will support the definition of the OGS from the beginning of the project, nominating a Ground Segment Manager who will report to the Project Manager (later to the Mission Manager). The definition of the Science Ground Segment will be done under the lead of an SGS Development Manager in the Science Operations Development Division at ESAC in Spain. This will be done in close interaction with the Project Scientist but formally reporting to the Project Manager. After handover of the responsibility from Project Manager to Mission Manager in the operations phase, the SGS will move from the Science Operations Development Division to the Solar System Science Operations Division.

7.2   Procurement philosophy

The proposed procurement scheme for Marco Polo is based on the concept that the payload (instruments and associated processing, data handling and control components) will be provided by PIs funded by national funding agencies of ESA member states. Also, the curation facility will be provided via nationally funded activities. The sampling tool and the associated transfer mechanisms are to be provided as part of the spacecraft.

ESA would have overall responsibility for:

- ▪ The overall spacecraft mission and design (via industrial contract)

- Provision of spacecraft equipment and integration of the spacecraft bus and payload module (via industrial contract)
- Equipment, sub-system and system testing (via industrial contract)
- Spacecraft launch and operations (Arianespace, ESOC and ESAC)
- Acquisition and distribution of data to the Operational and Science Ground Segments.

7.3 Development philosophy

Planetary protection constraints are of no concern as the mission is classified as Category II, thus less harsh than for Mars Express or Rosetta. Care has however to be taken concerning contamination to avoid that the sample will be polluted by Earth-brought contaminants. This can be done via standard cleanliness procedure as well as a well-established contaminant identification and tracking approach via witness plates and archiving during all integration steps of the spacecraft flight model and its payload.

The most critical items on Marco Polo are the sampling and landing mechanisms, the GNC/AOCS hardware and software, as well as the capsule. As a conclusion, a full model cycle (STM, EM, QM, and FM) could be proposed for these sub-systems. An avionics test bench will of course be implemented to verify and validate the spacecraft behaviour under any circumstances, in particular for the descent and sampling phase. To reduce costs, a simpler philosophy (EM/PFM or STM/PFM) is proposed for those sub-systems which need no intermediate qualification step (structure and thermal, antennas, transponders, propulsion equipment, solar arrays, battery, etc.).

An exemplary model philosophy for the different sub-systems of the spacecraft is shown in Table 18.

Table 18: Marco Polo model philosophy on sub-system level.

	STM	EM	QM	PFM	FM
Sampling mechanism	X	X	X		X
Landing mechanism	X	X	X		X
ERC	X	X	X		X
Other mechanisms		X	X		X
Structure	X			X	
Thermal	X			X	
Power				X	
AOCS, GNC		X	X	X	
Data Handling Unit		X		X	
Propulsion		X		X	
TT&C		X		X	
Science instruments		X		X	

7.4 Schedule

With a launch in December 2018 for the baseline ESA-defined scenario, the total time for development, manufacturing, assembly, integration, testing and launch campaign from beginning of Phase B2 to launch is 6 years and a half. This strictly requires that all technologies are at TRL 5 by the mission adoption. It is paramount that definition phase (Phase A/B1) and the proposed pre-development technology activities run on time and are well-coordinated to reach the required maturity by early 2012 so as to judge on the overall mission concept feasibility. Figure 55 gives a top-level master schedule.

ID	Task Name	Duration
1	**MARCO_POLO**	**2343 days**
2	**Milestones**	**2300 days**
3	Mission selection 1	1 day
4	SRR	1 day
5	Mission selection 2	1 day
6	PDR	1 day
7	CDR	1 day
8	AR	1 day
9	Margin	139 days
10	Launch date	1 day
11	**Phases**	**2335 days**
12	Definition Phase ITT	90 days
13	Definition phase B1 (2 parallel studies)	300 days
14	Mission selection process	90 days
15	Implementation phase ITT	90 days
16	Phase B2	300 days
17	Phase C	550 days
18	Phase D (incl. AIV)	650 days
19	Phase E1	90 days
20	**Pre-development technology activities**	**550 days**
21	**Payloads Procurement**	**1976 days**
22	Payload AO	60 days
23	Payload studies	400 days
24	Payload procurement	1516 days

Figure 55: Example of Marco Polo master schedule.

7.5 Science Management

The following text adds some details on the roles of the scientific players in the mission. It serves as a starting point for the Science Management Plan (SMP) which will be the top-level management document of Marco Polo to be agreed by the Science Programme Committee (SPC). For a collaborative mission a share of responsibilities between the participating agencies will be defined as a function of the collaboration scheme.

7.5.1 The Project Scientist

Once the mission enters the implementation phase, ESA will nominate a Project Scientist (PS) for Marco Polo. The PS will be located at ESTEC in the Solar System Missions Division, Research and Scientific Support Department (SRE-SM). He/she will be the Agency's interface with the PIs for scientific matters. The PS will chair the Science Working Team and coordinate its activities.

During all phases of the mission the PS will be responsible for all scientific issues within the project. The PS will monitor the state of implementation and readiness of instrument operations and data processing infrastructure. The Science Operations Department (SRE-O) will provide support on science operations and archiving.

7.5.2 Science Working Team

The Marco Polo Science Working Team (SWT) will consist of all PIs and Interdisciplinary Scientists (IDSs). The PS will chair the SWT. The SWT will monitor and advise ESA (and the collaborating agencies for a common mission) on all aspects of the Marco Polo mission that will affect its scientific performance. It will assist the PS in maximizing the overall scientific return within the established boundary conditions, advise on aspects of science coordination of all partners, and act as a focus for the interests of the scientific community of Marco Polo.

7.5.3 Modes of participation

The possible modes of participation to the Marco Polo programme are:

   (1) Principal Investigator (PI), heading an instrument consortium providing an instrument (= payload).
   (2) Co-Investigator (Co-I), a member of an instrument consortium providing an instrument.
   (3) Interdisciplinary Scientist (IDS), an expert in specific science themes connected to asteroids.

The detailed tasks of these participants will be described in the Science Management Plan.

7.5.4 Data rights

Marco Polo data will be made available in compliance with the established ESA rules concerning information and data rights and release policy. The PI teams will have a proprietary period where they can use the data within their team only, for scientific publications. After the proprietary period, the data has to be made available to the wider scientific community. The detailed data delivery schedule will be defined in the Archive Plan which will have to be agreed and signed by all PIs. Currently, a proprietary period of 6 months from receipt of the original science telemetry is envisaged.

The PIs will also be required to share data with the IDSs so as to enhance the scientific return from the mission, in accordance with procedures to be agreed and formalised within the SWT.

The PI teams will provide raw data and all relevant information on calibration and instrument properties to the Marco Polo science data archive. The data format will be compatible with the PSA.

The Science Ground Segment will be working together closely with the PI teams to produce data processing pipelines ensuring that the received data can be ingested quickly into the PSA. It will not perform any scientific analysis of the data. The PI teams will support the preparation of data processing pipelines installed at the SGS.

Scientific results from the mission have to be published by the PI teams in a timely manner, in appropriate scientific and technical journals. Proper acknowledgement of the services supplied by ESA (and JAXA, in the case of a common mission) will be made.

A Memorandum of Understanding between the involved agencies will be needed to fix:

- the data policy rules, the selected format and the length of the period after which the data have to become available to any user of the PSA;
- the criteria that will be adopted for the selection of the proposals of the study of the NEO samples resulting from a call to the worldwide scientific community on a competitive basis.

The PI teams will provide the agency(ies) with processed and useable data for Public Outreach purposes as soon as possible after their reception. The PI teams will also engage in supporting a Science Communication Plan.

7.6 Collaboration scenarios

During the last years we identified several possible collaboration scenarios with JAXA and NASA scientists and representatives. JAXA and NASA may contribute to various elements. Alternatively, it could be envisaged to participate as a 'mission of opportunity' (see appendix).

The Marco Polo study has been built on the lessons learnt from the JAXA Hayabusa sample return mission. The ESA baseline scenario would greatly benefit from the expertise of JAXA regarding various elements, in particular the GNC.

Moreover, the science objectives and mission design of Marco Polo create an eaxcellent opportunity for NASA collaboration. The Marco Polo mission is a synergetic fit with NASA's Strategic Goal for Planetary Science: "Advance scientific knowledge of the origin and history of the solar system, the potential for life elsewhere, and the hazards and resources present as humans explore space." Collaboration with NASA can be possible from the level of cooperating scientists (already in place) to the provision or sharing of key mission components. Specific NASA programme elements for fostering international collaboration include: SALMON (Stand Alone Missions of Opportunity), Discovery, and New Frontiers (see Appendix).

The final collaboration scheme will depend on the programmatic evolution of the involved agencies.

8   Communications and outreach

The public outreach possibilities of a mission like Marco Polo are considerable for two main reasons:

1. The enormous fascination of the general public for challenges such as the landing of a terrestrial robot on an alien world, expressed at each new step of planetary exploration (from the Surveyors on the Moon to Mars Pathfinder, from Spirit and Opportunity on Mars to Huygens at Titan). The Huygens probe is perceived as belonging to all of us and its achievements are seen as our own achievements.

2. The impact hazard and the interest of the media and people in this subject due to its link to the extinction of the dinosaurs and several disaster movies. On the strategic and political front there is considerable interest in prediction and mitigation of an NEA impact. Society has the right to expect that the scientific community will make a significant contribution to these efforts: we can do so, while still addressing the demands of fundamental planetary science, with a mission like Marco Polo.

Reaching out to the culturally different people from across Earth (Europe, Japan, China, India, North and South America) to provide a better understanding of the mission challenges/achievements is an important objective.

It is intended to set up an Outreach and Public Affairs (OPA) team composed of one representative of each scientific and technical team involved in the mission, to support the public relation services and/or press offices of the relevant space agencies with material and activities especially devoted to public outreach and education. The OPA team will organize at least one workshop per year designed to provide opportunities for Marco Polo Team-members to discuss and propose new tools and initiatives in the mission outreach activity.

From previous experiences, it was found that the quick regular release of news and information is very important to attract people's interest. We will develop and update continuously Marco Polo science multimedia tools such as images, video, animation, sounds, documents (producing posters, CD, DVD) to be distributed to the media, teachers and the general public. An important experience in that sense has been acquired in Japan during the Hayabusa mission. From the phase of approach to the asteroid to the end of the exploration, the information from the Hayabusa mission was continuously updated on the JAXA web site. Especially during the two touchdown events, the mission status was reported on the web in real time.

Another interesting activity performed by the Hayabusa team was to engrave people's names on the surface film of the target marker, an artificial landmark which reached the surface of the asteroid Itokawa (Figure 56). About 880 000 names from 150 countries were included after a public appeal. The Hayabusa mission thus attracted the interest of the public long before it was launched. At the time of the release of the target maker, the public attention was maximised.

The Hayabusa mission was thus successful in attracting the attention of the public. As a result of these efforts, not only written reports, but Manga cartoons and animations, many of very high quality, appeared on various amateur web sites. Even jazz music was composed specifically for the Hayabusa mission by a professional musician. As a result, many people became supporters of the Hayabusa mission.

Based on these previous experiences, the OPA team will undertake activities along those lines and promote various kinds of outreach and educational projects widely.
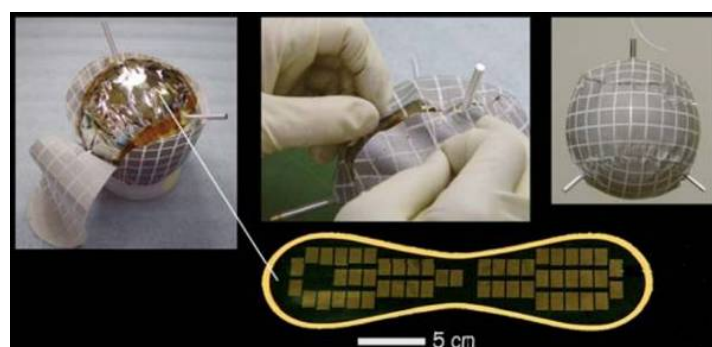
Figure 56: Target marker of the Hayabusa spacecraft. The names of about 880 000 people are engraved on its surface.

Together with the interested international and national scientific societies the team will seek to establish one or more Marco Polo mission awards. Activities that the team would like to consider recognized include:

- Presentations and posters of young students (high school, masters);
- PhD theses in asteroid science;
- Stories on the Marco Polo mission published in newspapers and monthly magazine.

The Marco Polo mission web page will be maintained for both internal communication among the various scientific/technical teams participating in the mission and outreach to the general public. We will look for a permanent location for the Marco Polo mission webpage and listserver, associated with ESA. We will develop and continually improve the value of the web page for both Marco Polo team members and the general public.

9 References

9.1 Scientific publications

Abe S. et al. 2006, Science 312, 1344.
Abe S. et al. 2008, LPSC XXXIX, 1391, 1594.
Alexander, C.M.O'D.*et al.*, 2008, Science 320, 1617
Amari S. et al. 1994, Meteoritics 29, 437.
Amelin Y. et al. 2002, Science 297, 1678.
Arteaga O. et al. 2009, Origin Life Evol. Biosph. in press
Barnouin-Jah O. et al. 2008, Icarus 188, 108.
Barucci M.A. et al.2002, Icarus 156, 202.
Barucci M.A. et al. 1998, Icarus 132, 388.
Barucci M.A. et al. 1987, Icarus 72, 304.
Bernatowicz T.J. et al. 2003, Geochim. Cosmochim. Acta 67, 4679.
Bernatowicz T.J. et al.*,* 2006, in Meteorites and the Early Solar System II, Univ. Arizona Press, 109
Binzel R.P. *et al.*, 2002a, in Asteroids III, Univ. Arizona Press, 255
Binzel R.P.*et al.*, 2002b, Bull. Am. Astron. Soc. 24, 840.
Binzel R.P. et al. 2004, Icarus 170, 259.
Bonner W.A. 1991, Origin of Life 21, 59.
Borg L.E. et al. 1999, Science 286, 90.
Bottke W.F. et al. 2002, Icarus 156, 399.
Bottke W.F. et al. 2005, Icarus 175, 111.
Bottke W.F. et al. 2007. Nature 449, 48.
Brock et al. 2000, Rev. Sci. Instrum. 71, 1306.
Bradley J.P. 1994, Science 265, 925.
Britt D.T. and Consolmagno G.J. 2000, Icarus 146, 213.
Brownlee D. et al. 2006, Science 314, 1711.
Buczkowski D.L. et al. 2008, Icarus 193, 39.
Bus S.J. and Binzel R.P. 2002a, Icarus 158, 106.
Bus S.J. and Binzel R.P. 2002b, Icarus 108, 146.
Campins H., *et al.*, 2009, Astron. Astrophys. 503, L17
Chapman, C.R. et al. 1996. Icarus 120, 231.
Chaussidon M. and Gounelle M., 2006, in Meteorites and the Early Solar System II, Univ. of Arizona Press, 323.
Cheng A.F. 2002, in Asteroids III, Univ. of Arizona Press, 351.
Chesley S. et al. 2003, Science 302, 1739.
Christoffersen R. et al. 1996, Meteoritics 31, 835.
Cody G.D. and Alexander C.M.O'D, 2005, GCA69, 1085.
Cody G.D. et al. 2008, MAPS 43, 353.
Dauphas, N. et al. 2000, Icarus 148, 508.
Delbo, M. et al. 2007, Icarus 190, 236.
Dell'Oro P. and Cellino A. 2008, ACM2008, LPIC 1405.
DeMeo F. and Binzel R.P. 2008, Icarus 199, 436.
Di Lellis A. et al. A.M. 1993, Il Nuovo Cimento 16, 743
Dotto E. et al., 2005, Comptes Rendus Physique Academie des Sciences, 6, 303.
Elsila J.E. et al., 2009, MAPS, in press.
Farinella P. and Vokrouhlicky D. 1999, Science 283, 1507.
Feigelson E.D. and Montmerle T. 1999, Annual Review of Astron. and Astroph., 37, 363.
Franchi I.A. 2008, Rev. Min. Geochem. 68, 345.
Fujiwara A. et al. 2006. Science 312, 1330.
Galy A. et al. 2000, Science 290, 1751.
Giorgini J.D. et al. 2008, Icarus 193, 1.
Gladman B.J. et al. 2000, Icarus 146, 176.
Gomes R. et al. 2005, Nature 435, 466.
Hartmann W. et al. 2007, Icarus 186, 11.
Hapke B. 2001, J. Geophys. Res. E5, 10039.
Harris A.W. 1998, Icarus 131, 291.
Heck P.R. 2009, ApJ 698, 1155.
Housen K. et al. 2009, Nature 402, 155.
Hunt, G.R. and Salisbury J.W. 1974, Environ. Res. Paper 496-AFCRL-TR-74-0625, 142.

Hunt G.R. and Salisbury J.W. 1975, Environ. Res. Paper 520-AFCRL-TR-750356, p. 49.
Hurych Z.D. et al. 1988, Phys. Rev. 38, 8002
Huss G.R et al. 2003, Geochim. Cosmochim. Acta 67, 4823.
Jacobsen S.B. 2003, Science 300, 1513
Jedicke R. 2008, BAAS 40, 435.
Jenniskens P. et al. 2009, Nature 458, 485.
Kanno A. *et al* 2003, Geophys. Res. Lett. 30., PLA 2-1.
Keller L.P. and McKay D.S. 1993, Meteoritics, 28, 378.
Keller H.U. et al. 2009, BAAS 41, 564.
Killen R.M. and Ip W.H. 1999, Rev. Geophys. 37, 361.
Lazzarin M. et al. 2006, Astrophys. J. 647, L179.
Lebowsky L.A. and Spencer J.R. 1989, in Asteroids II. Univ. of Arizona Press, Tucson, 128.
Leuw (de) S. et al. 2009, 40th LPI, Abstract 1794.
Loeffler M.J. et al. 2009, J. Geophys. Res. E 114, E03003.
Lowry S.C. et al. 2007, Science 316, 272.
Lu E.T. and Love S.G. 2005, Nature 438, 177.
Lyon I. et al. 2007, MAPS 42, 373.
Lyon, R.J.P. 1962, Stanford Res. Inst. Final Rep. Contract NASA, 49-04.
Martins Z. et al. 2008, EPSL 270, 130.
Maurette M., 2005, Micrometeorites and the mysteries of our origins. Springer-Verlag.
McKeegan K.D. et al. 2000, Science 289, 1334.
McKeegan K.D. et al. 2009, LPI, 40.2494M.
Messenger S. et al. 2003, Science 300, 105.
Meyer B.S. and Zinner E. 2006, in Meteorites and the Early Solar System II, Univ Arizona Press.
Michel P. et al. 2000. Icarus 145, 332.
Michel P. and Yoshikawa M. 2006, A&A 447, 817.
Michel P. et al. 2009, Icarus 200, 503.
Michel P. and Delbo M., Icarus, submitted.
Michikami et al. 2007, Science 316, 1011.
Mignard F. et al. 2007, Earth, Moon, and Planets 3-4, 97
Miller J.K. et al. 2002, Icarus 155, 3.
Miyamoto H. et al. 2007, Science 316, 1011
Modi et al. 2003, Nature 424,171.
Morbidelli A. et al. 2002, Icarus 158, 329.
Morbidelli A et al. 2006, MAPS 41, 875.
Müller T.G. and Lagerros J.S.V. 1998, Astron. Astrophys. 338, 340.
Nesvorny, D. et al. 2005, Icarus 173, 132.
Nguyen et al. 2007, The Astrophys. J. 656, 1223.
Nuth J.A. 2001, Am. Sci. 89, 230
Orsini S. et al. 2009a, AIP Conf. Proc. 1144, 76.
Peltzer E.T. and Bada J. L. 1978, Nature 272, 443.
Perozzi E. et al. 2001, PSS 49, 3.
Pizzarello S. and Cronin J. R. 2000, Geochim. Cosmochim. Acta 64, 329.
Pizzarello S. et al. 2006, in Meteorites and the Early Solar System II, Univ. Arizona Press, 625.
Plainaki C. et al. 2009, PSS 57, 384.
Rème H. et al. 1997, Space Science Reviews 79, 303.
Remusat L. et al. 2006, Earth and Planet. Sci. Let. 243**,** 15.
Richardson D.C. et al. 2002, in Asteroids III, Univ. Arizona Press, 501.
Richter L. 1998. Robotics and Autonomous Systems 23, 117
Riner M. A. et al. 2008, Icarus 198, 67.
Robert F. 2006, in Meteorites and the Early Solar System II, Univ. of Arizona Press, 341.
Rotundi A. et al. 2008 MAPS 43, 367.
Rubincam D.P. 2000, Icarus 148, 2.
Russell S. S., et al. 2006, in Meteorites and the Early Solar System II, 233.
Salisbury J.W. et al. 1991. Infrared spectral of minerals, Johns Hopkins Univ., Baltimore.
Saito et al. 2006, Science 312, 1341.
Sasaki, S. et al. 2001, Nature 410, 555.
Scheeres D. 2007, Icarus 189, 370.
Scheeres D. et al. 2007, Icarus 188, 425.
Scheeres D. and Gaskell R.W. 2008, Icarus 198, 125.
Shu F.H., et al. 1994, Astrophys. J., 429, 797.

Sigmund P. 1981, Sputtering by Ion Bombardment: A General Theoretical View, Sputtering by Particle Bombardment, I. Springer, New York.
Strazzulla G. et al. 2005, Icarus 174, 31.
Stuart J.S. and Binzel R.P. 2004, Icarus 170, 295.
Thomas P.C. et al. 2000, J. Geophys. Res. 105(E6), 15091.
Tsuchiyama A. et al. 2008, IPEWG Abstract Book
Villanueva G.L. et al. 2009, Astrophys. J. Letters, 690/1, L5
Vokrouhlicky D. et al. 2007, Icarus 191, 636.
Walsh K. et al. 2008, Nature 454, 188.
Wieser et al. 2005, J. Appl. Phys. 98, 034906-1.
Wurz P. 2000, The Outer Heliosphere: Beyond the Planets, Copernicus Gesellschaft e.V., Katlenburg-Lindau, Germany, 251.
Wurz P. and Lammer H. 2003, Icarus 164, 1.
Yamada M. et al. 1999. 30th LPI Abstract 1566.
Yano H. et al. 2006. Science 312, 1350.
Yeomans D. et al. 1997, Science 278, 2106.
Yeomans D. et al. 2000, Science 289, 2085.
Zega T.J. et al. 2007, MAPS 42, 1373.
Zolensky M.E. et al.. 2006. Science 314, 1735.

9.2   Technical documentation

[CDF FR]: Marco Polo Concurrent Design Facility study report, ESA/ESTEC, 2008
[CRAD]: Capsule Retrieval Assumptions Document, ESA/ESOC, DOPS-MGT-TN-1002-OPS-HSA
[MASCOT-DOI]: MASCOT report in response to the call of the 'Declaration of Interest', MSC-RY-ES-RP-0001
[MASCOT-SCIRD]: MASCOT Science Requirements Document, MSC-RY-ES-RD-0001
[MED]: Mission Environment Document, , ESA/ESTEC , SCI-PA/2008.014/Marco-Polo
[MOAD]: Mission Operations Assumptions Document, ESA/ESTEC, SRE-PA/2009.028/Marco-Polo
[PP]: Marco Polo Planetary Portection Document, ESA/ESTEC, SCI-PA/2008.013/Marco-Polo
[PDD]: Marco Polo Payload Definition Document, ESA/ESTEC, SCI-PA/2008/002/Marco-Polo
[SCI-RD]: Marco Polo Science Requirements Document, ESA/ESTEC, MP-RSSD-RS-001
[SOAD]: Science Operations Assumptions Document, ESA/ESTEC, MP-RSSD-TN-001

10   Index

11   List of acronyms

AarU	Aarhus University
ACE	Asteroid Charging Experiment
AIV	Assembly, Intergration and Verification
AMICA	Multi-Spectral Telescopic Imager on Hayabusa
AO	Announcement of Opportunity
AOCS	Attitude and Orbit Control System
APS	Active Pixel Sensor
APXS	Alpha-Particle X-ray Spectrometer
AR	Anti-reflection
ARD	Advanced Reentry Demonstrator
ASEM	Analytical Scanning Electron Microscopy
ASI	Agencia Spaziale Italiana
ASIC	Application Specific Integrated Circuit
ATR	Attenuated Total Reflection
ATV	Automated Transfer Vehicle
AU	Astronomical Unit
BELA	BepiColombo Laser Altimeter
CAI	Calcium aluminium rich inclusion
CC	Carbonaceous Chondrite
CDF	Concurrent Design Facility
CDPU	Command and data processing unit
CDTI	Centro para el Desarrollo Tecnologico Industrial
CEREGE	Centre Européen de Recherche et d'Enseignement des Géosciences de l'Environnement
CMOS	Complementary Metal Oxide Semiconductor
CNES	Centre National d'Etudes Spatiale
CNSR	Comet Nucleus Sample Return
Co-I	Co-Investigator
COSPAR	Committee on Space Research
CPEM	Circular Polarized Electromagnetic waves
CRAD	Capsule Recovery Assumptions Document
CRE	Cosmic ray exposure
CS-GS-MS	Compound specific gas source mass spectrometer
CT Scan	X-Ray Computed Tomography
CTP	Core Technology Programme
CUC	Close-Up Camera
CV	Cosmic Vision
DLR	Deutsches Zentrum für Luft- und Raumfahrt
DNA	Deoxyribonucleic acid
Dof	Degree of freedom
dof	Degree of freedom
DOI	Declaration of Interest
DPU	Digital processing unit
DS	Deep Space
DSM	Deep-Space Manoeuvre – or: Descent and Sampling Module
DTM	Digital terrain model
EBSD	Electro backscattered diffraction
EDX	Energy dispersive X-ray Spectrometer
EDXRF	Energy dispersive X-ray Fluorescence Spectrometer
EELS	Electron energy-loss spectroscopy
EGLO	Extended Global Monitoring (mission phase)
EM	Engineering Model
EMPA	Electron Microprobe Analyzer
ERC	Earth Re-entry Capsule
ESA	European Space Agency
ESA	Electrostatic Analyzer

ESAC	European Space Astronomy Centre
ESOC	European Space Operations Centre
ESR	Electron spin resonance
ESTEC	European Space Technology Centre
ETH	Eidgenössische Technische Hochschule (in Zürich)
FAR	Far formation flying (mission phase)
FDIR	Failure, Detection, Isolation and Recovery
FESM	Field emission scanning electron microscopy
FGI	Finnish Geodetic Institute
Fib	Focussed Ion Beam
FIB-SEM	Focussed Ion Beam – Scanning Electron microscope
FM	Flight Model
FOV	Field of View
FPA	Focal Plane Assembly
FPGA	Field-programmable gate array
FTIR	Fourier-transform infrared spectroscopy
FY	Fiscal year
GAP	Gas Analyzer Package
GC	Gas chromatograph
GC-MS	Gas Chromatography Mass Spectroscopy
GC-MS	Gas chromatograph – mass spectrometer
GLO	Global Characterisation (mission phase)
GNC	Guidance Navigation and Control
GS-MS	Gas source mass spectrometer
H	Absolute visual magnitude (*i.e.* the visual magnitude of an asteroid if observed a distance of 1 AU from the Earth and the Sun, and at a zero phase angle)
HGA	High gain antenna
HPLC	High performance liquid chromatography
ICPMS	Inductively Coupled Plasma Mass Analyzer
IDP	Interplanetary Dust Particle
IDS	Inter-Disciplinary Scientist
INAA	Instrumental Neutron Activation Analysis
INAF	Istituto Nazionale di Astrofisica (in Italy)
IR	Infrared
IR-GC-MS	Infrared Gas Chromatography Mass Spectroscopy
IR-LC-MS	Infrared Liquid Chromatography Mass Spectroscopy
ISM	Interstellar Medium
ISO	International Organization for Standardization – or: Infrared Space Observatory
ITT	Invitation to tender
JAXA	Japanese Space Agency
JPL	Jet Propulsion Laboratory
JSPEC	JAXA Space Exploration Center
L^{2}DMS	Laser Desorption Ionisation Mass Spectroscopy
LA-ICPMS	Laser Ablation – Inductive Coupled Plasma Mass Spectroscopy
LC	Liquid chromatograph
LC-MS	Liquid Chromatography Mass Spectroscopy
LED	Light emitting diode
LEO	Low-Earth Orbit
LEOP	Low-Earth Orbit Phase
LESIA	Laboratoire d'Etudes Spatiales et d'Instrumentation en Astrophysique (at Paris Observatory, France)
LGA	Low-Gain Antenna
LIDAR	Light Detection and Ranging – or: JAXA Laser Altimeter
LOC	Local Characterisation (mission phase)
LSST	Large Synoptic Survey Telescope
L	Launch
LV	Launch Vehicle
MAPIS	Marco Polo Imaging Spectrometer
MASCOT	Marco Polo Surface Scout
MBA	Main-Belt Asteroid
MC-ICPMS	Multiple collector inductively coupled plasma mass spectrometer
MCP	Micro-Channel Plate
MED	Mission Environment Document
MEX	Mars Express

MLI	Multi-Layer Insulation
MOAD	Mission Operations Assumptions Document
MOC	Mission Operations Centre
MP	Marco Polo
MRD	Mission Requirements Document
MS	Mass Spectroscopy
MS	Mass spectrometer
MSR	Mars Sample Return
MSL	Mars Simulation Laboratory at AarU
MSSL	Mullard Space Science Laboratory (at the University College London)
MTF	Modulation transfer function
n.d.	Not determined
NAC	Narrow Angle Camera
NASA	National Aeronautics and Space Administration
NEA	Near-Earth Asteroid
NEAR	near-Earth Asteroid Rendezvous mission, NEAR-Shoemaker
NG-MS	Noble Gas Mass Spectrometer
NHM	Natural History Museum
NIR	Near Infrared
NIRS	Near-Infrared Spectrometer
NHMD	Natural History Museum, Copenhagen
NHMS	Natural History Museum, Stockholm
NMR	Nuclear Magnetic Resonance
NPA	Neutral Particle Analyzer
OGS	Operational Ground Segment
OPA	Outreach and Public Affairs
ORB	Orbital module
OU	Open University (in Milton Keynes, UK)
P/L	Payload
Pan-STARRS	Panoramic Survey Telescope And Rapid Response System
PDD	Payload Definition Document
PDS	Planetary Data System
PenRad	Radiation Sensor
PFM	Proto-Flight Model
PI	Principal Investigator
PIXE	Proton-Induced X-ray Emission
ppb	parts per billion
ppm	parts per million
PRM	Propulsion Module
PS	Project Scientist
PSA	Planetary Science Archive
PSSRI	Planetary and Space Sciences Research Institute (at Open University, UK)
QE	Quantum efficiency
QM	Qualification Model
RCS	Reaction Control System
RD	Reference Document
RFDU	Radio Frequency Distribution Unit
RID	Requirements and Interfaces Document
RNA	Ribonucleic acid
RSE	Radio Science Experiment
S/C	Spacecraft
SALMON	Stand Alone Mission of Opportunity
SAM	Sampling operations phase (mission phase)
SCI-RD	Science Requirements Document
SCOS 2000	Spacecraft Operating System (version of the year 2000)
SCU	Sensor Control Unit
SEM	Scanning Electron Microscopy
SEM-EDX	Scanning electron microscope – Energy dispersive X-ray spectrometer
SGS	Science Ground Segment
SIMS	Secondary Ion Mass Spectroscopy
SM	System Margin

SMP	Science Management Plan
SOAD	Science Operations Assumptions Document
SOC	Science Operations Centre
SPC	Science Programme Committee
SRE	Directorate of Science and Robotic Exploration at ESA
SRE-O	Operations Department of ESA
SRE-OS	Solar System Missions Operations Division of ESA
SRE-P	Project Department of ESA
SRE-SM	Solar System Missions Division of ESA
S-SQUID-M	Superconducting SQUID Magnetometer
SST	Science Study Team
STFC	Science and Technology Facilities Council
STM	Structural and Thermal Model
STR	Star Tracker
SWT	Science Working Team
tbc	To be confirmed
tbd	To be defined
tbw	To be written
TC	Telecommand
TEM	Transmission Electron Microscopy
TIMS	Thermal Ionization Mass Spectrometer
TM	Telemetry
TMA	Three mirror anastigmatic
TOF	Time-of-Flight
TPS	Thermal protection system
TRL	Technology Readiness Level
TRP	Technology Research Programme
TWTA	Travelling Wave Tube Amplifier
UCL	University College London
UH	University of Helsinki
UHF	Ultra-High Frequency
UK	United Kingdom
UmU	Umea University
UpU	Uppsala University
US	United States
VEX	Venus Express
Vis-SWIR	Visual Short-Wavelength Infrared Spectrometer
VHF	Very High Frequency
VolDet	Volatile Detector and Regolith Microscope
WAC	Wide Angle Camera
wt%	Weight percent
WTR	Woomera Test Range
XAFS	X-Ray Absorption Spectroscopy
XANES	X-Ray Absorption Near the Edge Structure
XPS	X-Ray Photoelectron Spectroscopy
XRD	X-Ray Diffraction
XRF	X-Ray Fluorescence
XRS	X-Ray Spectroscopy/Spectrometer
XRMT	X-Ray Microtomography
YORP	Yarkovsky-O'Keefe-Radziewski-Paddack
ΔDOR	Delta differential one-way range
$\mu L^2 MS$	2-step Laser Mass Spectroscopy

12 Appendix

12.1 Potential contributions from JAXA & NASA to the baseline scenario

In the ESA baseline scenario, JAXA and NASA may contribute to various elements of Marco Polo.

Several NASA programmes foresee international collaboration. Within the programme SALMON (Stand Alone Missions of Opportunity), NASA is able to support the full mission participation of U.S. investigators and can also enable NASA as a partner providing science instruments, hardware or software components.

A JAXA contribution would benefit from the Hayabusa heritage. In particular they could provide engineering support regarding the GNC, s/c operations, and sample collection. Tracking support may also be provided using the two tracking stations in Japan. Scientific instruments (*e.g.* Lidar, XRS...) could also be developed in a partnership. JAXA also developed the Hayabusa re-entry capsule which would fit the re-entry conditions and interfaces of an ESA-defined mission.

Hayabusa is the only spacecraft so far that flew in the vicinity of a very small asteroid like Itokawa. JAXA has experience with the operations of a spacecraft around such a small body (Figure 57) and has obtained navigation data near Itokawa and at touchdown. Such real flight data would be very useful to derive a safe and robust plan for the Marco Polo proximity operations.
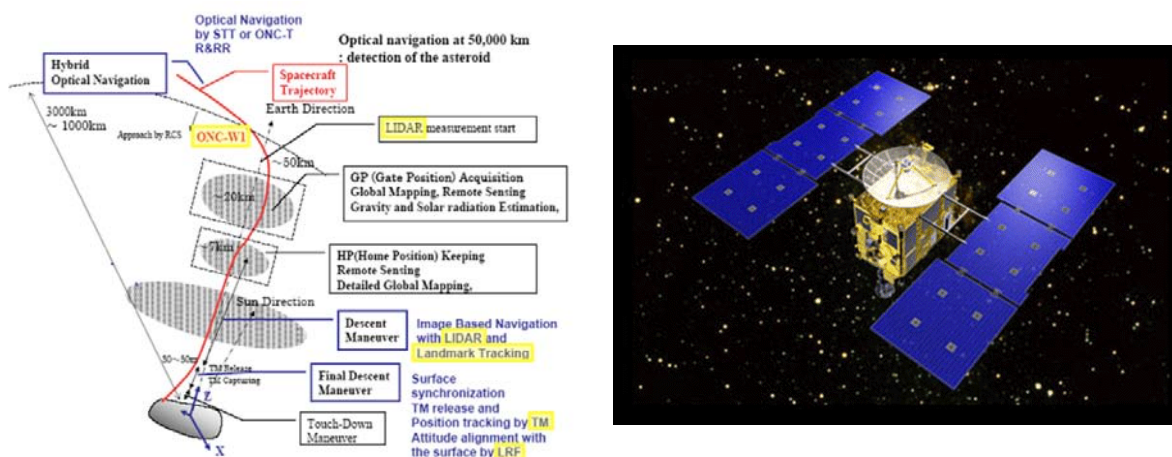
Figure 57: Hayabusa's proximity operations: asteroid descent trajectory (left) and artist concept of JAXA's spacecraft for small body sample return missions (right).

In recent discussions, JAXA's acting counterparts for Marco Polo have identified the following contributions to an ESA-led mission. In particular they envisage providing:

- Regarding GNC:
    - Engineering support by providing real data from Hayabusa for navigation training,
    - Specific hardware support (*e.g.* LIDAR),
    - supporting the mass, shape and density determination during the operations
- Tracking support
    - Range and Range Rate or doppler measurements
    - ΔDOR measurements
    - Receiving telemetry
- Heat shield of the Earth Re-Entry Capsule
- Provision of results from testing of sampling devices
- Science instruments

12.2 Participation as a mission of opportunity

The science objectives and mission design of Marco Polo create an excellent opportunity for either a JAXA or a NASA collaboration as an ESA mission of opportunity.

The Marco Polo mission is a synergetic fit with NASA's Strategic Goal for Planetary Science: "Advance scientific knowledge of the origin and history of the solar system, the potential for life elsewhere, and the hazards and resources present as humans explore space." Collaboration with NASA can be possible from the level of cooperating scientists (already in place) to the provision or sharing of key mission components. Within the New Frontiers, NASA is currently considering proposals that include near-Earth object sample return. If NASA selects an NEA mission for ongoing study or flight within the Discovery or New Frontiers programme this would open an opportunity for direct NASA - ESA dialogue on possible collaboration scenarios.

ESA has studied an ERC which can be provided to a mission by another space agency, using interface requirements from JAXA as an example.

The capsule design is presented in Section 5.1.6. In order to comply with a possible harsher mass-constraint, one option could be to also jettison the front heat shield. ESA would provide all ERC equipment, including the spin-ejection device and the heat shield. The details of the re-entry capsule depend on the finally-selected scenario, i.e. target, re-entry velocity, etc. but preliminary analysis show that a mass lower than 25 kg could be achieved. An example of possible JAXA/ESA interfaces regarding the re-entry capsule is given below.

ESA	JAXA
Capsule separation mechanism	Sample Container
Front / back heat shields	Sample Catcher
Sample heat shield	Sample transfer mechanism
ERC structure	ERC sealing mechanism
Parachute and/or crushables	
ERC electronics	
ERC thermal control	
Rescue beacon	

Table 19: Example of JAXA/ESA interfaces.
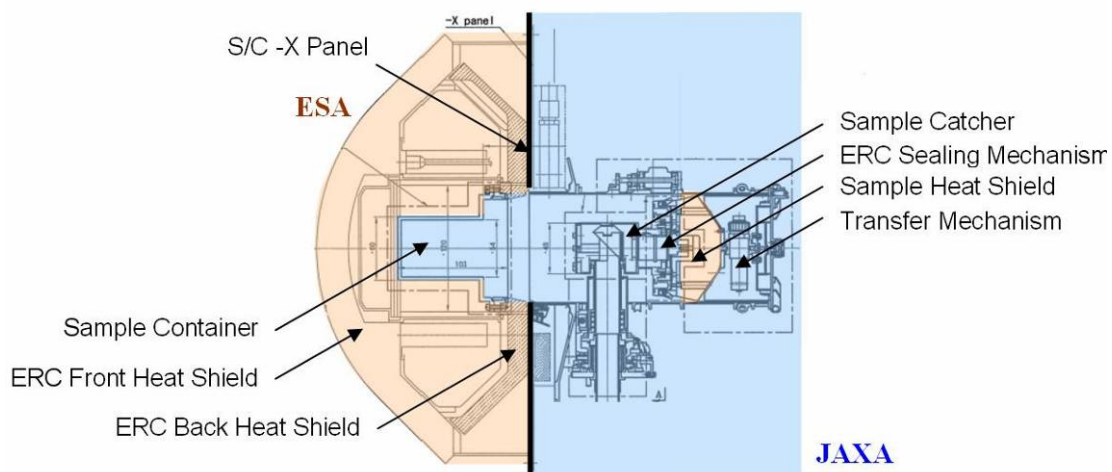
Figure 58: Example of JAXA/ESA interfaces. This drawing is based on the Hayabusa mission concept (http://www.isas.ac.jp/j/topics/topics/2007/0130.shtml).